NATIONAL TECHNICAL UNIVERSITY OF ATHENS (NTUA)

Investigation of the effect of seismological parameters on the risk estimation of a conventional reinforced concrete frame-wall, earthquake resistant building.

A Thesis By
Eng.Ibrahim Mohammed ElBatran

School of Civil Engineering
(**A**nalysis and **D**esign of **E**arthquake **R**esistant **S**tructures) **ADERS** Program
National Technical University of Athens, Greece

Under the supervision of
Prof. Psycharis Ioannis,
Dr.Taflampas Ioannis

Submitted in partial fulfillment of the requirements
For the degree of
Master of Science in structural Engineering

8/10/2014

National **T**echnical **U**niversity of **A**thens, 2014

Investigation of the effect of seismological parameters on the risk estimation of conventional reinforced concrete frame-wall, earthquake resistant building.

National **T**echnical **U**niversity of **A**thens, 2014

NATIONAL TECHNICAL UNIVERSITY OF ATHENS (NTUA)

Investigation of the effect of seismological parameters on the risk estimation of a conventional reinforced concrete frame-wall, earthquake resistant building.

A Thesis By
Ibrahim Mohammed ElBatran

School of Civil Engineering
(**A**nalysis and **D**esign of **E**arthquake **R**esistant **S**tructures) **ADERS** Program

Under the supervision of
Prof. Psycharis Ioannis,
Dr.Taflampas Ioannis

Submitted in partial fulfillment of the requirements
For the degree of
Master of Science in structural Engineering

8/10/2014

Accepted by the Graduate School

_____, _____

National **T**echnical **U**niversity of **A**thens, 2014

The undersigned have examined the thesis entitled '**Investigation of the effect of seismological parameters on the risk estimation of conventional reinforced concrete frame-wall earthquake resistant building**' presented by **Ibrahim ELBATRAN**, a candidate for the degree of **Master degree of Science in structural Engineering** and hereby certify that it is worthy of acceptance.

Date	Advisors name
Date	committee member name
Date	committee member name

Dedication

This thesis is dedicated to the blessed soul of my father Muhammad ELBATRAN.

Dad, you are living in my heart, and my mind. I hope all time to be moving on the path you wished me to go through, May you find the peace and happiness in the Jinnah Insha'Allah.

Ibrahim Muhammad ElBatran

أهدي هذا العمل المتواضع لروح أبى الطاهرة محمد البطران.

أبى أنت حى فى قلبى و فى عقلى دائما , أتمنى من الله أن أكون سائرا على الدرب الذى تتمناه لى, رحمك الله و تغمدك بواسع رحمته و فضله, و أسكنك فسيح جناته جنات الخلد و النعيم.

" قُلْ أَذَٰلِكَ خَيْرٌ أَمْ جَنَّةُ الْخُلْدِ الَّتِي وُعِدَ الْمُتَّقُونَ ۚ كَانَتْ لَهُمْ جَزَاءً وَمَصِيرًا (15) لَهُمْ فِيهَا مَا يَشَاءُونَ خَالِدِينَ ۚ كَانَ عَلَىٰ رَبِّكَ وَعْدًا مَسْئُولًا (16)" **سورةالفرقان 15, 16**

إبراهيم محمد البطران

Acknowledgment

I would like to thank my supervisors, Prof. Psycharis Ioannis, Dr.Taflampas Ioannis for the guidance, encouragement and advice they had provided me during my study in National Technical University of Athens.

I`m also extremely thankful to prof. Papadrakakis, Dr.Plevris, for their care, assistance in anything we face inside or outside the university, and their continuous and efficient support all over the time we stayed in Greece since we came, it was a really a pleasant enjoyable stay.

I would like to thank all the academic staff who taught us in the courses and also the secretary at National Technical University of Athens (NTUA) for their aid and support.

I`m grateful to Prof. Sameh Mehanny, prof of structural engineering at Cairo University in Egypt for his continuous support, and frequent visits to us in Greece.

I should give all the credits of my academic engineering life to Prof.Nayer A.EL-ESNAWY, professor of Structural Engineering at Cairo University who have and will continue to be a great influence on me; Thank you for all what you did all over the time since I was honored to meet and deal with you, I learnt from you lots of valuable things not only in my academic life but also my daily life as well. Thank you so much for taking the time from your busy schedule to write a letter of recommendation for my graduate school application. I hope I would be always at your expectations.

Last but not least, I`m deeply in infinite debit to my mother and my sister Eng.Manal M.ElBatran for their infinite loyalty in serving me and providing me with all my needs, no words can express my appreciation and gratitude to them…

Abstract

In this paper the seismic risk of conventional seven-story reinforced-concrete frame-wall building to near-field strong ground motions records is presented. The purpose of this investigation is to establish the effect of magnitude, directivity and distance to the fault on the seismic risk of a sample of buildings, designed according to the up to date seismic codes available in their region. As a first step, the fragility curves, associated with the different limit states regarding the response of the examined buildings, are estimated, following the methodology incorporated in the HAZUS procedure for individual structures. A large sample of ground motion time histories, effectively representing the seismic events for which near field records are available, is used as input motion for the selected buildings. The records examined adequately represent the diversification regarding the referred seismological characteristics that affect the strong ground motion. Subsequently, the response of the examined buildings to the selected ground motions is estimated and compared to the fragility curves already established according to the HAZUS procedures. The referred seismological characteristics of the ground motion are associated to the probability of attaining particular limit states for each building under examination. As a result, a correlation is established between the magnitude, directivity and attenuation characteristics of the ground motion and the limit states attained by the building. The magnitude effect has already been appreciated as a crucial factor affecting structural response. This investigation indicates that the directivity and distance to the fault effects are of equal significance. Characteristically, the range of structural response values for different directivity or attenuation effects may present a difference of an order of magnitude. The sensitivity of the estimation of seismic risk to the referred parameters indicates that their incorporation in procedures such as HAZUS must be as detailed and accurate as possible.

Table of Contents

List of figures

List of Tables

Chapter1

1. Introduction

Earthquakes ground motions that are recorded by stations located at "near-fault" regions convey different and risky characteristics compared to that of those recorded at "far-fault" regions. The main difference is an intense long pulse period that is clearly obvious in the velocity time history record due to what is known as "forward directivity" effects.

Such a phenomenon may result in serious and severe damage and even may lead to collapse of flexible structures especially high rise buildings; inheriting relatively large natural periods.

Unfortunately Seismic design codes are based on "far-fault" ground motion data only which do not show the other characteristics of "near-fault" ground motions and therefore code provisions for structures in near-fault regions are inappropriate.

In this study the effect of near-fault ground motions are investigated, along with other seismological parameters such as earthquake magnitude and distance from the fault, in order to see their effects on the seismic response of a conventional seven-story reinforced-concrete frame-wall building, and hence be able to perform a risk estimation for that building under certain earthquake event.

Using SAP2000, a static non-linear Pushover Analysis is made, in order to follow step by step the formation and development of the plastic hinges -whose probable locations were predefined before performing the analysis in accordance to FEMA 356 -and hence we could determine the displacements associated with each structural damage limit state that is defined according to HAZUS methodology.

The values of the displacements related to each limit state are then used to develop the fragility curves of the examined building following the methodology incorporated in the HAZUS procedure for individual structures.

Using also SAP2000, A large sample of 290 "near-fault" ground motion records – Acceleration Time Histories- obtained from 24 earthquakes would be used in this investigation to widely show the effect of the seismological parameters on the risk estimation of such a frame-wall building under a certain ground motion.

The report is formed out of seven chapters, the first chapter is an introductory to the procedure followed in this report, and a summary for each chapter presented in this report.

A detailed description for the frame-wall building is provided in chapter 2, involving the general description of the building layout, also detailed descriptions showing the dimensions,

reinforcement, for the structural elements forming the building ;beams, column, & Shear wall, also the properties of the materials used ; concrete and reinforcement steel.

In Chapter 3, the results obtained from the nonlinear static Pushover using SAP2000 are shown such as the relation between the base shear and displacement of top floor, displacements associated with the damage limit states according to HAZUS methodology, and finally constructing the fragility curve associated with each damage limit state.

In Chapter 4, the sample of the ground motion records time histories, effectively representing the seismic events for which near field records are available, used as input motion for our mentioned building is presented.

In chapter 5, results arising from applying the "near-fault" ground motion record to the building using SAP2000 are obtained; these results are the maximum top floor displacement that the building undergoes due to that certain ground motion record.

The displacement value gives an indication for at which structural damage state the building will suffer when subjected to such a ground motion, these results are given in a tabulated form for each earthquake showing the maximum displacement and the corresponding predefined limit damage state.

Moreover, applying these results to the fragility curves shows us the probability of exceeding a certain damage limit state under that certain ground motion record.

The conclusions upon reviewing the results obtained are summed up in the last chapter which is chapter 6 to show the sensitivity of the building to each seismological parameter.

Chapter 2

2. Building Layout

2.1 General description.

The building considered for this study to examine its seismic response due to seismic loadings arising from near-field ground motions is a seven-story building of reinforced concrete mixed system of columns and wall. The building was designed at the University of California at Berkeley for use in a research project, which involved both American and Japanese researchers, in order to study the seismic behavior of a mixed system consisting of columns and wall. The results of the research project published in the report An evaluation of the design and analytical seismic response of a seven - story reinforced concrete frame - wall structure", of Finley A. Charney and Vitelmo V. Bertero.

The building consists of three parallel frames. The two outer panels (panel A and C) composed only of columns while the inner (panel B) of columns and a central wall. Below are a plan view (Figure 2.1) and the section of the structure (figure 2.2).

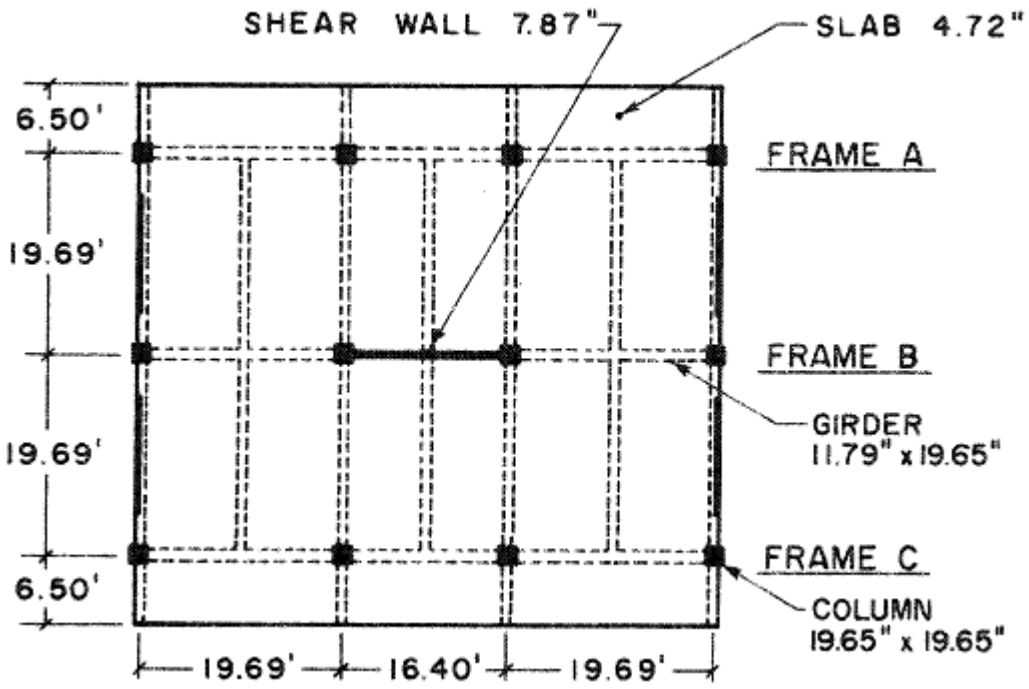

Figure 2.1 Building Top View

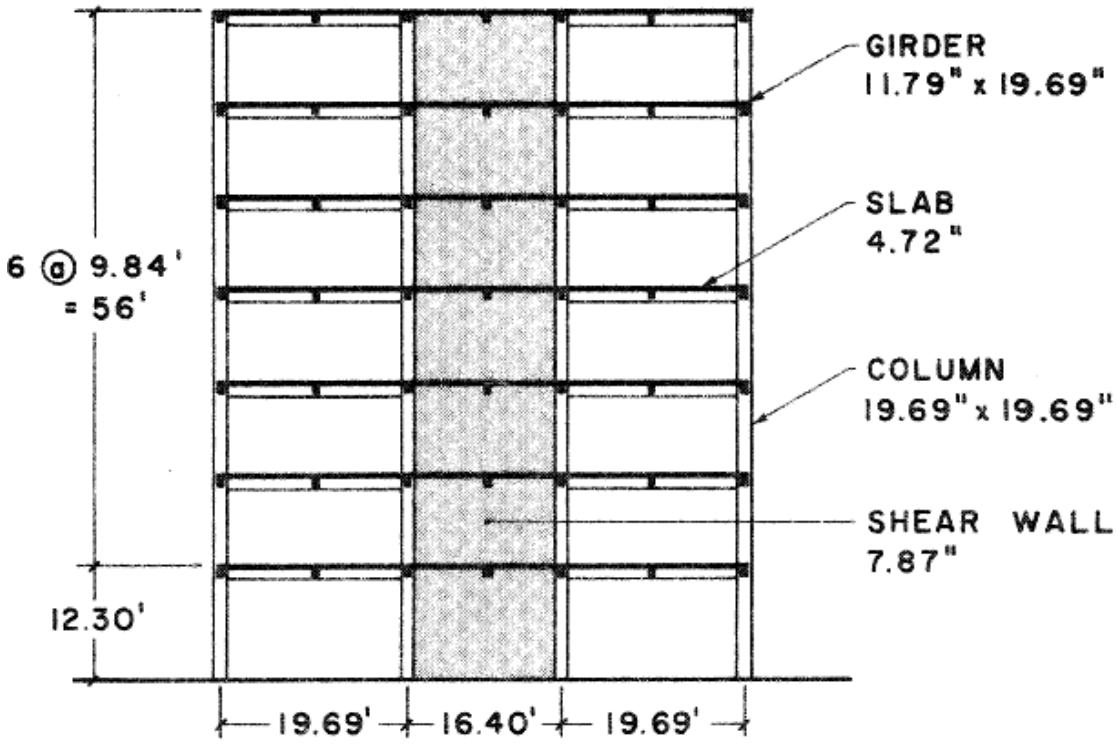

Figure 2.2 Building Section Elevation**.**

2.2 Materials.

2.2.1 Concrete.

The concrete used to build the original set so as to have resistance cylindrical specimen 28 days equal to 26.5 Mpa or 3.85 KSI (1 KSI = 6.89 MPa) and the composition was made with normal weight aggregates and cement Type 1 Portland. Figure 2.3 below shows the stress-strain Relationship.

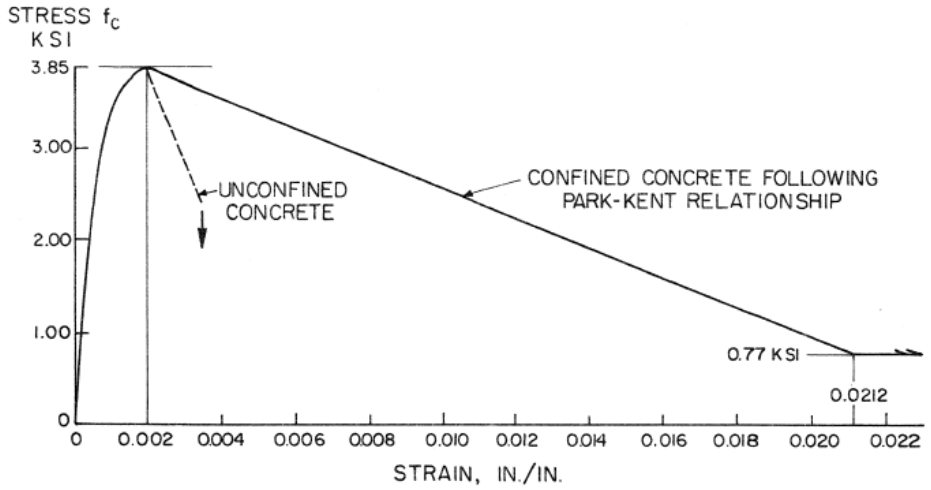

Figure 2.3 Stress-strain curve for unconfined and confined concrete.

2.2.2 Reinforcement.

Based on Japanese factory references samples rod diameters from F13 to F22, the average yield stress was equal to 59.25 KSI (408 MPa), while the average tensile strength was equal to 85 KSI (586 MPa). Note that this average yield stress is higher by 18.5 percent than the specified value. So for the next analysis consider yield stress 59.25 KSI (408 MPa), tensile strength 85 KSI (586 MPa), modulus 29000 KSI (200000 MPa) and strain-hardening 441 KSI. The stress-strain curve of the steel is given in Figure 2.4.

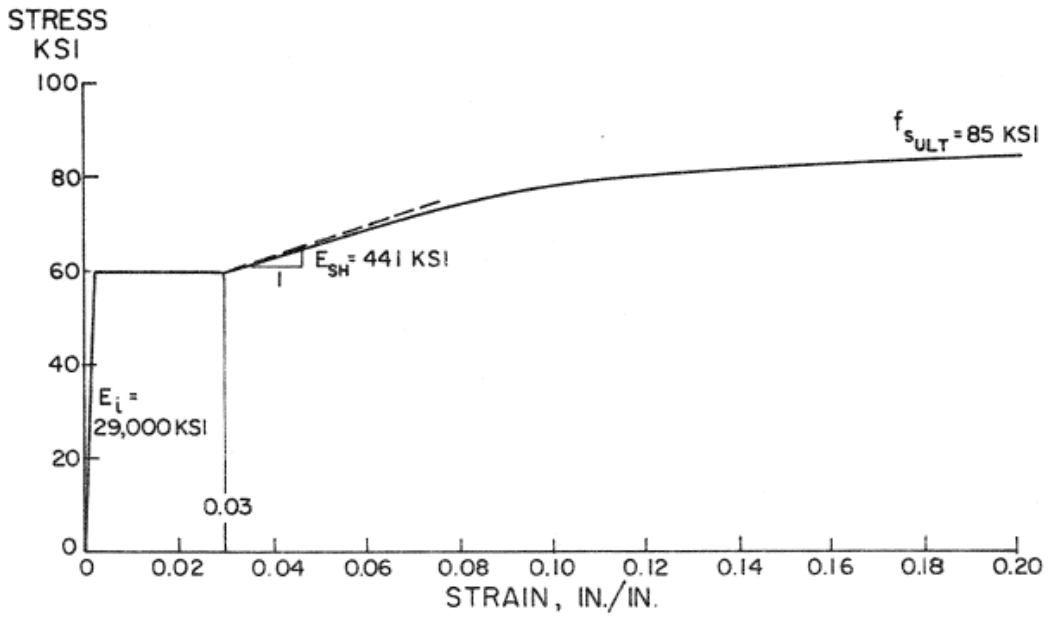

Figure 2.4 Stress-strain curve for steel.

2.3 Manufacturing Concerns.

2.3.1 Beams.

The x-section of the beam of typical construction is shown in Fig.2.5 and the side view of the Fig. 2.6. In these figures are given the dimensions of the beam, and the provision of longitudinal and transverse RFT. These rules shall govern all beams of frames A, B and C.

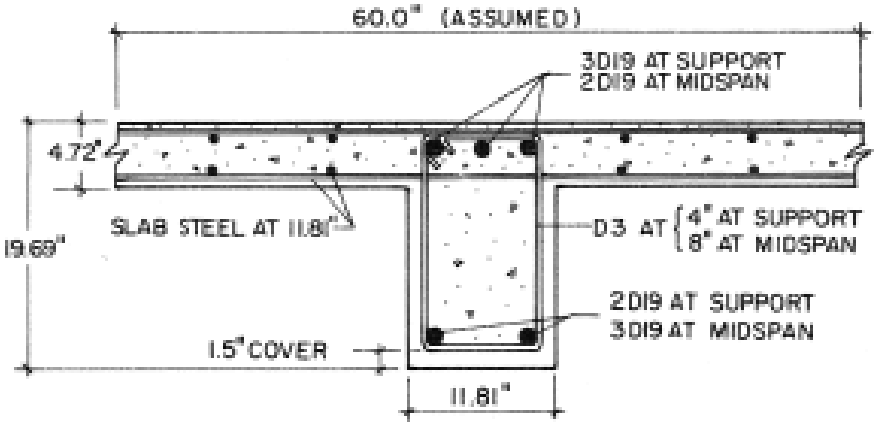

Figure 2.5 Beam`s Cross-section.

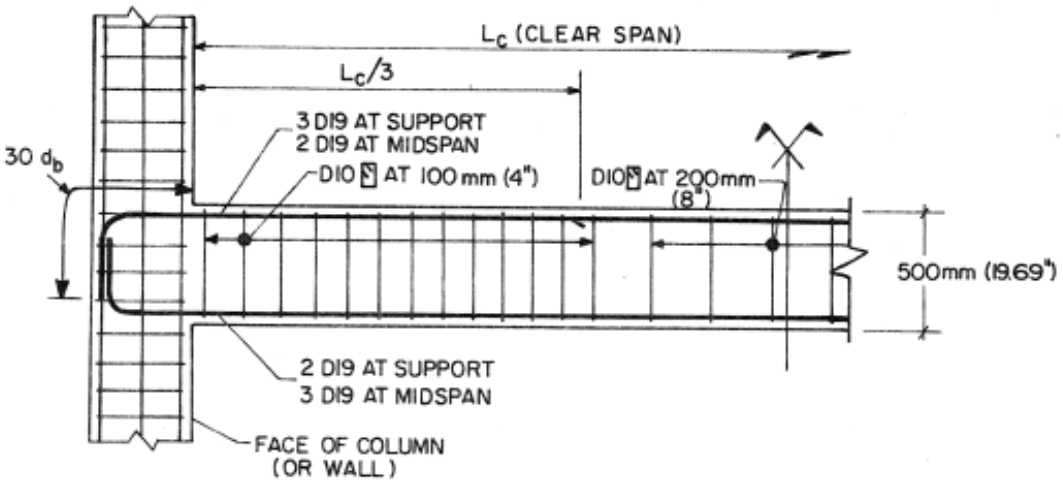

Figure 2.6 Beams Side View.

The provision of primary reinforcement, as shown in Figures satisfies all the requirements of the regulation; including the requirement that the compression reinforcement is a cross section is at least 50 percent of the tensile. The intersection is considered with effective width equal to 1.52 m which is less than the distance from the center of a plate as the center of the next.

2.3.2 Columns

The cross section of a typical column of the model is given in the figure below. This section with the exception to the stirrups is the same for all the columns of the structure.

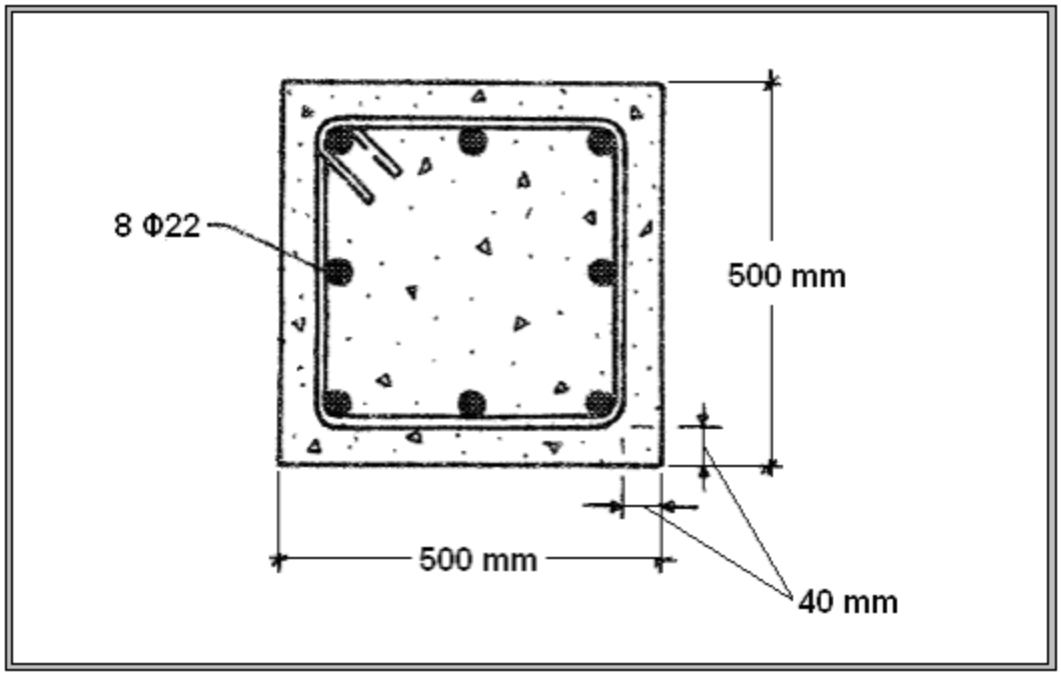

Figure 2.7 Typical Column`s Cross Section.

The details of the stirrups of the columns vary among members of the structure. There are three different types of transverse reinforcement. For all columns of the second floor and all upper floors, connectors consist of bars diameter D10, square ring, and spaced 100 mm height of the column. For the columns of the first floor has selected the following provision: From the base of the column and by the fourth of the height, the stirrups again comprises rods D10 square layout boosted cross-linkers , as shown in the figure below, again spaced 100 mm. The rest of the column height of the layout is similar to the columns of the overlying floors, as described above. For columns lying at the edges of the wall, it is similar to the base of the columns of the first floor. In summary, all the above are shown in Figure 2.8.

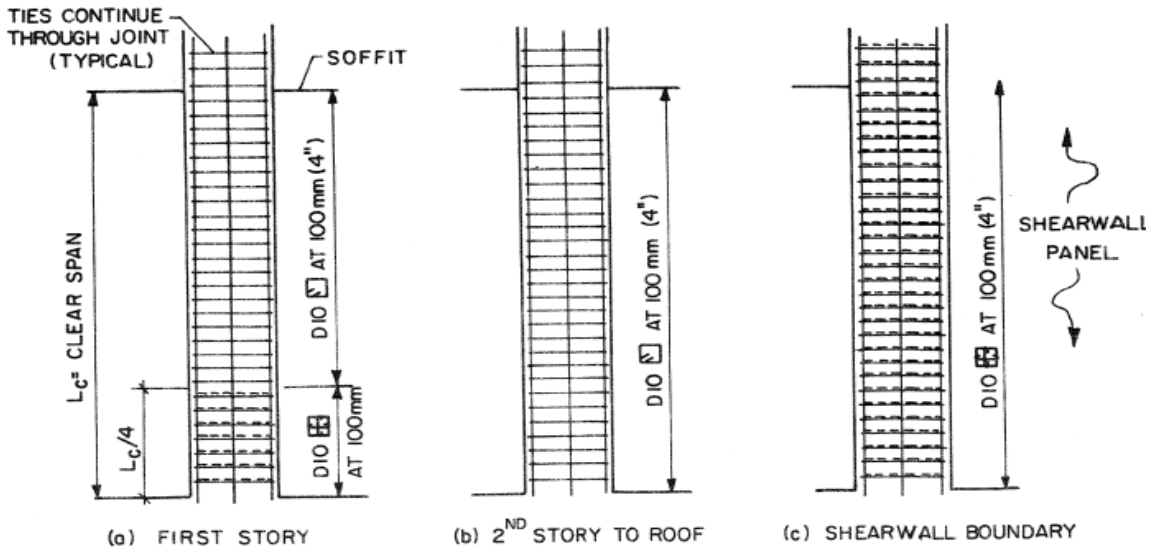

Figure 2.8 Stirrups Details for columns.

2.3.3 Wall

The wall, located in the center of the building is without a doubt the most important element of the building, as it is the component that gives the construction of most of rigidity. It is a composite cross section with rectangular core and edges of greater width, the core has a thickness of 200 mm and a length of 4.5 m and the reinforcement consists of rods F10 diameter spaced at 200 mm in both horizontal and vertical faces of the two walls. The ends of the wall are columns having the typical cross section column, of which was shown its top view in Figure2.5 and the section in Figure 2.8 (c). The section plan view of the entire wall is given in Figure 2.9, while the vertical section in Figure 2.10.

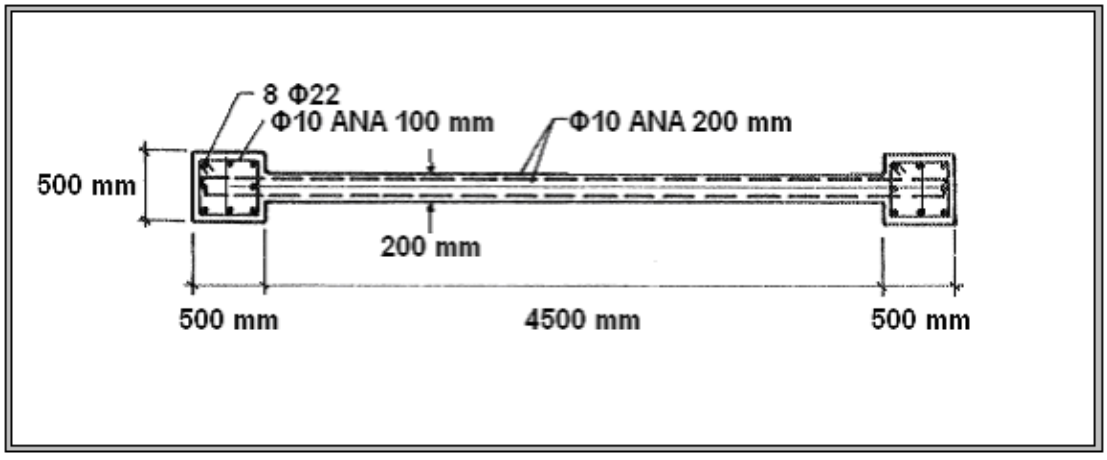

Figure 2.9 Wall Section Plan view.

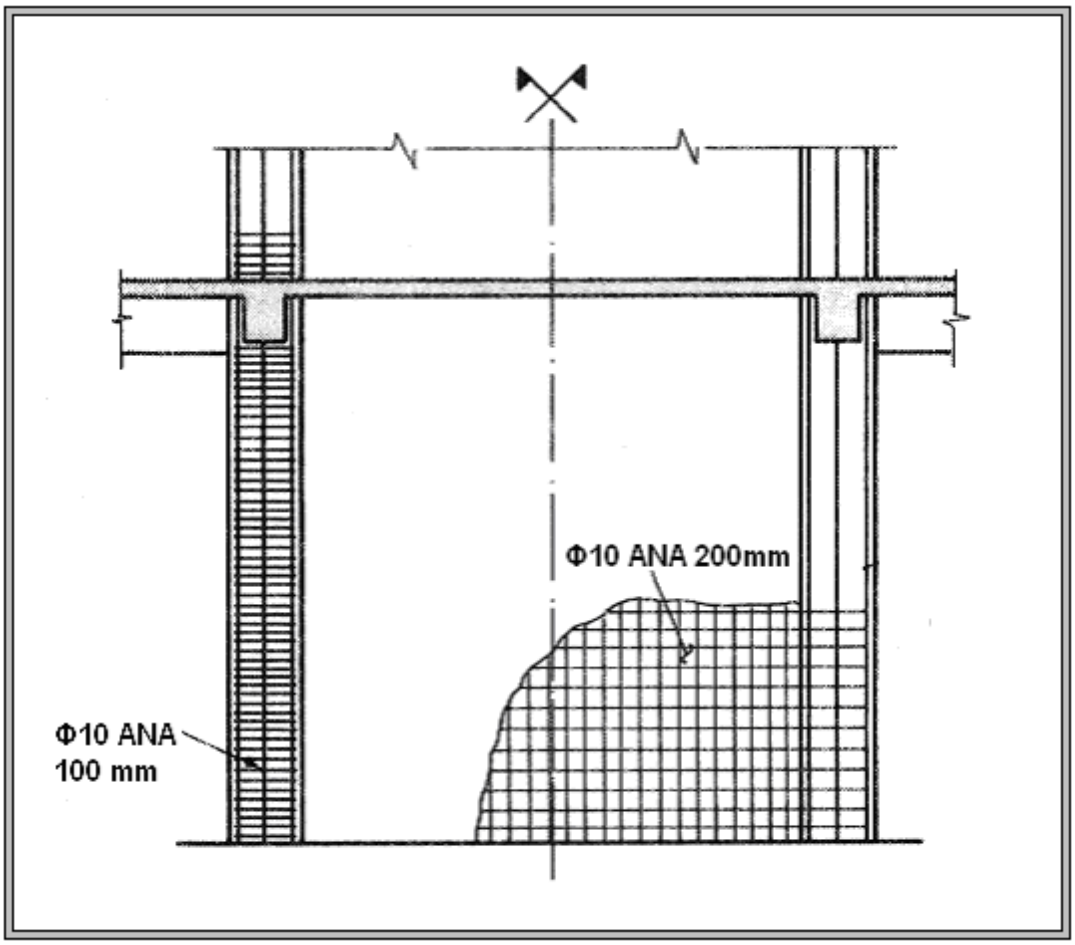

Figure 2.10 Wall Vertical section

2.4 Modeling of the building on program SAP2000.

To allow for comparison between the results of the research program of the University of Berkeley and those of the thesis, it was preferred simulation operator- program to become a model 2D. So the three panels (A, B and C) are placed next to each other, while the height of each floor is rigid couplings that connect the beams of each floor of a frame with those on the same floor of the adjacent frame. This ensures that diaphragmatic function, and attach the slabs of the building will be taken into account by the program during the analysis and movements developing at nodes on each floor levels will be same for all frames at the same height. The following figure2.11 given model operator as introduced in the SAP2000.

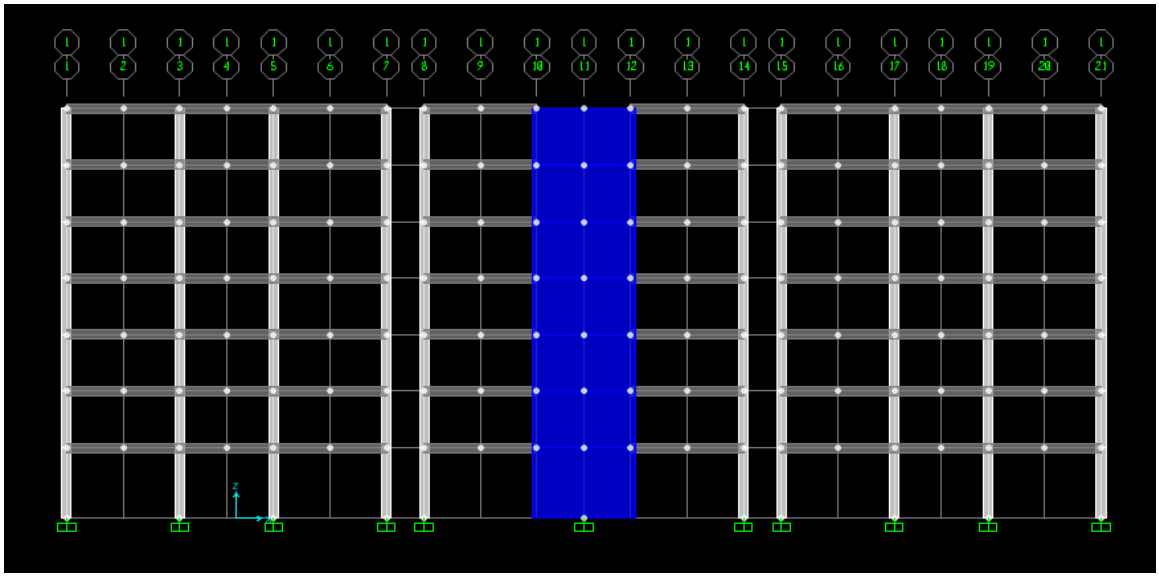

Figure 2.11 Building 2D Model.

The carrier materials are weightless, and each frame is loaded with both distributed and with concentrated loads. Distributed loads on the same weights of materials of the beams, and the dead and live loads of the slabs, all with a coefficient equal to one. The division of the area of the slabs in surfaces portions transmitted to each beam shown in the figure 2.12 below.

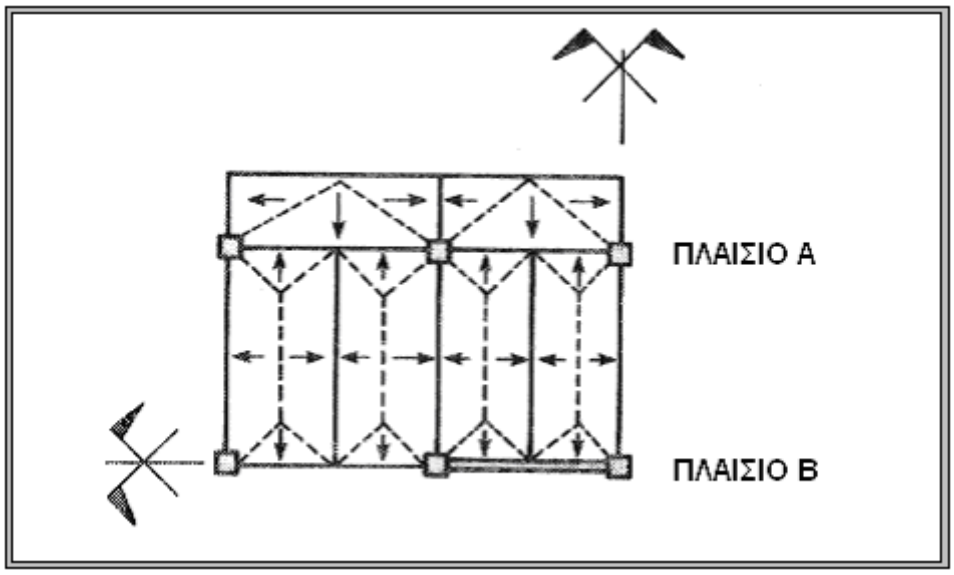

Figure 2.12 Beams portion from slabs loads.

Finally, at each level are grouped masses which correspond to loads (dead and live) transmitted within the transverse beams in them, and also weights of columns leading to these nodes. The ultimate static load each beam eventually introduced in the model of the program is given in the figure 2.13 below.

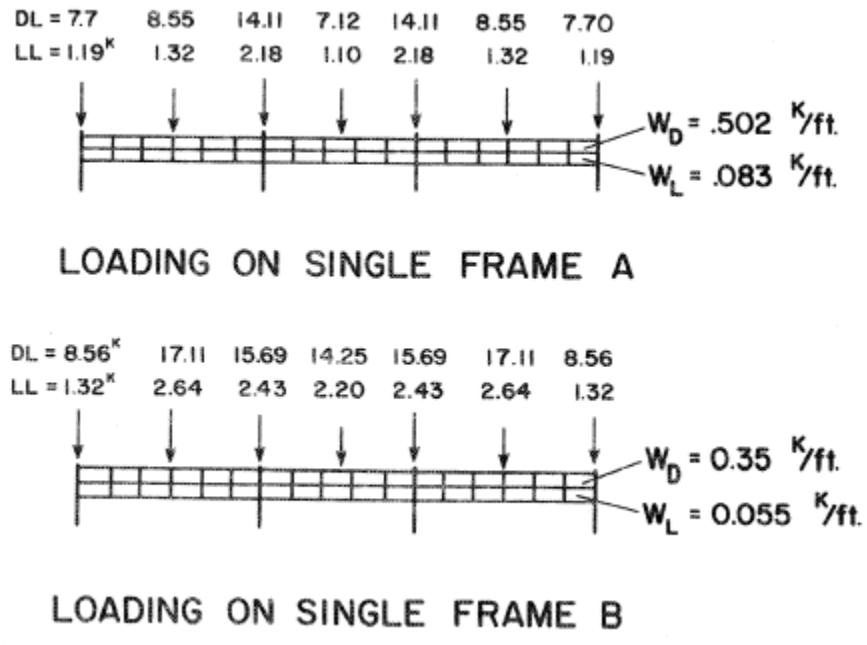

Figure 2.13 Prototype Gravity Loading.

What deserves special mention is the input model of the wall in the program as the cross section of the wall of this building is core rectangular at core and square shaped ends –columns- wider than that of the core which was not among the available sections provided by the program. This problem is overcome by use of an equivalent rectangular cross section in the model finally introduced in the program which gives moment diagrams - curvatures same as the cross section of the actual wall. The analysis was performed using the program Fagus - 5. The results of the analysis are given in the following figures 2.14,2.15

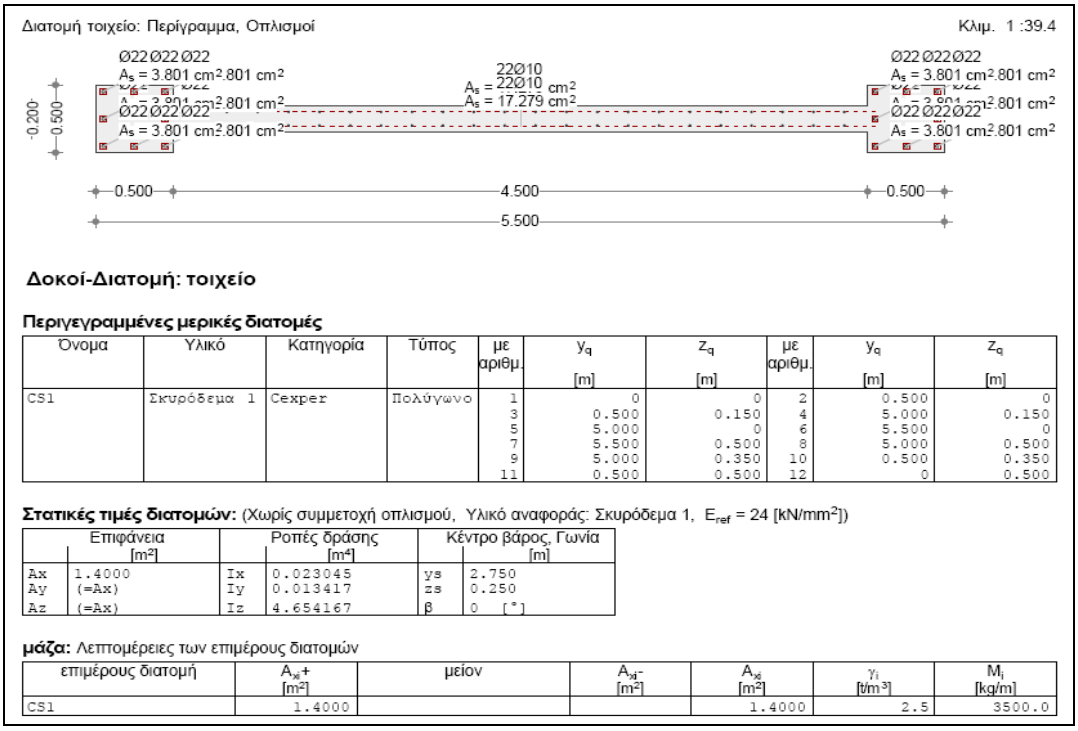

Δοκοί-Διατομή: τοιχείο

Περιγεγραμμένες μερικές διατομές

Όνομα	Υλικό	Κατηγορία	Τύπος	με αριθμ.	y_q [m]	z_q [m]	με αριθμ.	y_q [m]	z_q [m]
CS1	Σκυρόδεμα 1	Cexper	Πολύγωνο	1	0	0	2	0.500	0
				3	0.500	0.150	4	5.000	0.150
				5	5.000	0	6	5.500	0
				7	5.500	0.500	8	5.000	0.500
				9	5.000	0.350	10	0.500	0.350
				11	0.500	0.500	12	0	0.500

Στατικές τιμές διατομών: (Χωρίς συμμετοχή οπλισμού, Υλικό αναφοράς: Σκυρόδεμα 1, E_{ref} = 24 [kN/mm²])

	Επιφάνεια [m²]		Ροπές δράσης [m⁴]		Κέντρο βάρος, Γωνία [m]
Ax	1.4000	Ix	0.023045	ys	2.750
Ay	(=Ax)	Iy	0.013417	zs	0.250
Az	(=Ax)	Iz	4.654167	β	0 [°]

μάζα: Λεπτομέρειες των επιμέρους διατομών

επιμέρους διατομή	A_x+ [m²]	μείον	A_{xi}- [m²]	A_{xi} [m²]	γ_i [t/m³]	M_i [kg/m]
CS1	1.4000			1.4000	2.5	3500.0

Figure 2.14 Elements actual section

M-x-Diagram:

N = -467.25 -938.95 -1410.65 -1882.35 -2354.05 -2848.00 -3293.00 kN

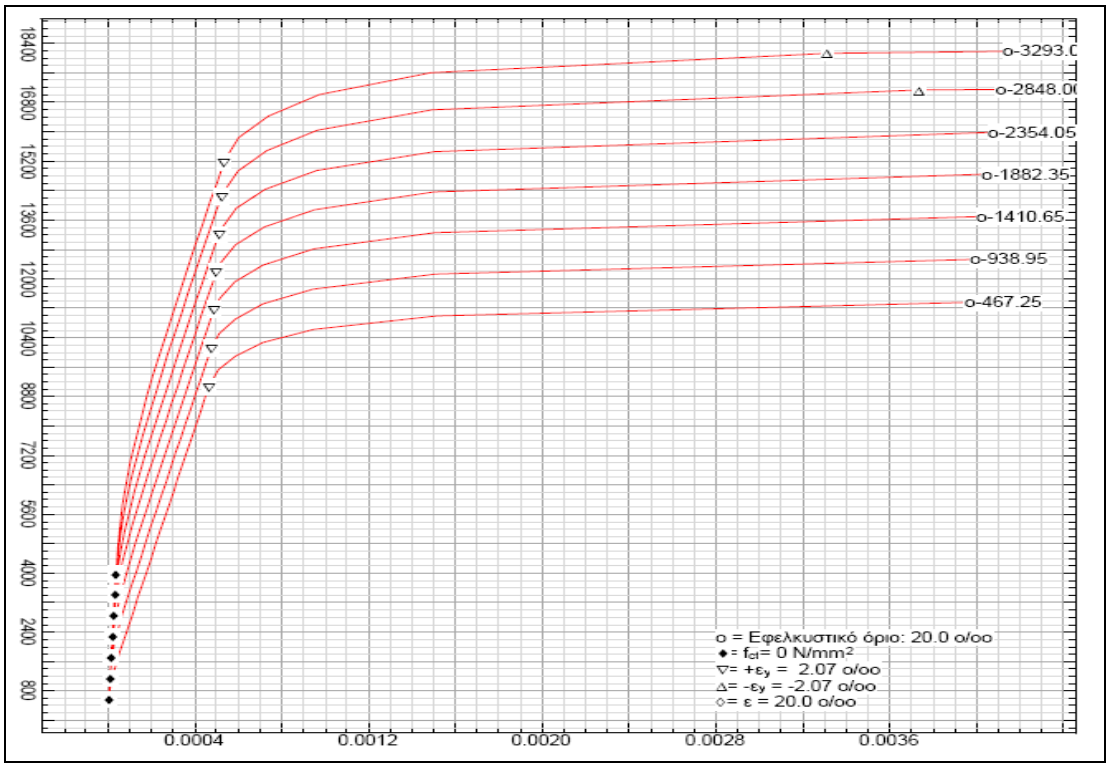

Figure 2.15 Diagram moments - real sectional curvatures

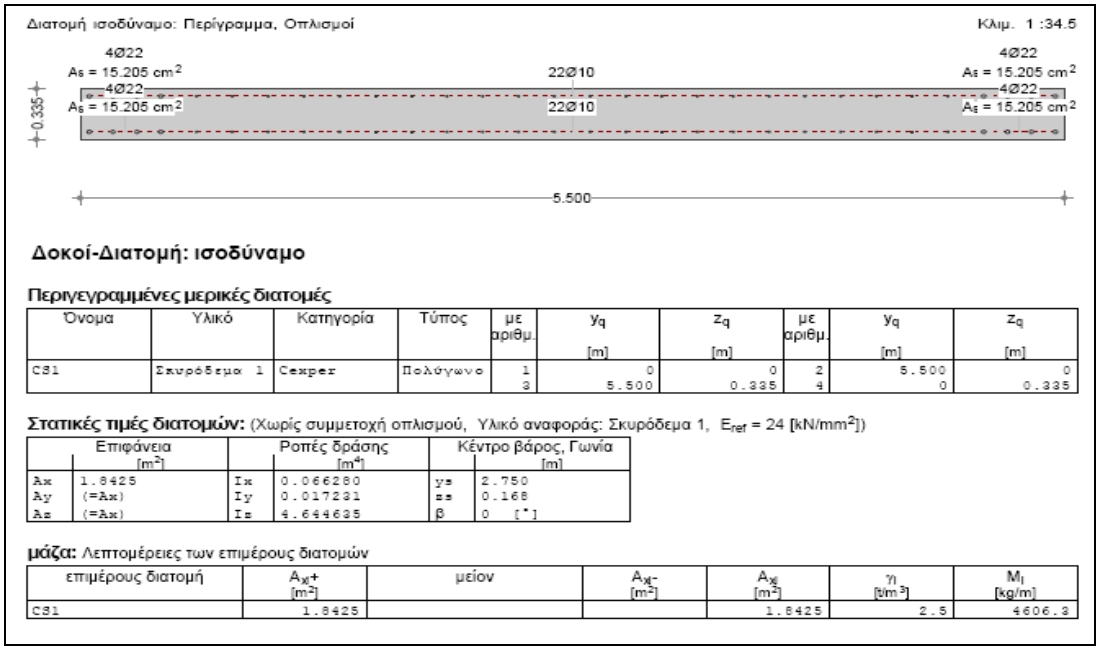

Δοκοί-Διατομή: ισοδύναμο

Περιγεγραμμένες μερικές διατομές

Όνομα	Υλικό	Κατηγορία	Τύπος	με αριθμ.	y_q [m]	z_q [m]	με αριθμ.	y_q [m]	z_q [m]
C31	Σκυρόδεμα 1	Cexper	Πολύγωνο	1 3	0 5.500	0 0.335	2 4	5.500 0	0 0.335

Στατικές τιμές διατομών: (Χωρίς συμμετοχή οπλισμού, Υλικό αναφοράς: Σκυρόδεμα 1, E_{ref} = 24 [kN/mm²])

	Επιφάνεια [m²]		Ροπές δράσης [m⁴]		Κέντρο βάρος, Γωνία [m]
Ax	1.8425	Ix	0.066280	ys	2.750
Ay	(=Ax)	Iy	0.017231	zs	0.168
Az	(=Ax)	Iz	4.644635	β	0 [°]

μάζα: Λεπτομέρειες των επιμέρους διατομών

επιμέρους διατομή	A_{xl}+ [m²]	μείον	A_{xl}- [m²]	A_{xl} [m²]	γ_l [t/m³]	M_l [kg/m]
C31	1.8425			1.8425	2.5	4606.3

Figure 2.16 Identification of equivalent rectangular.

M-x-Diagram:

N = -467.25 -938.95 -1410.65 -1882.35 -2354.05 -2848.00 -3293.00 kN

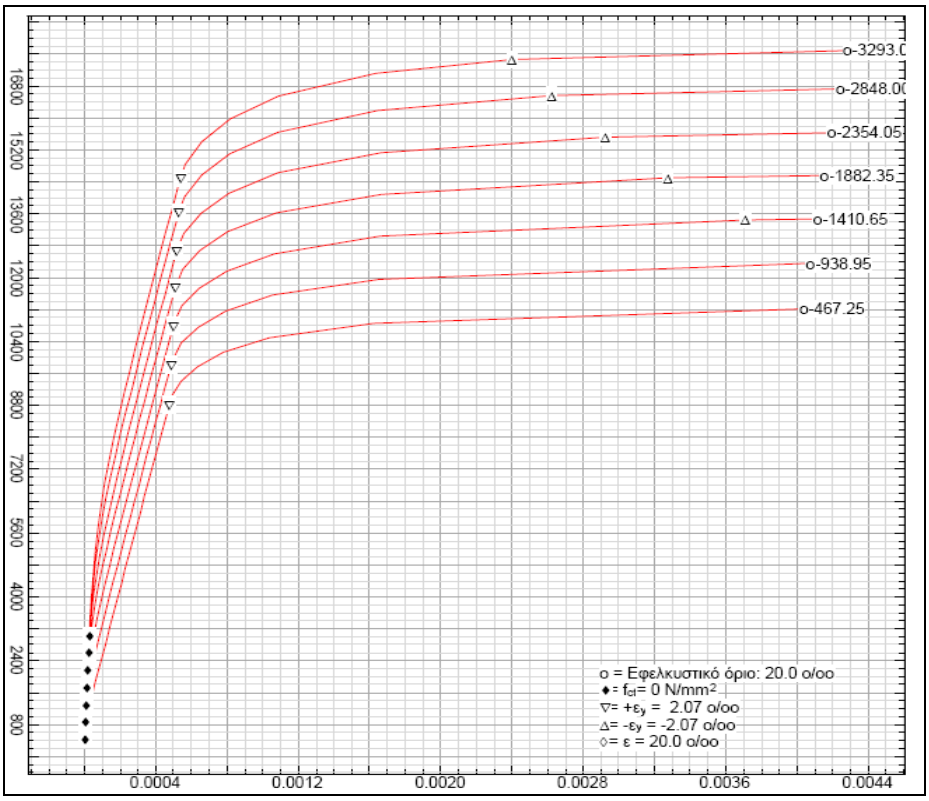

Figure 2.17 Diagram moment - curvature equivalent rectangular.

Chapter 3

3. Development of the building`s structural Damage Limit states and associated Fragility curves.

3.1 Methodology.

Using SAP2000, a static non-linear Pushover Analysis is made, in order to follow step by step the formation and development of the plastic hinges -whose probable locations were predefined before performing the analysis in accordance to FEMA 356 -and hence we could determine the displacements associated with each structural damage limit state that is defined according to HAZUS methodology.

The values of the displacements related to each limit state are then used to develop the fragility curves of the examined building following the methodology incorporated in the HAZUS procedure for individual structures.

3.1.1 Pushover analysis.

The recent advent of performance based design has brought the nonlinear static pushover analysis procedure to the forefront. Pushover analysis is a static, nonlinear procedure in which the magnitude of the structural loading is incrementally increased in accordance with a certain predefined pattern. With the increase in the magnitude of the loading, weak links and failure modes of the structure are found. The loading is monotonic with the effects of the cyclic behavior and load reversals being estimated by using a modified monotonic force-deformation criteria and with damping approximations. Static pushover analysis is an attempt by the structural engineering profession to evaluate the real strength of the structure and it promises to be a useful and effective tool for performance based design.

The ATC-40 and FEMA-273 documents have developed modeling procedures, acceptance criteria and analysis procedures for pushover analysis. These documents define force-deformation criteria for hinges used in pushover analysis. As shown in Figure 1, five points labeled A, B, C, D, and E are used to define the force deflection behavior of the hinge and three points labeled IO, LS and CP are used to define the acceptance criteria for the hinge. (IO, LS and CP stand for Immediate Occupancy, Life Safety and Collapse Prevention respectively.) The values assigned to each of these points vary depending on the type of member as well as many other parameters defined in the ATC-40 and FEMA-273 documents.

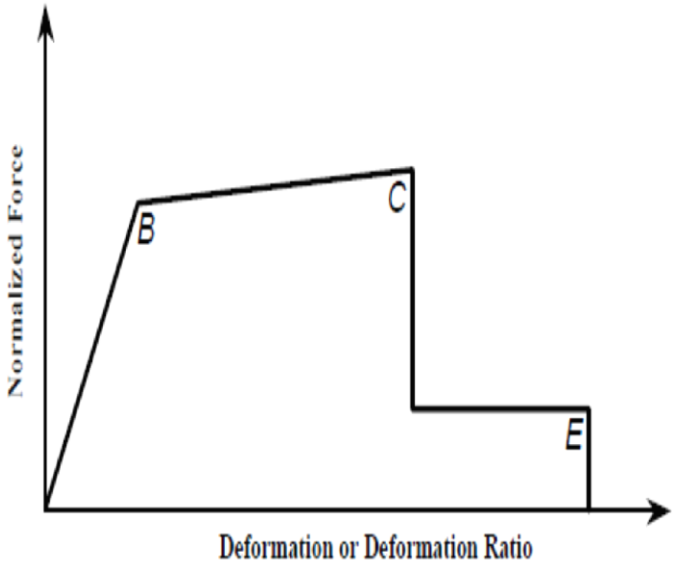

Figure 3.1 Idealized Component Load versus Deformation.

For analysis monitored displacement of the building roof was chosen as 1m (one meter). The resulting pushover curves in positive Y- direction, in terms of Base Shear vs. Roof Displacement (V-Δ), have shown in Figure 6.1. The slope of the pushover curves is gradually reduced with the increase of the lateral displacement of the building.

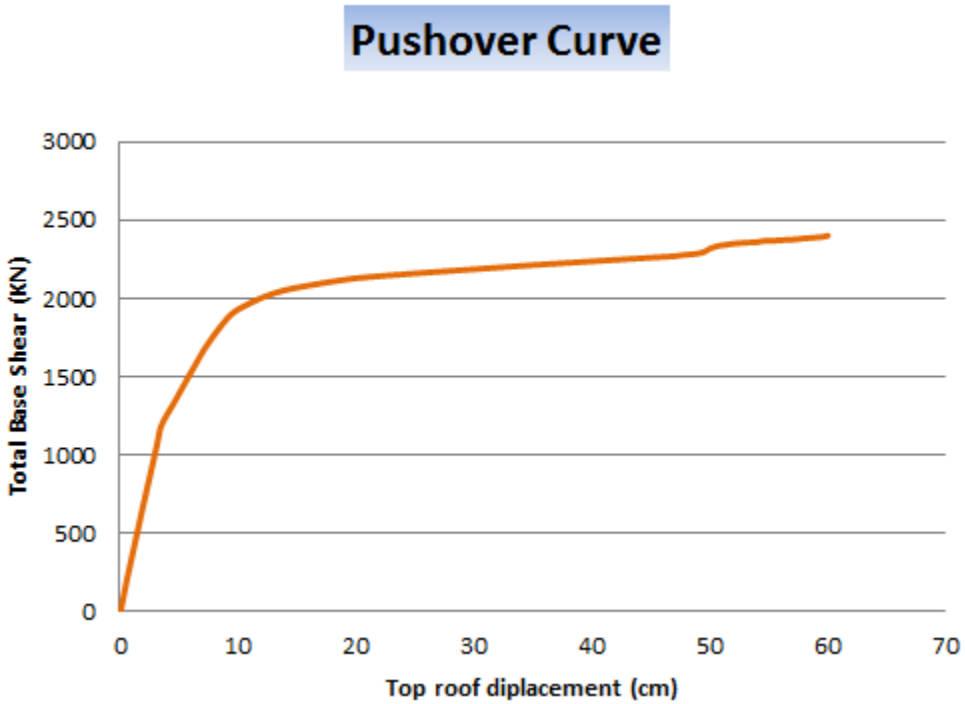

Figure 3.2 Push-over curve of the frame-wall building imported from SAP Analysis.

3.1.2 Defining Limit Damage States

Following HAZUS procedure to determine the limit states as In figure 3.2, Structural Damage Limit states are obtained as shown in table1.

Damage State	Component		
	Fraction[2]	Limit[3]	Factor[4]
Slight	> 0%	C	1.0
Moderate	≥ 5%	C	1.0
Extensive	≥ 25%	C	1.0
Complete	≥ 50%	E	1.0 - 1.5[5]

Figure 3.3 Damage Limit States Boundaries.

Direction	Limit State	Base shear (KN)	Displacement (m)
Y	Yield	1055	0.030978
	Slight	2200	0.3229
	Moderate	2210	0.34893
	Partial Collapse	2229	0.4769
	Collapse	2360	0.5427

Table 1 Performance level of building at different limit states.

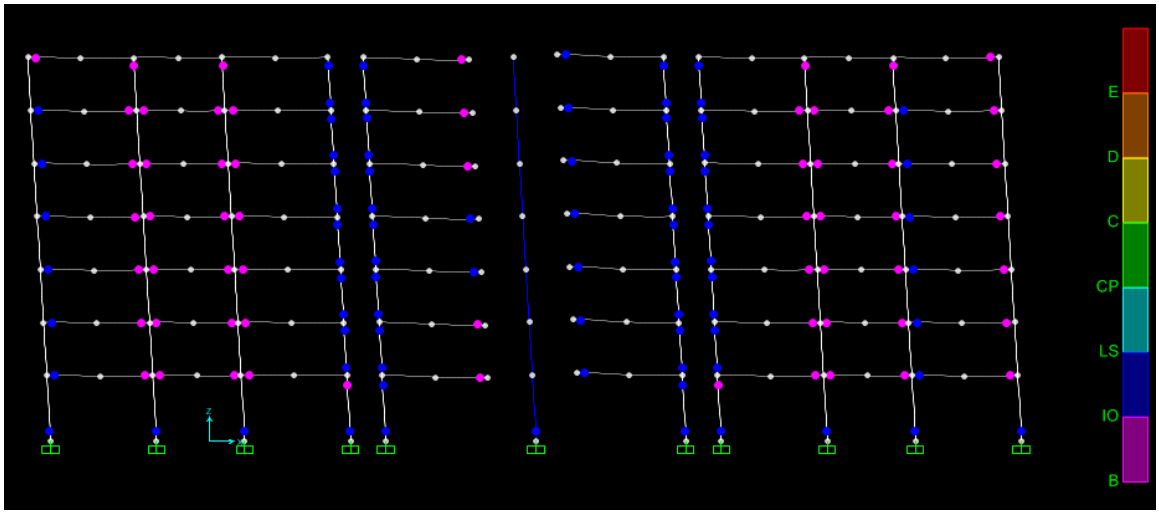

Figure 3.4 (slight damage state)

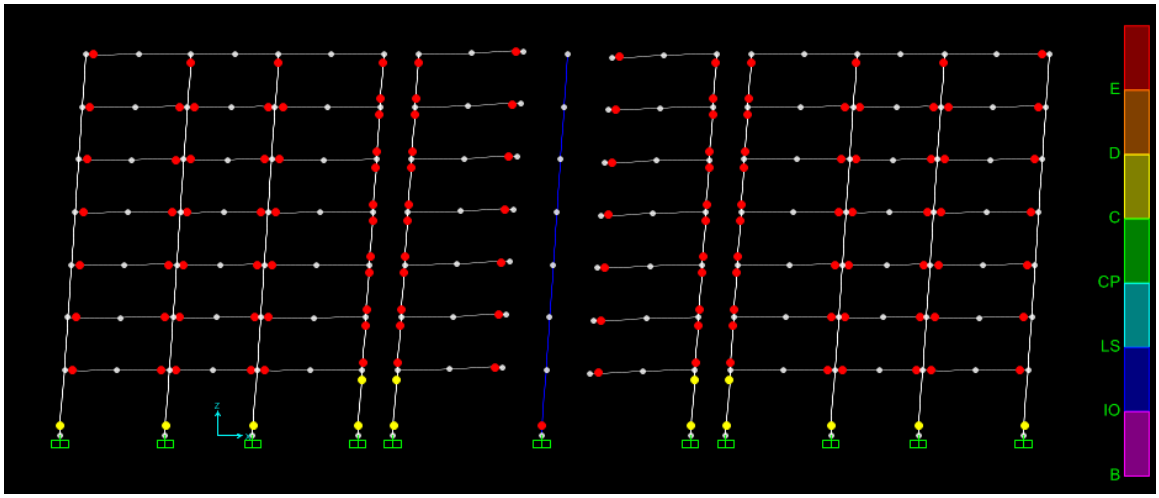

Figure 3.5 (collapse state at the controlled displacement)

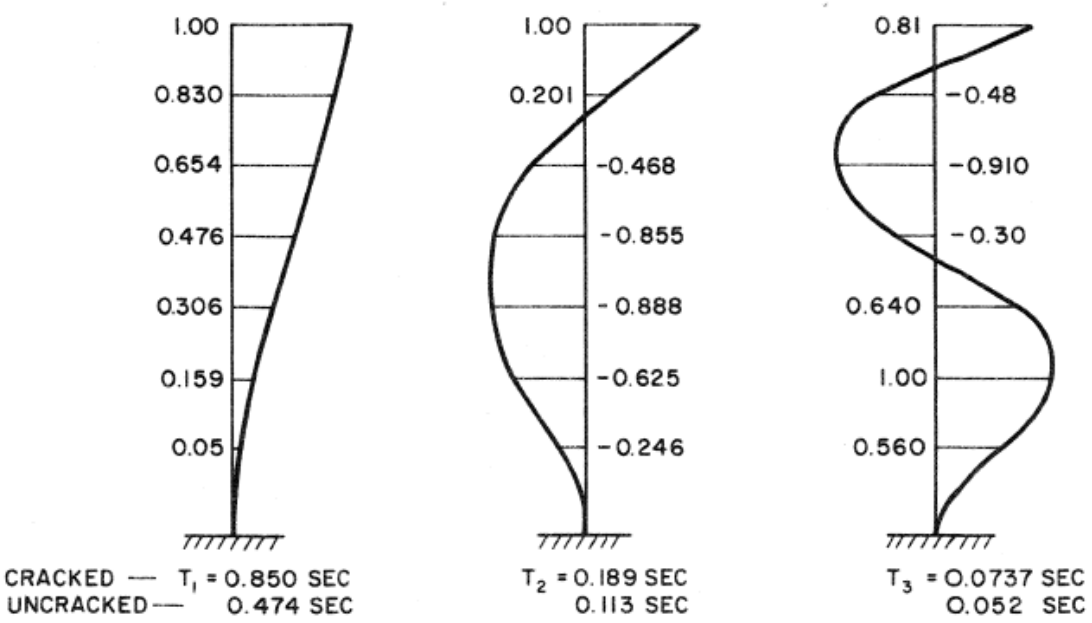

Figure 3.6 Mode Shapes and periods of vibrations.

3.1.2 Development of Fragility Curve.

On the basis of HAZUS Methodology four vulnerability curves have been developed corresponding to light, moderate, extensive and totally collapse limits of the building. Another fifth curve namely yield curve was incorporated when first plastic hinge was formed during P-O analysis.

The vulnerability of the building is represented the following;

The first green curve, which represents the phase in which the building yields, corresponding to a mean displacement 0.030978m (i.e. the time when maximum displacement 0.030978 m occurred and the first plastic hinge is formed).

The light blue curve which defines the slight limit, i.e. the time when the first failure plastic hinge, corresponding to a mean value of 0.3229 m.

The blue curve that defines the medium level fault corresponds to the point on the pushover in which only 5% of plastic hinges failed and is equivalent to average price movement equal to 0.34894 m.

The yellow curve which defines the extensive damage, i.e. 25% of plastic hinges fail, corresponding to a mean value 0.4769 m.

Finally, red curve that defines the total damage, i.e. 50% of plastic hinges fail, corresponding to a mean displacement 0.5427 m. In Figure 6.7 the pushover curve and the average displacement which define the fault levels are presented.

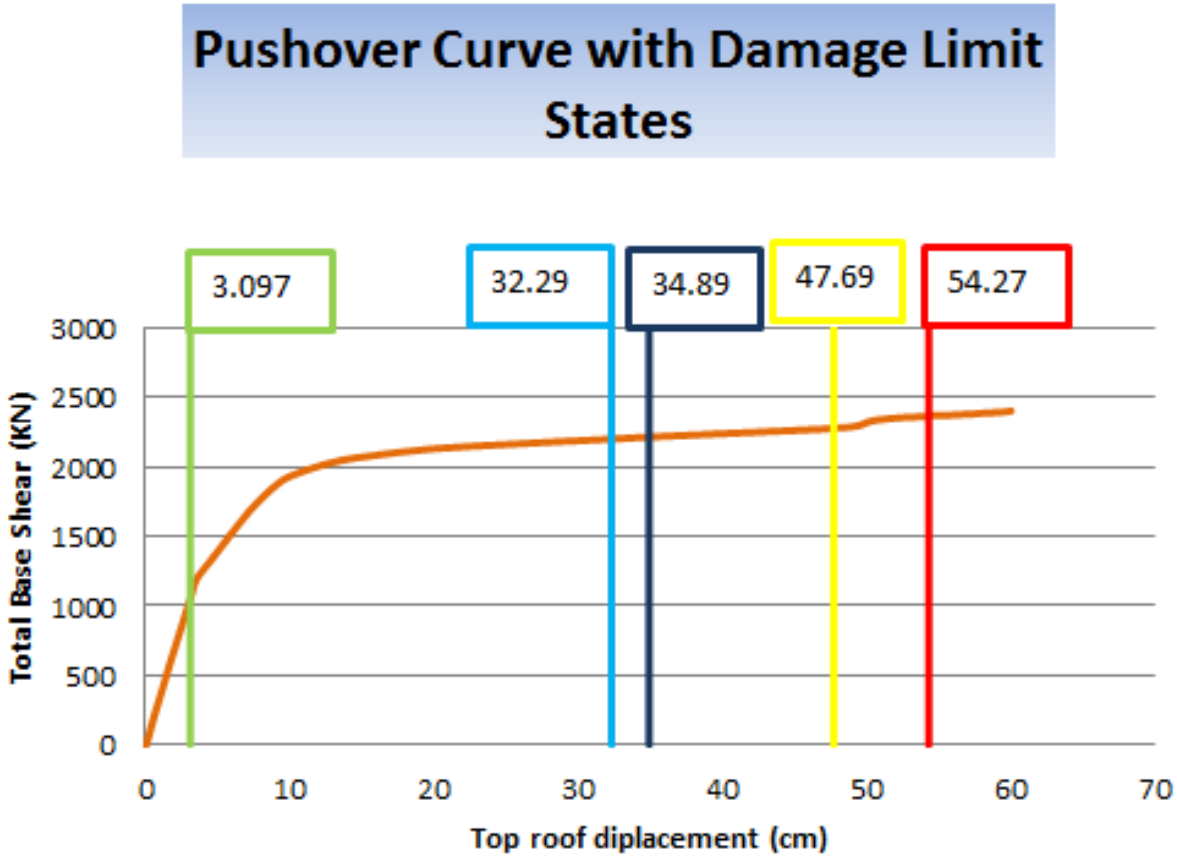

Figure 3.7 Push over curve with defined damage limit state using Hazus criteria

Therefore, by applying the equation 3-16 estimated the value of the standard deviation for each level. So for the value for the yield curve βds = 1, while for the slight = 0.6, moderate = 0.8 and extensive and collapse limit βds = 1. The equation for calculating the probability distribution of fragility curve is given below.

$$P[ds|S_d] = \Phi\left[\frac{1}{\beta_{ds}} \ln\left(\frac{S_d}{\bar{S}_{d,ds}}\right)\right]$$

(Equation 6.1)

Where,

d_s damage limit state .
$S_{d,ds}$ the median value of the spectral shift.
β_{ds} the standard deviation of the natural logarithm of spectral movement for fault level ds.
Φ the function probability distribution normal distribution.
Replacing the equation the values of spectral displacement SD, ds and the standard deviation βds. for each level, the five curves vulnerability, and are given in Figure 6.5.

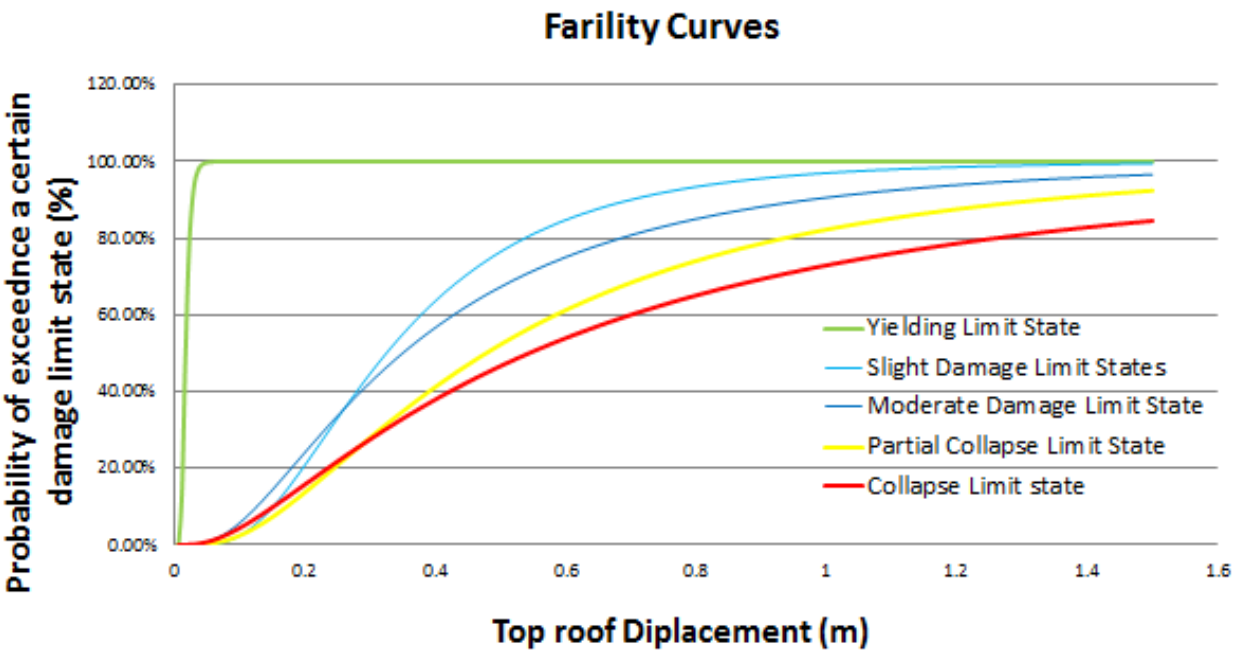

Figure 3.8 Fragility curve of a Frame-wall building.

From the Figure 6.8 it is visible that the uncertainty to attain a limit state is decreasing from yielding 100% to the collapse state 70-75% respectively. The maximum displacement experienced by the structure during non-linear static analysis is 0.5427m that leads to the complete collapse mechanisms of structure.

Chapter 4

4. Ground motions used in this study.

In this study, we used 22 earthquakes subsets having a range in magnitude Mw between 5.6 and 7.6. The minimum fault distance was C/D=0.1 km.

All the near field records are affected by forward directivity effect. Reviewing the earthquakes that account site characteristics and the corresponding displacement of a single degree of freedom (SOF) system provides an expected displacement of a building under referred ground shaking. The details of each earthquake that is recorded location, faulting mechanisms, type of directivity and closest distance are tabulated in table 5.1.

No	LOCATION	DATE	Mw	F/M	STATION	S/C	DIR/TY	C/D	COMP.	SDmax
1	Imperial Valley CA, USA	19/05/1940	6.6	SS	El Centro	SL	B	8.0	180 - 270	26.07 – 36.40
2	Parkfield,CA,USA	27/6/1966	6.0	SS	Cholame Shandon Array 2 (CO2)	SL	F	0.1	65	38.65
					Cholame Shandon Array 5 (CO5)	SL	F	5.2	85 - 355	20.01 - 11.78
					Cholame Shandon Array 8 (CO8)	SL	F	9.2	50 - 320	16.21 - 14.34
					Temblor Station 2 (TMB)	-	F	6.5	205 - 295	10.95 - 7.55
3	San Fernando,CA,USA	9/2/1971	6.7	SS	Pacoima Dam (PCD)	HR	F	3.0	254 - 164	23.38 - 88.53
4	Gazli,USSR	17/5/1976	6.7	RV	Karakyr Point (KAR)	SR	N	3.0	0 - 90	82.29 - 68.15
5	Tabas,Iran	16/9/1978	7.1	RV	Tabas (TAB)	SL	N	1.2	74 - 344	243.73 - 131.32
6	Coyote Lake ,CA,USA	8/6/1979	5.6	SS	Gilroy Array 1 (GA1)	H	F	9.0	230 - 320	1.47 - 2.74
					Gilroy Array 2 (GA2)	R	F	7.2	50 - 140	4.91 - 11.39
					Gilroy Array 3 (GA3)	SL	F	5.1	50 - 140	11.49 - 9.55
					Gilroy Array 4 (GA4)	SL	F	3.5	270 - 360	8.18 - 10.15
					Gilroy Array 6 (GA6)	SL	F	1.2	230 - 320	58.51 - 33.95
					San Martin Coyote Creek (SMCC)	SR	B	0.2	160 - 250	3.37 - 4.81
7	Imperial Valley, CA,USA	15/10/1979	6.4	SS	Aeropurto Mexicall (AEP)	-				
					Agrarias (AGR)	SL	F	0.4	45 – 315	31.14 – 8.73
					El Centro Array 3, Pine Union Schl (E03)	SL	N	0.6	33 – 273	21.89 – 27.79
					El Centro Array 4, Anderson Rd (E04)	SL	F	11.7	140 – 230	54.26 - 55.52
					El Centro Array 5, James Rd (E05)	SL	F	6.0	140 – 230	68.96 - 123.84
					El Centro Array 6, Huston Rd (E06)	SL	F	2.7	140 – 230	112.33 - 127.06
					El Centro Array 7, Imperial Val. Cl (E07)	SL	F	0.3	140 – 230	66.62 - 155.55
					El Centro Array 8, Cruickshank Rd (E08)	SL	F	1.8	140 – 230	65.21 - 117.6
					El Centro Array 10, Hospital (E10)	SL	F	5.0	140 – 230	79.31 - 85.67
					Bonds Corner (BCR)	SL	F	9.6	320 – 50	51.48 - 92.28
					Calexico Fire Station (CXO)	SL	F	2.0	230 – 140	33.94 - 28.93
					Mexicall Casa Flores (MXC)	SL	N	11.0	225 – 315	49.42 - 27.93
					Compuertas (CMP)	SL	N	10.4	0 – 270	11.33 - 14.08
					Meloland Route Overpass (EMO)	SL	B	15.5	15 – 285	12.78 -12.12
					Brawley Airport (BRA)	SL	F	1.2	0 – 270	51.06 - 111.05
					Differential Array-Dogwood Rd (EDA)	SL	F	8.2	225 – 315	31.15 - 56..58
					Post Office,Hotville (HVP)	SL	F	6.3	0 – 270	48.69 - 92.10
						SL	F	6.9	315 - 225	76.50 - 69.72
8	Mexicali Valley, Mexico	9/6/1980	6.4	SS	Cerro Prieto (CPR)	HR	F	6.5	45 - 315	24.49 - 9.04
9	Morgan Hill,CA,USA	24/4/1984	6.2	SS	Anderson Dam,Downstream (AND)	SL	F	2.6	250 – 340	11.80 - 13.32
					Coyote Lake Dam,San Martin (CLD)	SR	F	0.1	195 – 285	16.33-28.51
					Halls Valley (HAL)	SL	B	2.0	150 - 240	4.93-12.64
10	Nahanni, Canada	23/12/1985	6.7	RV	Iverson,NW Territories (SITE 1)	HR	N	9.4	10 – 280	29.04-34.37
					Slide Mountain (SITE2)	HR	N	5.2	240 - 330	13.44-11.72

11	Palm Springs,CA,USA	8/7/1986	6.1	OB	Cabazon Post Office (CAB)	SL	F	6.0	180 – 270	6.44 - 7.05
					Desert Hot Springs (DSP)	SL	N	6.4	0 – 90	15.42 - 9.79
					North Palm Springs Post Office (NPS)	SL	F	4.0	210 – 300	24.95 - 11.03
					Palm Springs Airport (PSA)	-	F	10.8	0 – 90	7.69 - 7.31
					Whitewater Trout Farm (WWT)	SR	F	6.5	180 - 270	11.08 - 7.80
						SL				
						SL				
12	Superstition Hills,CA,USA	24/11/1987	6.4	SS	Parachute Test Site (PTS)	-	F	0.7	225 – 315	89.62 – 51.31
					Superstition Mountain (SSM)	SR	N	5.7	45 – 135	14.47 - 19.76
					Poe Road (POE)	-	N	10.7	270 – 360	24.99 - 28.25
					Kornbloom Poad (KRN)	H	N	17.8	270 – 360	15.60 - 15.15
					Westmorland Fire station (WST)	R	F	13.2	90 – 180	68.58 - 77.22
					El Centro (ELC)	-	F	13.6	0 – 90	95.43 - 103.15
						-				
						SL				
						SL				
13	Loma Prieta,USA	17/10/1989	6.9	OB	Corralitos (COR)	SR	N	2.3	0 – 90	20.77 - 28.73
					Gavilan College Physics Sci. Bldg .(GIL)	SL	N	10.5	67 – 337	12.28 - 13.78
					Gilroy 1-Gavilan Coll. Water Tank (G01)	SR	N	10.1	0 – 90	13.91 - 12.29
					Lexington Dam-Left Abutment (LXD)	SR	F	6.7	0 – 90	33.75 - 42.97
					Los Gatos Presentation Center (LGP)	H	F	3.0	0 – 90	115.24 - 31.58
					Saratoga-Aloha Avenue (STG)	R	F	8.3	0 – 90	30.76 - 72.16
					Gilroy Historic Building (GHB)	SL	F	11.1	90 – 180	21.62 - 10.24
					Capitola Fire Station (CAP)	-	B	15.8	0 – 90	34.12 - 15.82
					Branciforte Drive (BRN)	SL	B	11.5	0 – 90	22.46 - 14.21
						-				
14	Sierra Madre,CA, USA	28/6/1991	5.6	RV	Cogswell Dam (COG)	-	F	9.4	65 – 155	1.90 - 4.72
					Eaton Canyon Park-Altadena (ETN)	SL	F	9.6	0 – 90	7.13 - 2.62
					Mt. Wilson-Caltech Station (MTW)	H	F	11.9	0 – 90	3.32 - 2.57
					San Marino-SW Academy (SNM)	R	F	15.6	0 - 90	2.73 - 2.24
						SL				
15	Erzincan, Turkey	13/3/1992	6.6	SS	Erzincan (ERZ)	SL	F	2.0	0 - 90	56.46 - 71.02
16	Petrolia,CA,USA	25/4/1992	6.9	RV	Cape Mendocino (CAP)	H	F	7.8	0 – 90	73.13 - 36.23
					Petrolia (PGS)	R	F	8.9	0 – 90	30.15 - 50.75
					Fortuna (FOR)	SL	N	13.5	0 – 90	42.75 - 32.34
					Rio Dell (RIO)	SL	N	13.1	270 - 360	35.93 –21.56
						-				
						SR				
						SL				
						-				
						SR				
17	Landers,CA,USA	28/6/1992	7.3	SS	Joshua Tree-Fire Station (JSH)	SL	B	11.6	0 – 90	19.09 - 35.07
					Lucerne Valley (LUC)	SL	F	1.1	0 – 90	36.74 – 156.90
18	Northridge,CA, USA	17/1/1994	6.7	RV	Jensen Filtration Plant (JFA)	SL	F	5.2	22 – 292	109.88 - 72.43
					Pacoima Kagel Canyon (PKC)	H	N	7.4	90 – 360	43.64 - 21.30
					Newhall,LA Country Fire Station (NWH)	R	F	6.5	90 – 360	38.92 - 60.13
					Arleta,Nordhoff Fire Station (SFY)	SL	N	8.0	90 – 360	21.31 - 29.37
					Pacoima Dam-Downstream (PCD)	SL	F	7.2	175 – 265	17.84 - 16.53
					Rinaldi Receiving Station (RRS)	H	F	6.0	318 – 228	66.95 - 58.09
					Sylmar Converter Station (SCG)	R	F	5.1	52 – 142	131.88 - 87.25
					Sylmar Converter Station East (SCH)	SL	F	5.0	11 – 281	97.63 - 69.41
					Sepulveda Veterans Hospital (VSP)	SL	F	8.0	270 – 360	29.70 - 55.36
					Los Angeles Dam (LDW)	SL	F	5.6	334 – 64	48.01 - 51.30
					Sylmar Country Hospital (SYH)	SL	F	5.5	90 – 360	59.99 - 77.68
					Canoga Park Epiphany Church (CPC)	SL	N	13.7	196 – 106	47.26 - 26.13
					Canyon Country (CCY)	SL	F	12.9	0 – 270	31.60 - 19.65
					LA Fire Station 108 (LF5)	SL	B	19.2	35 – 125	15.00 - 10.04
					LA Fire Station 99 (LF6)	SL	B	17.3	9 – 279	34.00 - 36.96
					LA UCLS Grounds (ULA)	SL	B	19.9	90 – 360	11.59 - 26.65
					LA Westlake School (LWS)	SL	B	19.0	0 – 90	8.00 - 10.14
					Newhall,Pico Canyon (NWS)	SL	F	5.3	46 – 316	83.66 - 47.60
					North Hollywood Coldwater Can. (NHW)	SL	N	11.8	270 – 180	26.10 - 29.72
					Northridge White Oak Cov.Church (NRG)	SL	F	11.5	90 – 180	53.81 - 28.39
						SL	N	12.4	0 – 90	20.12 - 17.26
						SL	N	9.3	0 – 90	21.38 - 29.07
						SL	B	14.8	90 – 360	38.62 - 42.64
						SL				
						SL				
						-				

					Simi Valley (SMI) Sun Valley Grace Comm.. Church (SVG) Tarzana Nursery (TAR)	SR				
19	Hanshin (Kobe), Japan	17/1/1995	6.8	SS	Kobe University (KBU) Kobe Port Island,Surface (KPI) Takarazuka (TAZ) Takatori (TAK) Nishi-Akashi (NIS)	H R SL SL SL SL	F F F F N	0.7 3.2 0.4 1.1 10.5	0 – 90 0 – 90 0 – 90 0 – 90 0 – 90	41.58 - 24.14 77.52 - 67.44 50.88 - 41.71 114.89 - 95.42 28.13 - 32.22
20	Izmit, Turkey	17/8/1999	7.4	SS	Arcelik Arge Lab (ARC) Yarimca Petkim (YPT)	SR SL	F F	14.0 2.6	0 – 270 0 - 270	36.13 - 78.02 107.42 - 145.02
21	Chi-Chi,Taiwan	20/9/1999	7.6	RV	CHY024 CHY028 CHY101 TCU049 TCU051 TCU052 TCU053 TCU054 TCU055 TCU065 TCU067 TCU068 TCU071 TCU072 TCU074 TCU075 TCU076 TCU078 TCU082 TCU087 TCU089 TCU101 TCU102 TCU103 TCU116 TCU120 TCU122 TCU129	SL SL SL SL SL SL SL SL SL SL SL SL SL SL SL SL SL SL SL SR SR SL SL SL SL SR SL SL	F N F F F F F F F F F F F F F F F F F F F F F F F F F F	7.7 2.3 7.7 2.7 6.9 0.8 4.6 4.7 6.5 0.1 0.2 0.2 4.1 6.8 11.4 0.6 2.3 5.4 5.0 5.8 6.2 1.5 0.6 4.4 11.5 6.1 8.5 1.5	90 – 360 90 – 360 90 – 360 90 - 360 90 – 360 90 – 360 90 – 360 90 – 360 90 - 360 90 – 360 90 – 360 90 – 360 90 – 360 90 - 360 90 – 360 90 – 360 90 – 360 90 – 360 90 - 360 90 – 360 90 – 360 90 – 360 90 – 360 90 - 360 90 – 360 90 – 360 90 - 360 90 – 360	96.88 - 111.29 52.39 - 53.66 107.61 - 223.06 152.55 – 150.49 121.08 - 164.26 338.74 – 496.22 130.10 – 166.76 140.54 – 154.95 40.25 – 135.96 248.53 - 182.93 188.42 – 110.20 597.22 – 768.98 49.43 – 108.32 101.14 – 96.47 55.73 - 46.24 144.31 - 109.91 69.75 – 69.84 69.18 – 24.59 148.13 – 140.59 158.30 – 83.87 64.53 – 51.24 165.26 - 122.05 199.98 - 123.92 180.67 - 75.22 90.14 - 97.47 90.55 - 125.74 115.11 - 105.40 125.95 - 73.84
22	Duzce, Turkey	12/11/1999	7.1	OB	Duzce (DZC) Bolu (BOL)	SL SL	N F	8.3 19.9	180 – 270 0 - 90	145.65 - 159.53 49.54 - 30.70

Table 2 Near-field ground motion having different site characteristics

Where:

M_w: Magnitude of the Earthquake

F/M: Fault Mechanism: SS-Strike slip, RV-Reverse, OB-Obverse.

S/C-Site Code: HR-hard rock, SR-sedimentary and conglomerate rock, SL-soil and alluvium.

DIR/TY: Directivity: F-forward, N-neutral, B-backward.

C/D: Closest distance:

Normal distance from fault trace for events:1, 4, 5, 7, 8, 9, 10, 11, 15, 20, 22, 23, 25

Normal distance from fault plane for events: 12, 13, 14, 16, 17, 19, 21, 24

Distance from point source (i.e. hypo central distance): 2, 3

COMP: location of recorded station

SD_{max}: Maximum Spectral Displacement

Chapter 5

5. Earthquakes Risk Estimation Results on the structure.

5.1 Methodology.

Results arising from applying the "near-fault" ground motion record to the building using SAP2000 are obtained; these results are the maximum top floor displacement that the building undergoes due to that certain ground motion record.

A non-linear Direct Integration method was employed with an input parameter of time step size 0.01 sec, a total number of output time step 3000 to 6000 (30 sec to 60 sec) depend upon the length of the accelerogram. To consider a geometric non-linearity, P-Delta plus large displacement effects are also taken into account. All accelerograms are applied in positive y-direction (U2) and a damping near to 5 % is used in this analysis.

The displacement value gives an indication for at which structural damage state the building will suffer when subjected to such a ground motion, these results are given in a tabulated form for each earthquake showing the maximum displacement and the corresponding predefined limit damage state.

Moreover, applying these results to the fragility curves shows us the probability of exceeding a certain damage limit state under that certain ground motion record.

5.2 Results.

The tabulated results are based on the location, displacement, type of directivity, distance from the fault and the five damage levels attained by the model under the seismic records.

For a particular maximum displacement which is smaller than the average displacement of the vulnerability curve for the yield (0.030978m), the limit state is given the designation non-yield For a particular maximum displacement which is larger than the average displacement of the vulnerability curve for the yield (0.030978m), but less than the slight limit state displacement value (0.3239), it is given the designation yield (green). For a maximum displacement value located between the slight Disp. Limit Value (0.0309m) and the moderate limit value (0.3489) , it is categorized as (light blue), and designated as a slight damage state. Accordingly, the maximum displacement between the vulnerability curves of moderate limit state (0.3489m) and Partial collapse limit state (0.4769), characterized as moderate state of damage. The displacement between the Partial Collapse (0.4769 m) and extensive damage (0.5427 m), would be classified as partial collapse (protected life) having the yellow color. And the displacements that are more than complete damage limit state (0.5427 m), characterized as complete collapse of the building having the red color indication.

5.2.1 IMPERIAL VALLEY CA, USA 1940

Location	Mw	Dir/Ty	C/D	Displacement	Limit State
ELC 180-1	6.6	B	8.0	0.231	SLIGHT
ELC 270-1				0.1733	SLIGHT

Table 3 Table of Displacements and damage levels for recording station in Imperial Valley, USA 1940.

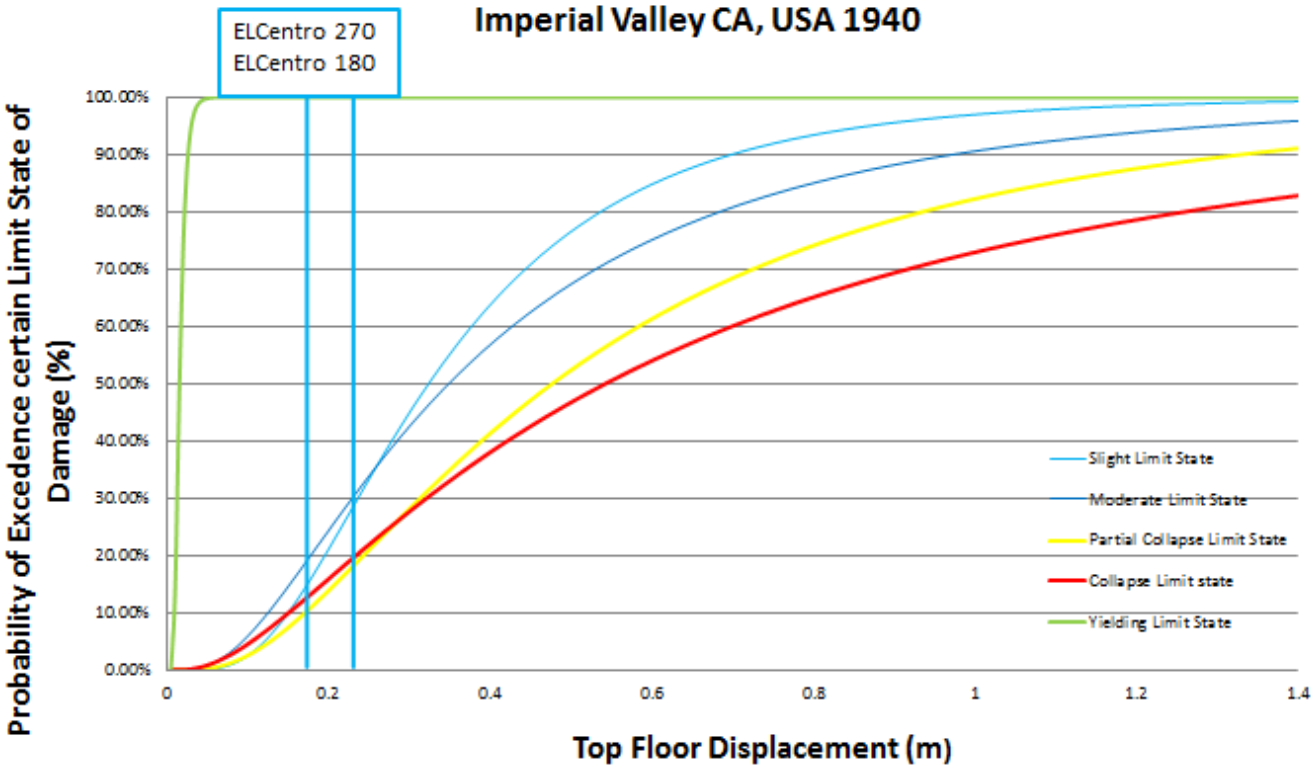

Figure 5.1 Fragility curves showing damage limit state for recording station in Imperial Valley, USA, 1940.

Imperial Valley earthquake from 1940, had a magnitude of Mw=6.6. The stations exhibit a backward directivity. The results place our building in the slight damage state area. This is the result of the big distance of the station from the rift.

5.2.2 IMPERIAL VALLEY CA, USA 1979

Location	Mw	Dir/Ty	C/D	Displacement (m)	Limit State
AEP 045-1	6.4	F	0.4	0.2521	YIELD
AEP 315-1				0.0768	YIELD
AGR 033-1		N	0.6	0.1944	YIELD
AGR 273-1				0.2476	YIELD
E03 140-1		F	11.7	0.3184	YIELD
E03 230-1				0.1612	YIELD
E04 140-1		F	6.0	0.2783	YIELD
E04 230-1				0.4255	MODERATE
E05 140-1		F	2.7	0.3889	SLIGHT
E05 230-1				0.6055	COLLAPSE
E06 140-1		F	0.3	0.4006	MODERATE
E06 230-1				0.5789	COLLAPSE
E07 140-1		F	1.8	0.2954	YIELD
E07 230-1				0.4822	PARTIAL COLLAPSE
E08 140-1		F	5	0.3112	YIELD
E08 230-1				0.2891	YIELD
E10 320-1		F	9.6	0.2802	YIELD
E10 050-1				0.3141	YIELD
BCR 230-1		F	2.0	0.1683	YIELD
BCR 140-1				0.2702	YIELD
CXO 225-1		N	11.0	0.071	YIELD
CXO 315-1				0.06947	YIELD
MXC 000-1		N	10.4	0.09511	YIELD
MXC 270-1				0.1383	YIELD
CMP 015-1		B	15.5	0.0452	YIELD
CMP 285-1				0.03571	YIELD
EMO 000-1		F	1.2	0.3724	MODERATE
EMO 270-1				0.6604	COLLAPSE
BRA 225-1		F	8.2	0.155	YIELD
BRA 315-1				0.2157	YIELD
EDA 000-1		F	6.3	0.2548	YIELD
EDA 270-1				0.394	MODERATE
HVP 315-1		F	6.9	0.2488	YIELD
HVP 225-1				0.252	YIELD

Table 4 Table of Displacements and damage levels for recording station in Imperial Valley, USA 1979.

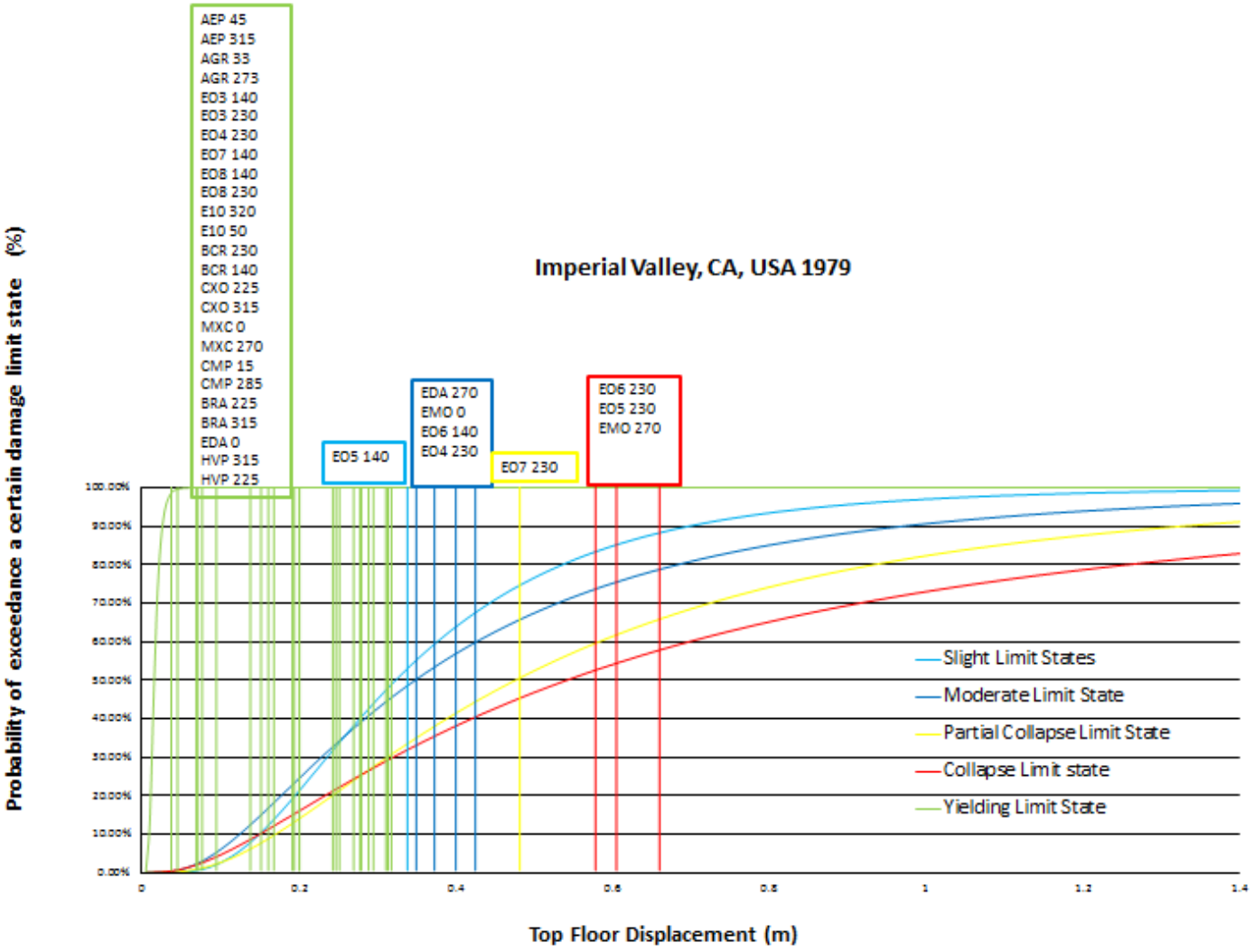

Figure 5.2 Curves showing damage limit state for recording station in Imperial Valley, USA, 1979.

The earthquake in the Imperial Valley from 15-10-1979 had a magnitude of 6.4. Most of the stations showed forward directivity, but AGR, CXO and MXC showed neutral directivity. the displacement that put the building in the collapse damage state such as E05, E06, EMO, are influenced by the fact that the stations are very near the rift and a have forward directivity. Below is given the Map 8.1 for a better understanding of the diversity of displacement.

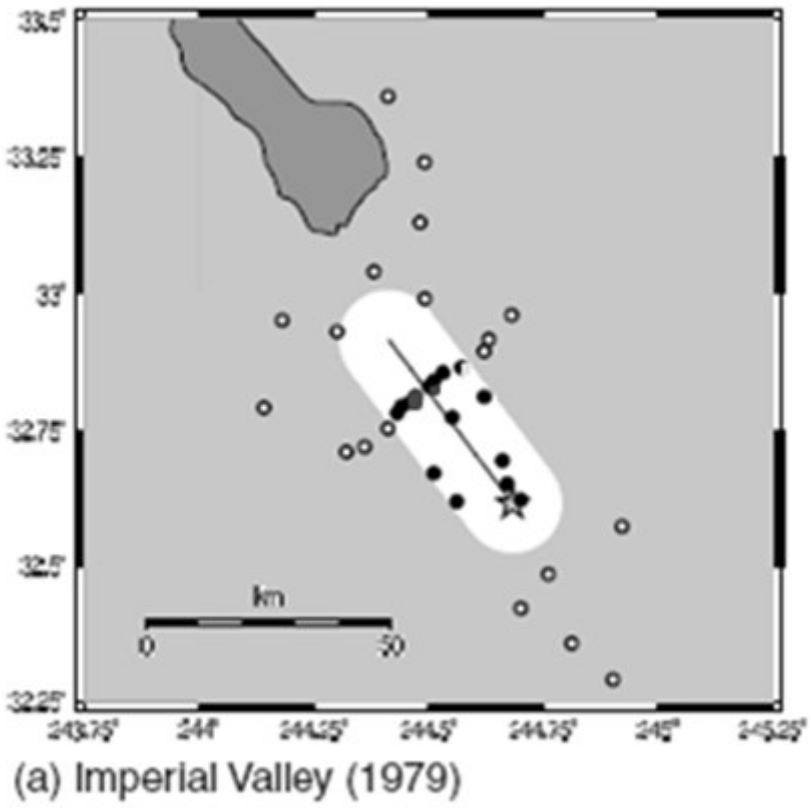

Figure 5.3 Map of stations in relation to the rupture of the earthquake area in IMPERIAL Valley, CA, USA, 1979.

5.2.3 IZMIT, TURKEY

Location	Mw	Dir/Ty	C/D	Displacement (m)	Limit State
ARC 000-1	7.4	F	14	0.5695	COLLAPSE
ARC 090-1				0.1145	YIELD
YPT 000-1		F	2.6	0.2949	YIELD
YPT 090-1				0.3243	SLIGHT

Table 5 Table of Displacements and damage levels for recording station in Izmit, Turkey.

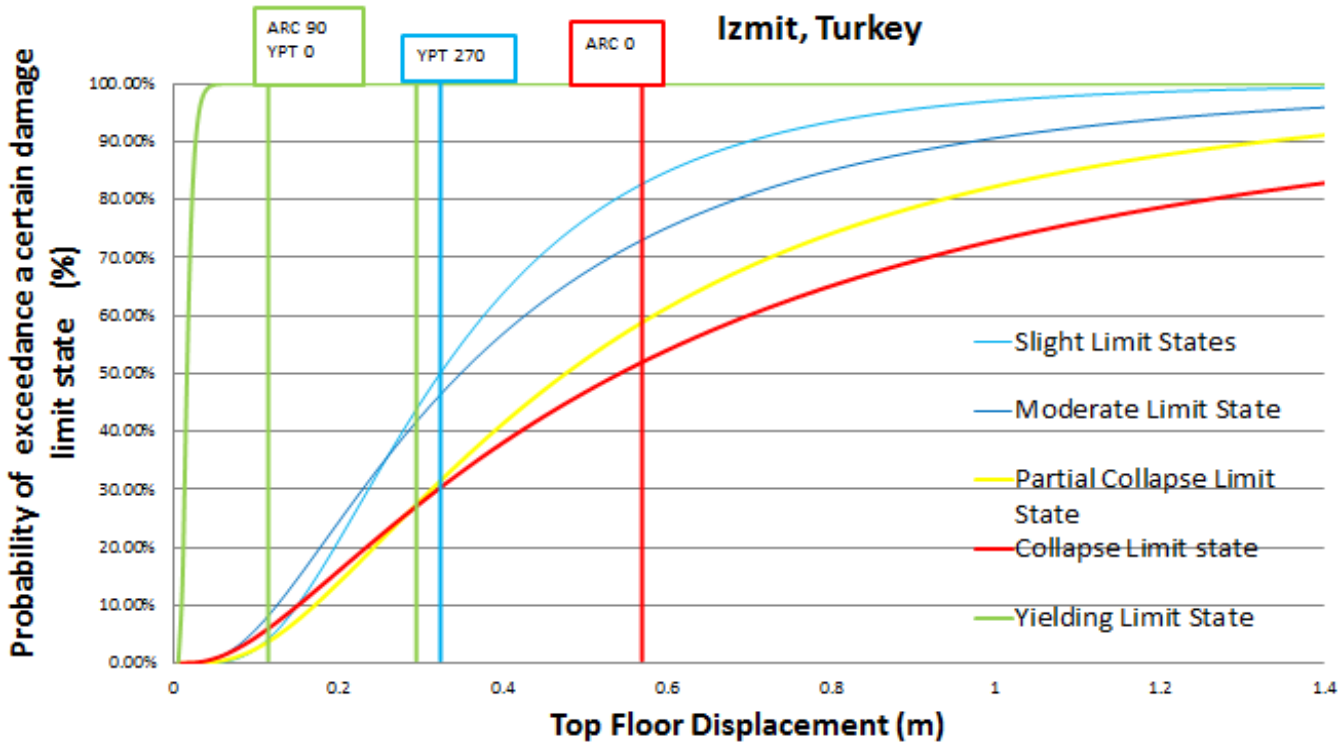

Figure 5.4 Fragility curves showing damage limit state for recording station in Izmit, Turkey.

The Izmit earthquake had a magnitude of 7.4 on Richter's scale. It was recorded by 2 stations ARC and YPT. Both of them showed a forward directivity pattern, but ARC was at a far distance from the trace of the fault, 14 km, even though it forces the building to collapse.

5.2.4 LANDERS, CA, USA

Location	Mw	Dir/Ty	C/D	Displacement (m)	Limit State
JSH 000-1	7.3	B	11.6	0.1155	YIELD
JSH 090-1				0.1834	YIELD
LUC 000-1		F	1.1	0.1588	YIELD
LUC090-1				0.6247	COLLAPSE

Table 6 Table of Displacement and damage levels for recording station in Landers, CA, USA.

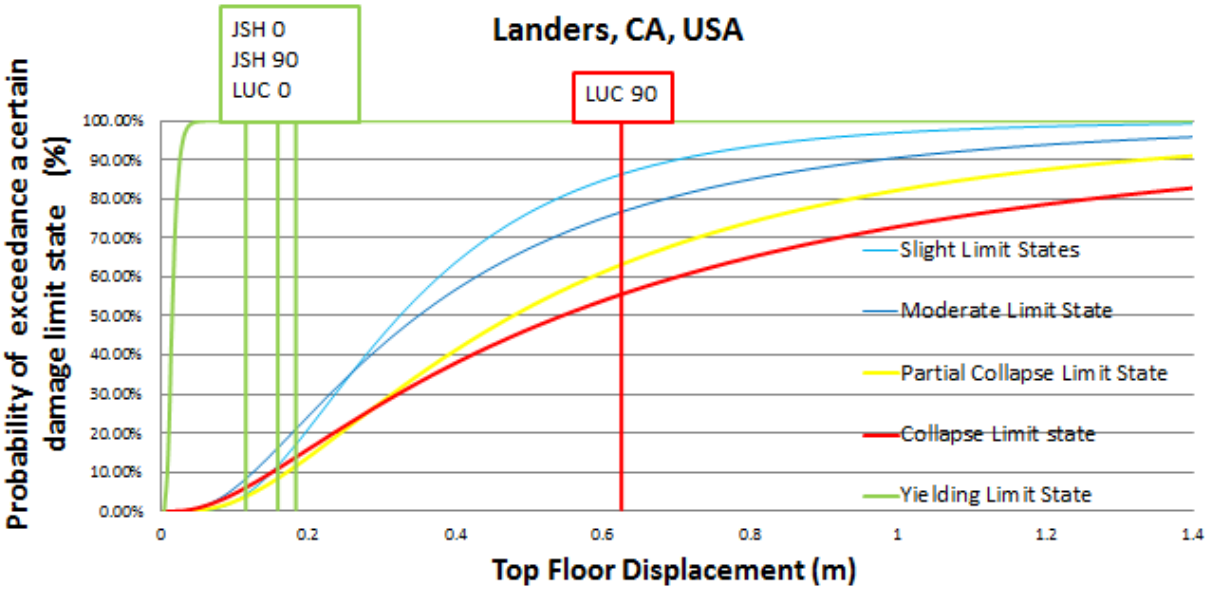

Figure 5.5 Fragility curves showing damage limit state for recording station in Landers, USA.

The earthquake from Landers, had a magnitude of 7.3 on Richter's scale. The JSH station received backward directivity and is at far distance from the trace of the fault (11.6 km) as a consequence the building lies in the yielding area. In contrast, the LUC station showed a pulse nature and also a short distance from the trace of the rift (1,1 km) played significant role in the results, resulting in building collapse. The map below shows the rupture and the locations of stations. Even if the earthquake magnitude was great and showed a forward directivity, it seems that the distance of the rift played an important role in the building's behavior.

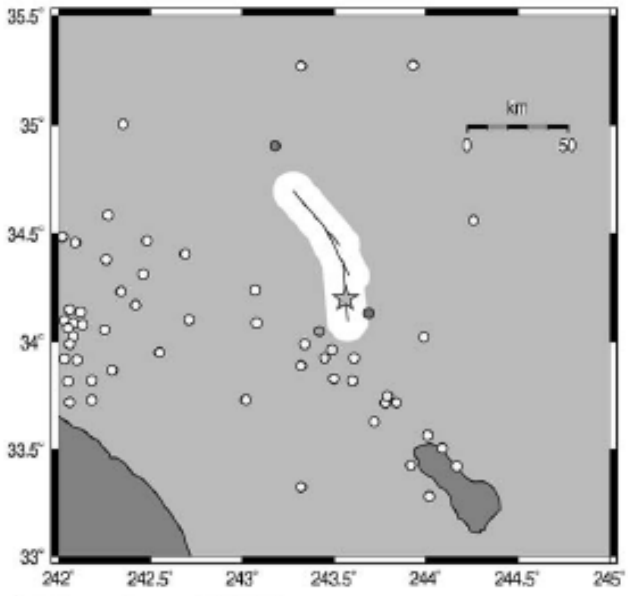

Figure 5.6 Focus earthquake LANDERS, CA, USA (indicated by the asterisk), recording stations positions**.**

5.2.5 LOMA PRIETA, USA

Location	Mw	Dir/Ty	C/D	Displacement (m)	Limit State
COR 000-1	6.3	N	2.3	0.1929	YIELD
COR 090-1				0.1686	YIELD
GIL 067-1		N	10.5	0.1091	YIELD
GIL 337-1				0.07021	YIELD
G01 000-1		N	10.1	0.08572	YIELD
G01 090-1				0.1236	YIELD
LGP 000-1		F	3.0	0.6772	COLLAPSE
LGP 090-1				0.2634	YIELD
STG 000-1		F	8.3	0.281	YIELD
STG 090-1				0.2057	YIELD
GHB 090-1		F	11.1	0.2264	YIELD
GHB 180-1				0.1076	YIELD
CAP 000-1		B	15.8	0.1471	YIELD
CAP 090-1				0.1025	YIELD
BRN 000-1		B	11.5	0.1758	YIELD
BRN 090-1				0.08594	YIELD

Table 7 Table of Displacements and damage levels for recording station in Loma Prieta, USA.

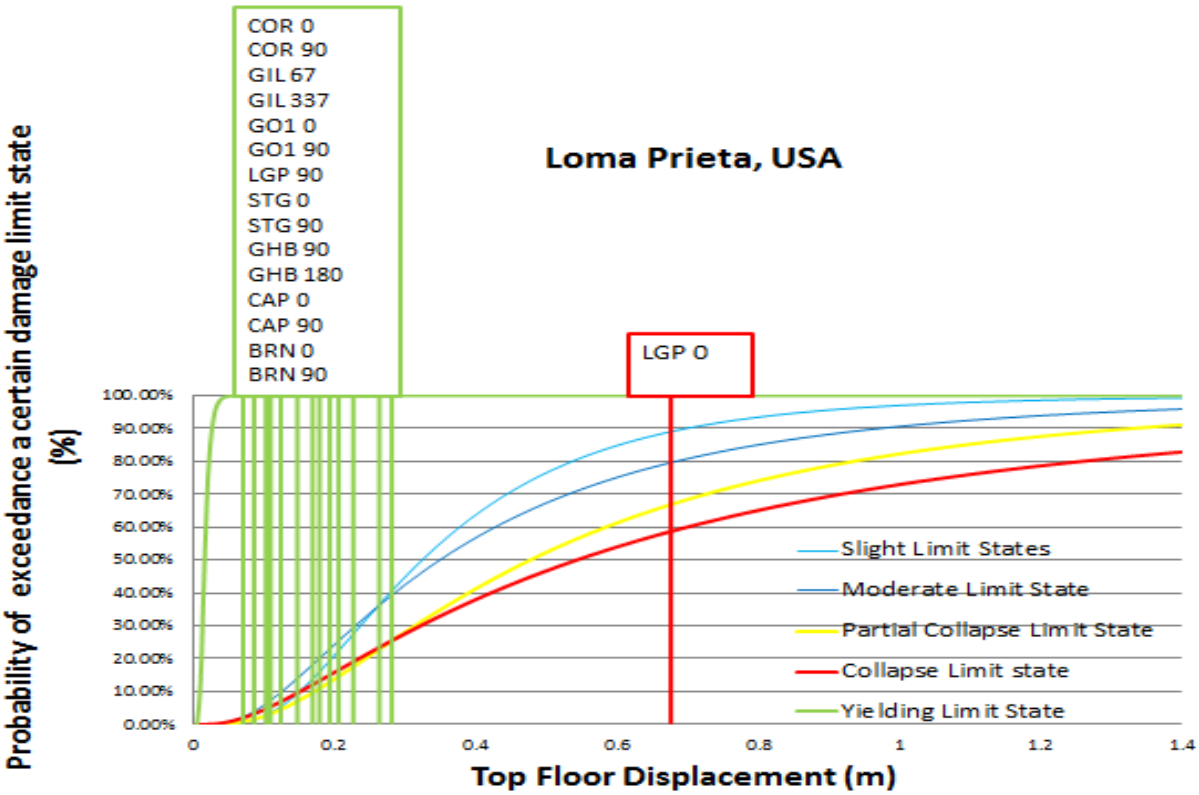

Figure 5.7 Fragility curves showing damage limit state for recording station in Loma Prieta.

The Loma Prieta earthquake had a magnitude of 6.9 on Richter's scale. The displacement provided by the recordings places our building mostly in the yield zone. LGP station shows a forward directivity an small distance from the surface of the rift (3 Km) . Other recordings that have neutral directivity or backward directivity recorded at relatively a big distance of the rift.

5.2.6 MEXICALI VALLEY, MEXICO

Location	Mw	Dir/Ty	C/D	Displacement (m)	Limit State
CPR 045-1	6.4	F	6.5	0.4827	PARTIAL COLLAPSE
CPR 315-1			6.5	0.3307	SLIGHT

Table 8 Table of Displacements and damage levels for recording station in Mexicali Valley, Mexico.

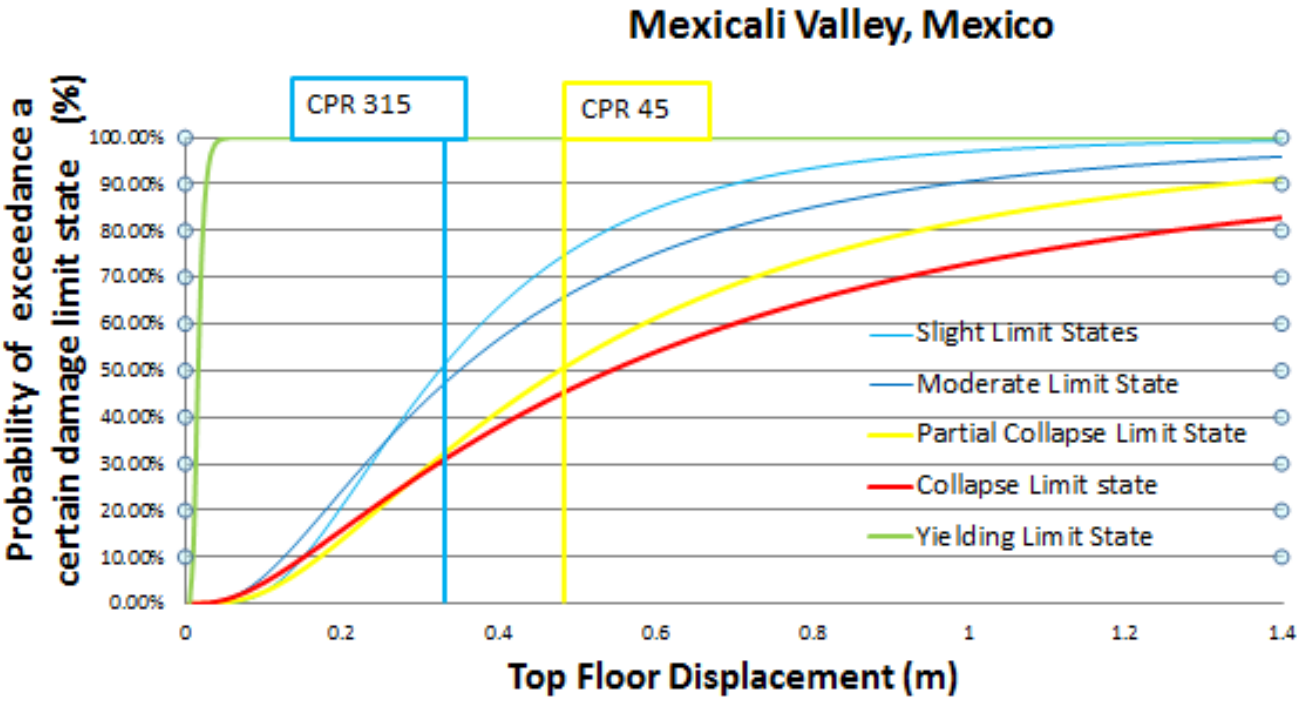

Figure 5.8 Fragility curves showing damage limit state for recording station in Mexicali Valley.

Mexicali Valley earthquake had a magnitude of 6.4 on Richter's scale, showing a forward directivity. The recording for CPR 45 puts building in the partial collapse zone Even if the earthquake magnitude was great and showed a forward directivity; it seems that the pulse amplitude played an important role in the building's behavior.

5.2.7 MORGAN HILL, CA, USA

Location	Mw	Dir/Ty	C/D	Displacement (m)	Limit State
AND 250-1	6.2	F	2.6	0.08687	YIELD
AND 340-1				0.09897	YIELD
CLD 195-1		F	0.1	0.1478	YIELD
CLD 285-1				0.2477	YIELD
HAL 150-1		B	2.0	0.04385	YIELD
HAL 240-1				0.1455	YIELD

Table 9 Table of Displacements and damage levels for recording station in Morgan Hill, USA.

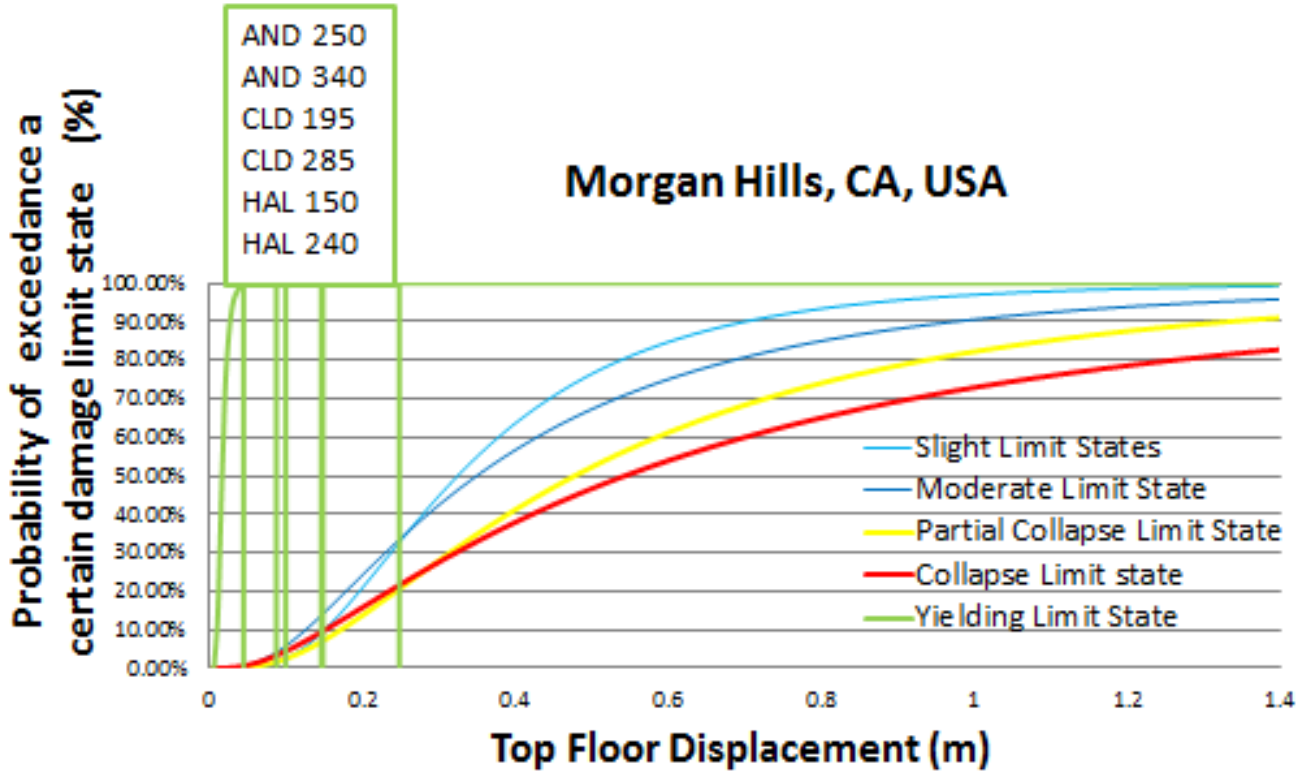

Figure 5.9 Fragility curves showing damage limit state for recording station in Morgan Hill.

Morgan Hill earthquake had a magnitude of 6.2 on Richter's scale. The epicenter of the quake was located near Mount Hamilton in the Diablo Range of the California Coast Ranges, although nearby communities, including Morgan Hill did not suffered serious damage. Recordings revealed that the building maintained a yielded area.

5.2.8 NAHANNI, CANADA

Location	Mw	Dir/Ty	C/D	Displacement (m)	Limit State
SITE1 010-1	6.7	N	9.4	0.1232	YIELD
SITE1 280-1				0.2046	YIELD
SITE2 240-1		N	5.2	0.09321	YIELD
SITE2 330-1				0.1237	YIELD

Table 10 Table of Displacements and damage levels for recording station in Nahanni, Canada.

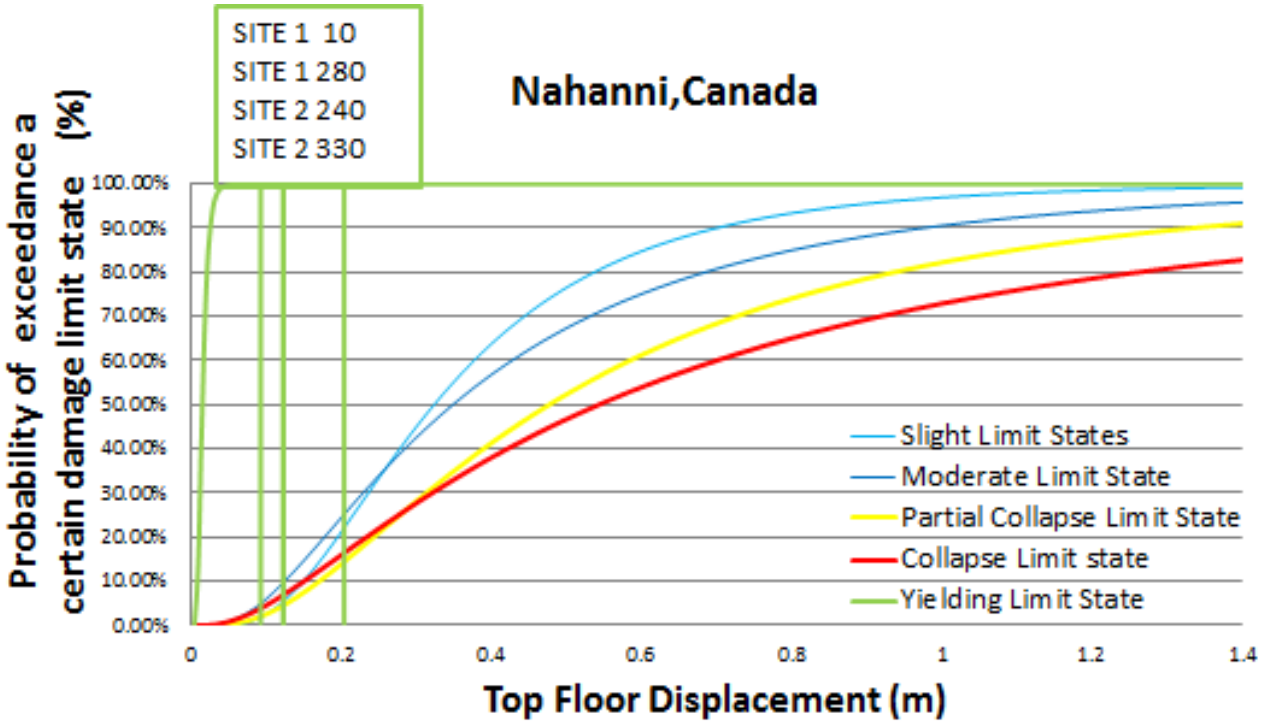

Figure 5.10 Fragility curves showing damage limit state for recording station in Nahanni River, Canada.

The earthquake in the South Nahanni River in Canada had a seismicity of 6.7 on Richter's scale but with neutral directivity. Both the stations have maintained the building damage state at the yielded zone with small difference between the displacements. The neutral directivity, the distance from the surface of the epicenter and the intensity of the earthquake affects the results.

5.2.9 PALM SPRINGS, CA, USA

Location	Mw	Dir/Ty	C/D	Displacement (m)	Limit State
CAB 180-1	6.1	F	6.0	0.04894	YIELD
CAB 270-1				0.05459	YIELD
DSP 000-1		N	6.4	0.1603	YIELD
DSP 090-1				0.0899	YIELD
NPS 210-1		F	4.0	0.3074	YIELD
NPS 300-1				0.09457	YIELD
PSA 000-1		F	10.8	0.05885	YIELD
PSA 090-1				0.05447	YIELD
WWT 180-1		F	6.5	0.1229	YIELD
WWT 270-1				0.07498	YIELD

Table 11 Table of Displacements and damage levels for recording station in Palm Springs, USA.

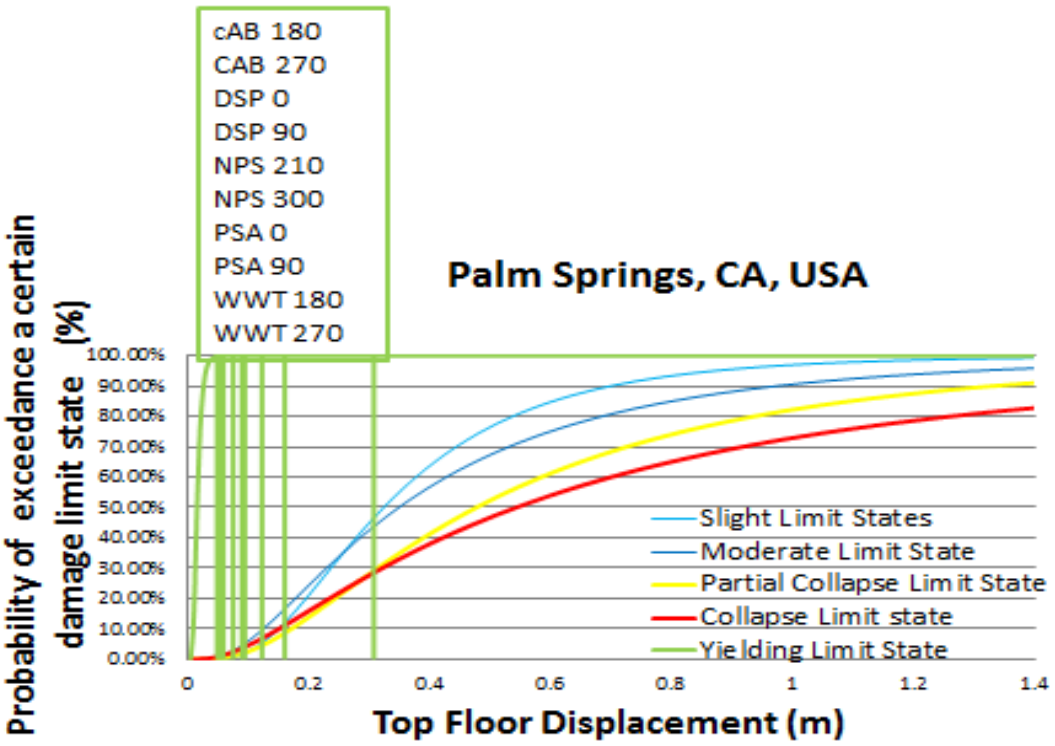

Figure 5.11 Fragility curves showing damage limit state for recording station in Palm Springs.

The Palm Spring earthquake had a magnitude of 6.1 on Richter's scale. The stations revealed a forward directivity except the station DSP, which exhibits a neutral directivity. The results revealed that the NPS station at the distance of 4 km from the rift, places, the building in the upper limit of the yield zone. The rest of the stations place the building in the start of the yielding zone, with an average distance from the rift ranges from 6 to 11 km.

5.2.10 SUPERSTITION HILLS, CA, USA

Location	Mw	Dir/Ty	C/D	Displacement (m)	Limit State
PTS 225-1	6.4	F	0.7	0.52	P.COLLAPSE
PTS 315-1				0.32	MODERATE
SSM 045-1		N	5.7	0.1299	YIELD
SSM 135-1				0.09692	YIELD
POE 270-1		N	10.7	0.1967	YIELD
POE 270-1				0.2085	YIELD
KRN 270-1		N	17.8	0.1466	YIELD
KRN 360-1				0.1581	YIELD
WST 090-1		F	13.2	0.1285	YIELD
WST 180-1				0.1611	YIELD
ELC 000-1		F	13.6	0.2239	YIELD
ELC 090-1				0.3452	SLIGHT

Table 12 Table of Displacements and damage levels for recording station in Superstition Hills.

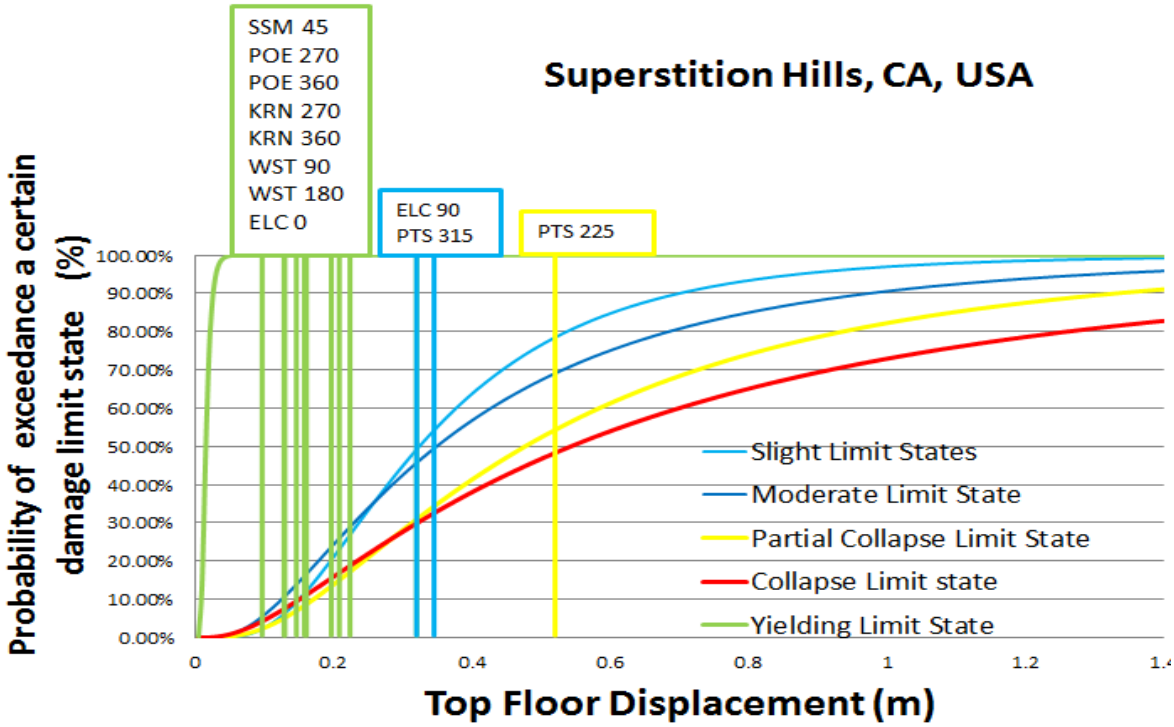

Figure 5.12 Fragility curves showing damage limit state for recording station in Superstition Hills.

The Superstition Hills Earthquake has a magnitude of 6.4 on Richter's scale. The recording stations have the neutral or forward directivity. A special case is PTS. The recordings put the building in the moderate and partial collapsed zone for both directions, mainly because of the forward directivity plus the small distance of the station with the rift (0.7 Km). The other results are placing the building in the yielding zone, until slight damage one.

5.2.11 TABAS, IRAN

Location	Mw	Dir/Ty	C/D	Displacement (m)	Limit State
TAB 074-1	7.1	N	1.2	0.5497	COLLAPSE
TAB 344-1				0.4625	P.COLLAPSE

Table 13 Table of Displacements and damage levels for recording station in Tabas, Iran.

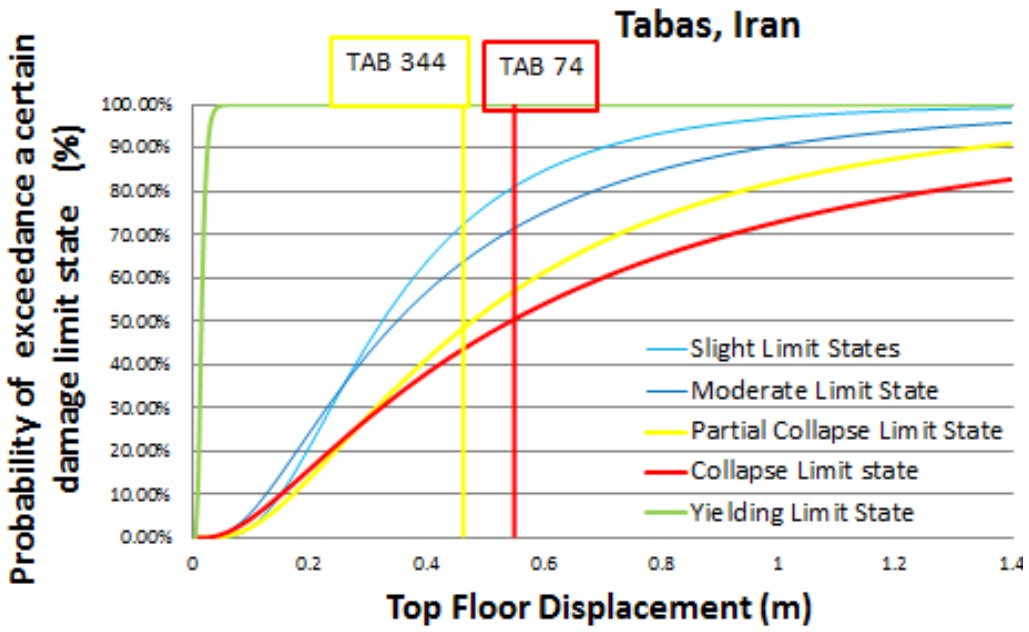

Figure 5.13 Fragility curves showing damage limit state for recording station in Tabas, Iran

The earthquake in Tabas had a magnitude of 7.1; The TAB record gave a top displacement of building places it in the Partial Collapse and Collapse zone. A very small distance of the station from the trace of the rift (1.2 Km), but the directivity was neutral contributed to this result. It must be the distance and the intensity of the EQs which cause the building to be in these two damage states.

5.2.12 SAN FERNANDO, CA, USA

Location	Mw	Dir/Ty	C/D	Displacement (m)	Limit State
PCD 164-1	6.7	F	3.0	0.476	PARTIAL COLLAPSE
PCD 254-1				0.1946	YIELD

Table 14 Table of Displacements and damage levels for recording station in San Francisco, USA.

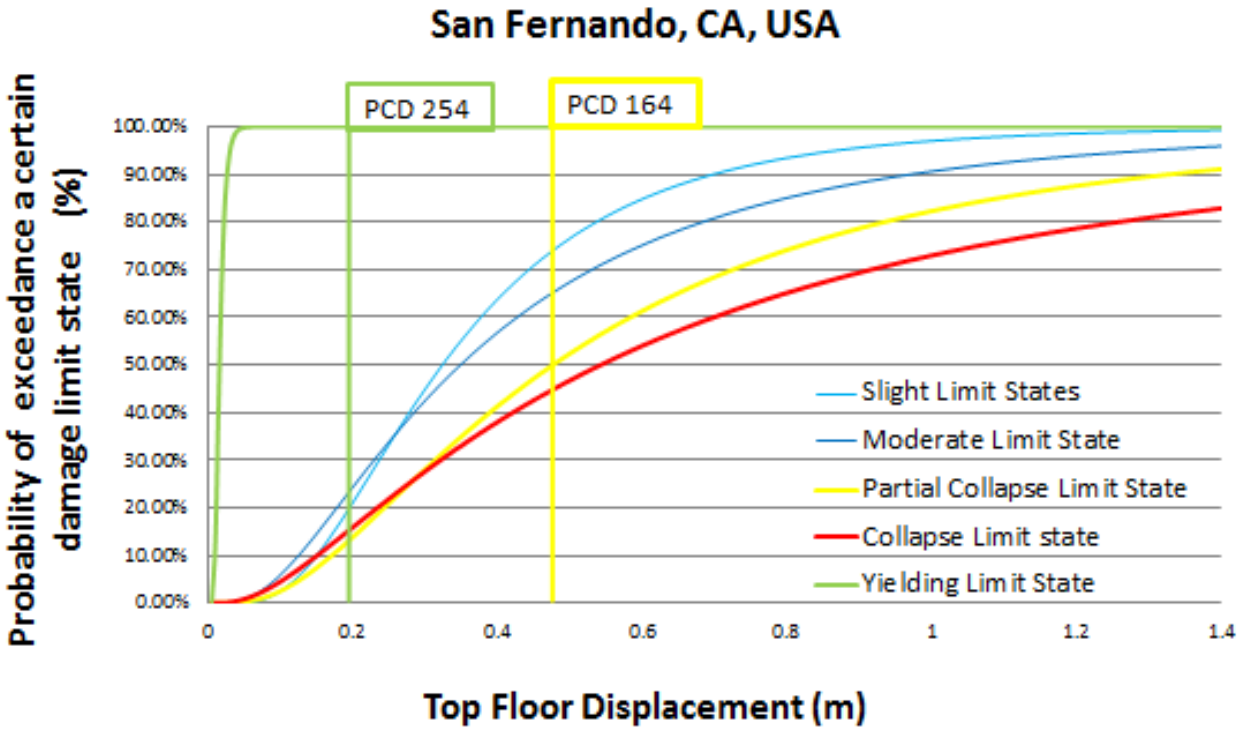

Figure 5.14 Fragility curves showing damage limit state for recording station in San Francisco.

The earthquake in San Fernando had a magnitude of 6.7 on Richter's scale, forward directivity, and the distance from the trace of the fault is 3 km, also the seismic intensity high The record PCD 254 gave displacement that just put the building in the yield zone, while the other record PCD-164 pushes the building to suffer a partial collapse damage state.

5.2.13 SIERRA MADRE, CA, USA

Location	Mw	Dir/Ty	C/D	Displacement (m)	Limit State
COG 065-1	5.6	F	9.4	0.1768	YIELD
COG 155-1				0.04544	YIELD
ETN 000-1		F	9.6	0.06537	YIELD
ETN 090-1				0.01824	NON-YIELD
MTW 000-1		F	11.9	0.03122	YIELD
MTW 090-1				0.01932	NON-YIELD
SNM 000-1		F	15.6	0.02286	NON-YIELD
SNM 090-1				0.02225	NON-YIELD

Table 15 Table of Displacements and damage levels for recording station in Sierra Madre, USA.

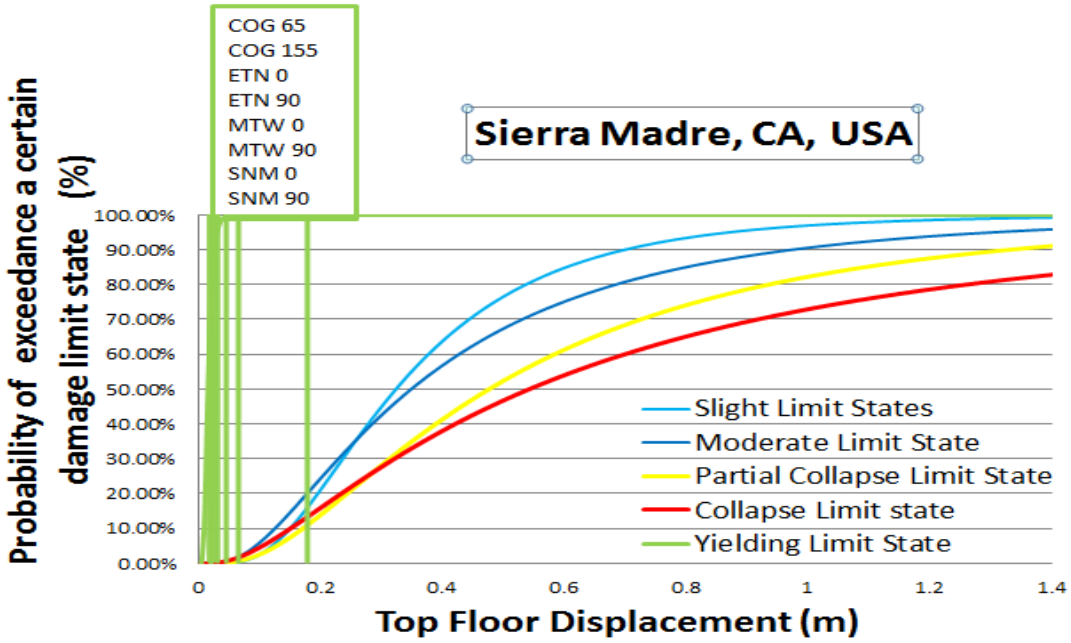

Figure 5.15 Fragility curves showing damage limit state for recording station in Sierra Madre.

The earthquake from Sierra Madre, California had a magnitude of 5.6 on the Richter scale. All the seismic excitations maintained the building in the yield and non-yielding zones only recording small displacements. Although, in other words, that the seismic triggers showed a forward directivity, the great distance of stations from the surface of the fault in combinations with the small magnitude of the earthquake, justifies the low values od peak displacement of the building.

5.2.14 PARKFIELD, CA, USA

Location	Mw	Dir/Ty	C/D	Displacement (m)	Limit State
CO2 065-1	6.0	F	0.1	0.3675	MODERATE
CO5 085-1		F	5.2	0.1243	YIELD
CO5 355-1				0.05648	YIELD
CO8 050-1		F	9.2	0.04539	YIELD
CO8 320-1				0.04917	YIELD
TMB 205-1		F	6.5	0.03906	YIELD
TMB 295-1				0.05707	YIELD

Table 16 Table of Displacements and damage levels for recording station in Park field, USA.

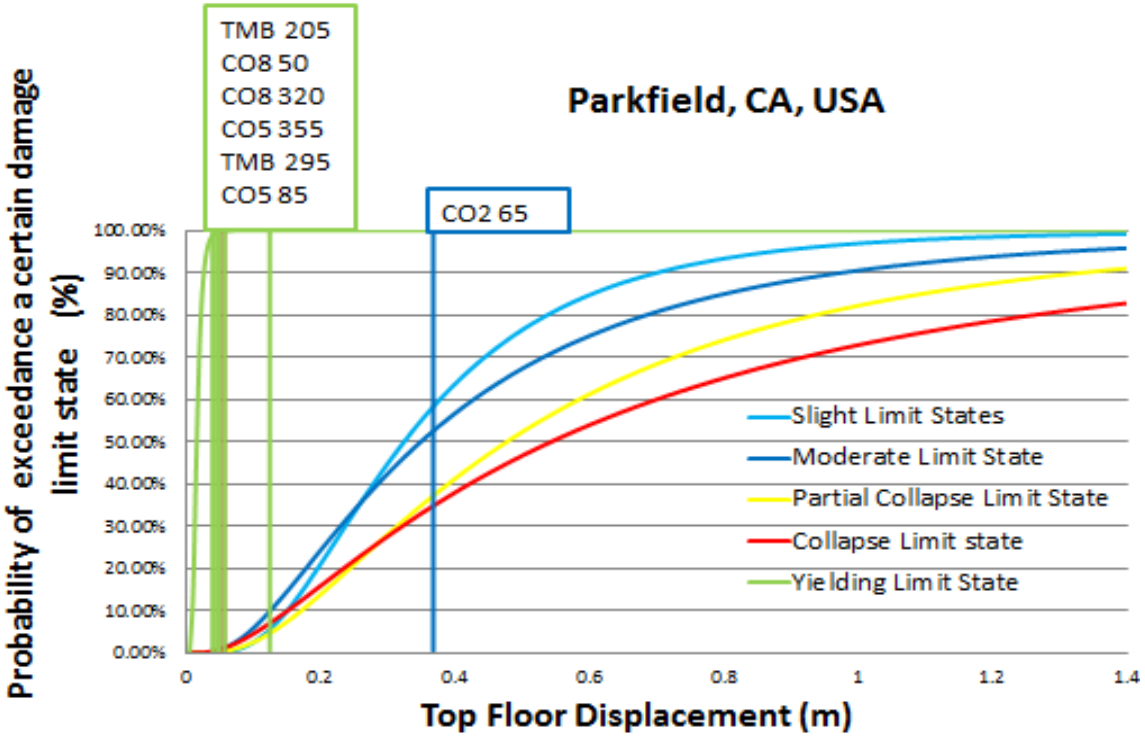

Figure 5.16 Fragility curves showing damage limit state for recording station in Park field, USA.

The Park field Earthquake had a magnitude of 6 on the Richter's scale. The stations record a forward directivity for all the station. The results place our building in the yielded area, with CO5 85 near the upper limit of the yield zone, While station CO2 065, due to its small distance from the rift, just 0.1 km, brings our building in the moderate area.

5.2.15 CHI-CHI, TAIWAN

The Chi-Chi earthquake was recorded by 422 free- strong motion instruments, including about 60 recordings within 20 km of the fault and 10 recordings within 3 km of the fault, making this by far the best recorded large earthquake ever.

The surface rupture from the September 21, 1999 Taiwan earthquake extends for about 75km along the north-south trending Chelungpu with vertical displacements of 1-8 km. At the fault's northern end, near Fengyuan, it curves toward the northeast and splinters into complex branches. This area of faulting, which trends towards the northeast, extends for an additional 10 km and was not previously considered an active fault.

More than 10 000 aftershocks were recorded in the first 3 weeks following the main shock, including over 100 felt events and 5 aftershocks of magnitude greater than 6.0.

Location	Mw	Dir./Ty	C/D	Displacement (m)	Limit State
CHI 024 090-1	7.6	F	7.7	0.3285	SLIGHT
CHI 024 360-1				0.2537	YIELD
CHI 028 090-1		N	2.3	0.4196	MODERATE

CHI 028 360-1			0.2861	YIELD
CHI 101 090-1	F	7.7	0.4013	MODERATE
CHI 101 360-1			0.5266	PARTIAL COLLAPSE
TCU 049 090-1	F	2.7	0.1629	YIELD
TCU 049 360-1			0.1971	YIELD
TCU 051 090-1	F	6.9	0.187	YIELD
TCU 051 360-1			0.2355	YIELD
TCU 052 90-1	F	0.8	0.3501	MODERATE
TCU 052 360-1			0.483	P.COLLAPSE
TCU 053 090-1	F	4.6	0.1416	YIELD
TCU 053 360-1			0.1973	YIELD
TCU 054 090-1	F	4.7	0.1349	YIELD
TCU 054 360-1			0.191	YIELD
TCU 055 090-1	F	6.5	0.2342	YIELD
TCU 055 360-1			0.2935	YIELD
TCU 065 090-1	F	0.1	0.6219	COLLAPSE
TCU 065 360-1			0.4485	MODERATE
TCU 067 090-1	F	0.2	0.6327	COLLAPSE
TCU 067 360-1			0.2831	YIELD
TCU 068 090-1	F	0.2	0.561	COLLAPSE
TCU 068 360-1			0.608	COLLAPSE
TCU 071 090-1	F	4.1	0.302	YIELD
TCU 071 360-1			0.2168	YIELD
TCU 072 090-1	F	6.8	0.2033	YIELD
TCU 072 360-1			0.283	YIELD
TCU 074 090-1	F	11.4	0.4531	MODERATE
TCU 074 360-1			0.1883	YIELD
TCU 075 090-1	F	0.6	0.6001	COLLAPSE
TCU 075 360-1			0.155	YIELD
TCU 076 090-1	F	2.3	0.2799	YIELD
TCU 076 360-1			0.3027	YIELD
TCU 078 090-1	F	5.4	0.1684	YIELD
TCU 078 360-1			0.1423	YIELD
TCU 082 090-1	F	5.0	0.1987	YIELD
TCU 082 360-1			0.2883	YIELD
TCU 087 090-1	F	5.8	0.1489	YIELD
TCU 087 360-1			0.1672	YIELD
TCU 089 090-1	F	6.2	0.1661	YIELD
TCU 089 360-1			0.1349	YIELD
TCU 101 090-1	F	1.5	0.242	YIELD
TCU 101 360-1			0.2587	YIELD
TCU 102 090-1	F	0.6	0.4985	PARTIAL COLLAPSE
TCU 102 360-1			0.5071	PARTIAL COLLAPSE
TCU 103 090-1	F	4.4	0.2519	YIELD
TCU 103 360-1			0.1582	YIELD
TCU 116 090-1	F	11.5	0.2409	YIELD

TCU 116 360-1			0.2431	YIELD
TCU 120 090-1	F	6.1	0.4222	YIELD
TCU 120 360-1			0.1837	YIELD
TCU 122 090-1	F	8.5	0.193	YIELD
TCU 122 360-1			0.2218	YIELD
TCU 129 090-1	F	1.5	0.30	YIELD
TCU 129 360-1			0.2031	YIELD

Table 17 Table of Displacement and damage level for recording station in Chi-Chi, Taiwan.

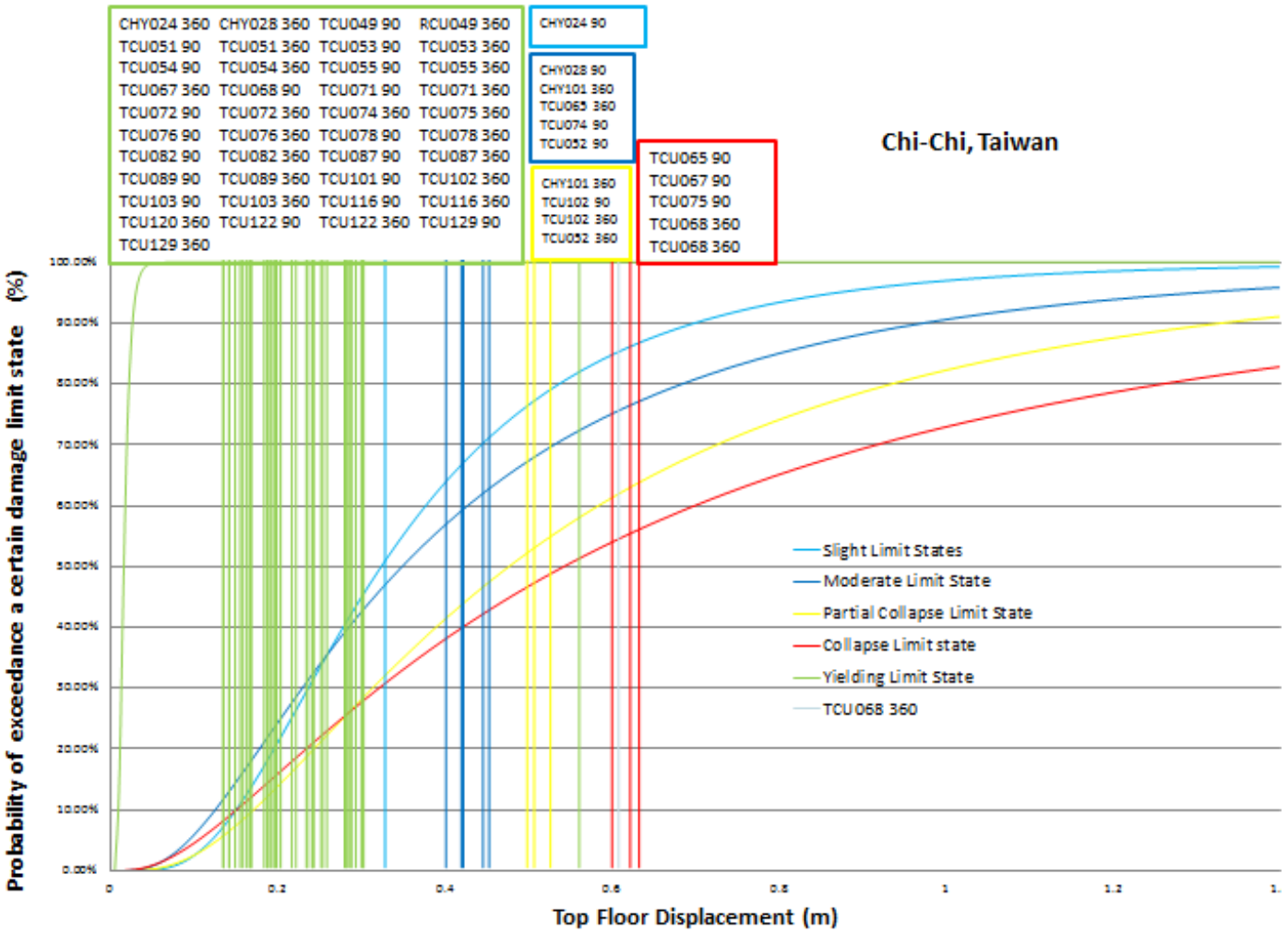

Figure 5.17 Fragility curves showing damage limit state for recording station in Chi-Chi, Taiwan.

The Chi-Chi Earthquake has a seismic magnitude of 7.6. The stations are showing a forward directivity, except Chi028 (neutral directivity).Mostly of the results maintained the building in the upper limit of the yield zone, exception being made by the station TCU068 (90,360), TCU065 90, TCU075 90 , TCU067 90 which places our building in the collapsed area, the main cause being the combination of the forward directivity, near position distance of the stations from the rift, and the magnitude of the earthquake, made the building not capable to resist

to its lateral load. Other stations like TCU052 360 TCU102 (90,360), and CHY101 360 placed the building in the partially collapsed area, again making the correlation between its directivity and the distance of the station from the rift.

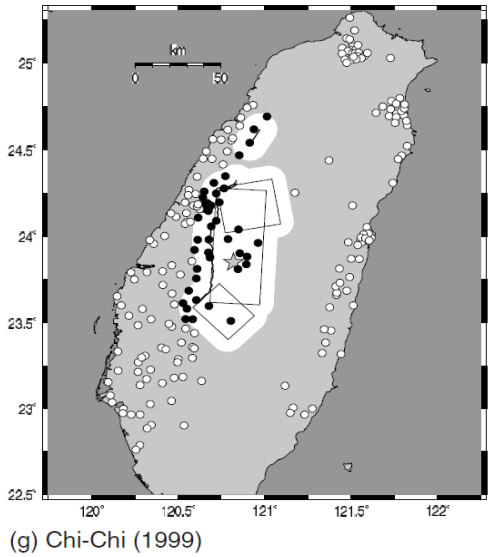

Figure 5.18 Map in which the black lines show the view of surface rupture based on the models of failure.

Stations within 10 km from the view of the Gulf (white areas in figure) are classified as nearby field, and are marked with black circles. The stations that are further away are shown with white circles. The star indicates the epicenter of the quake.

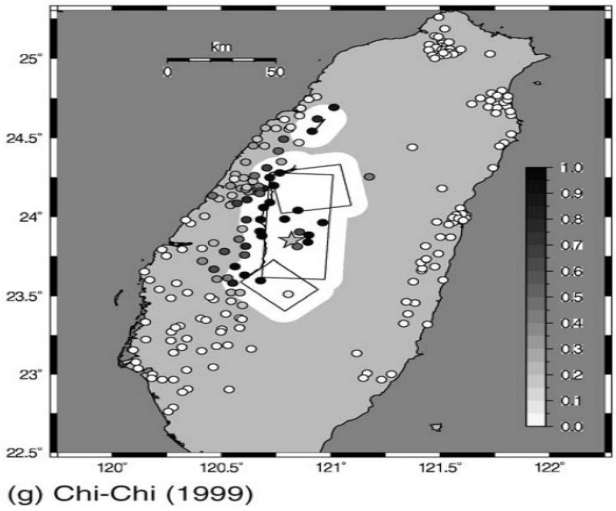

Figure 5.19 Map in which the dark spot are likely to be used as stations which are located in a region near the source.

All stations use the same color code for the scale. The symbols for the failure and the focus is the same as before.

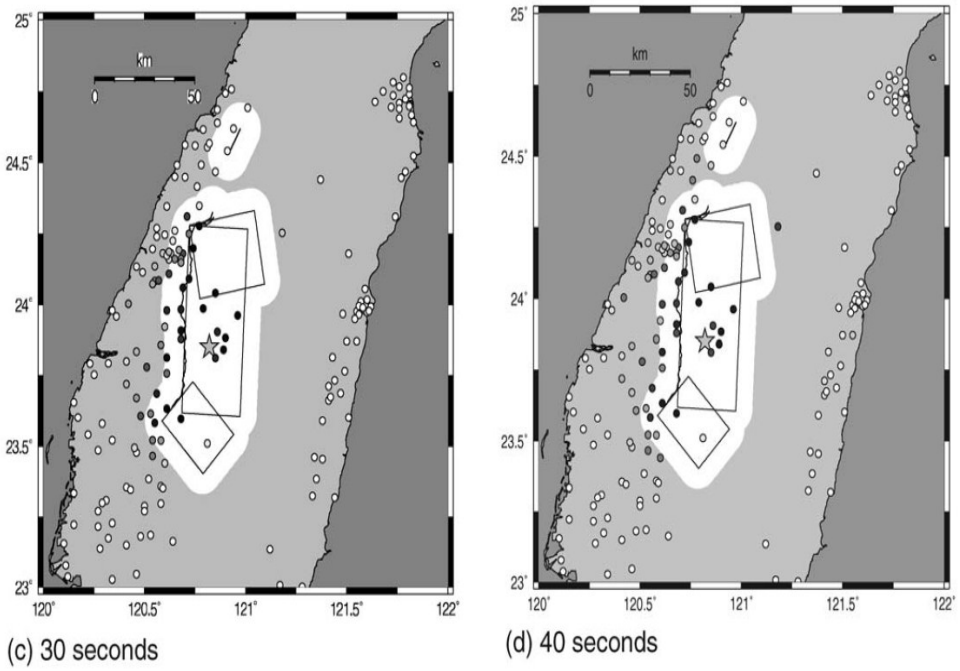

Figure 5.20 Maps showing snapshots of the potential near the source for the Chi-Chi earthquake,

according to the best discreet from the Bayesian approach. The large circle is the theoretical front rupture assuming that the rupture speed is 2 kilometers per second.

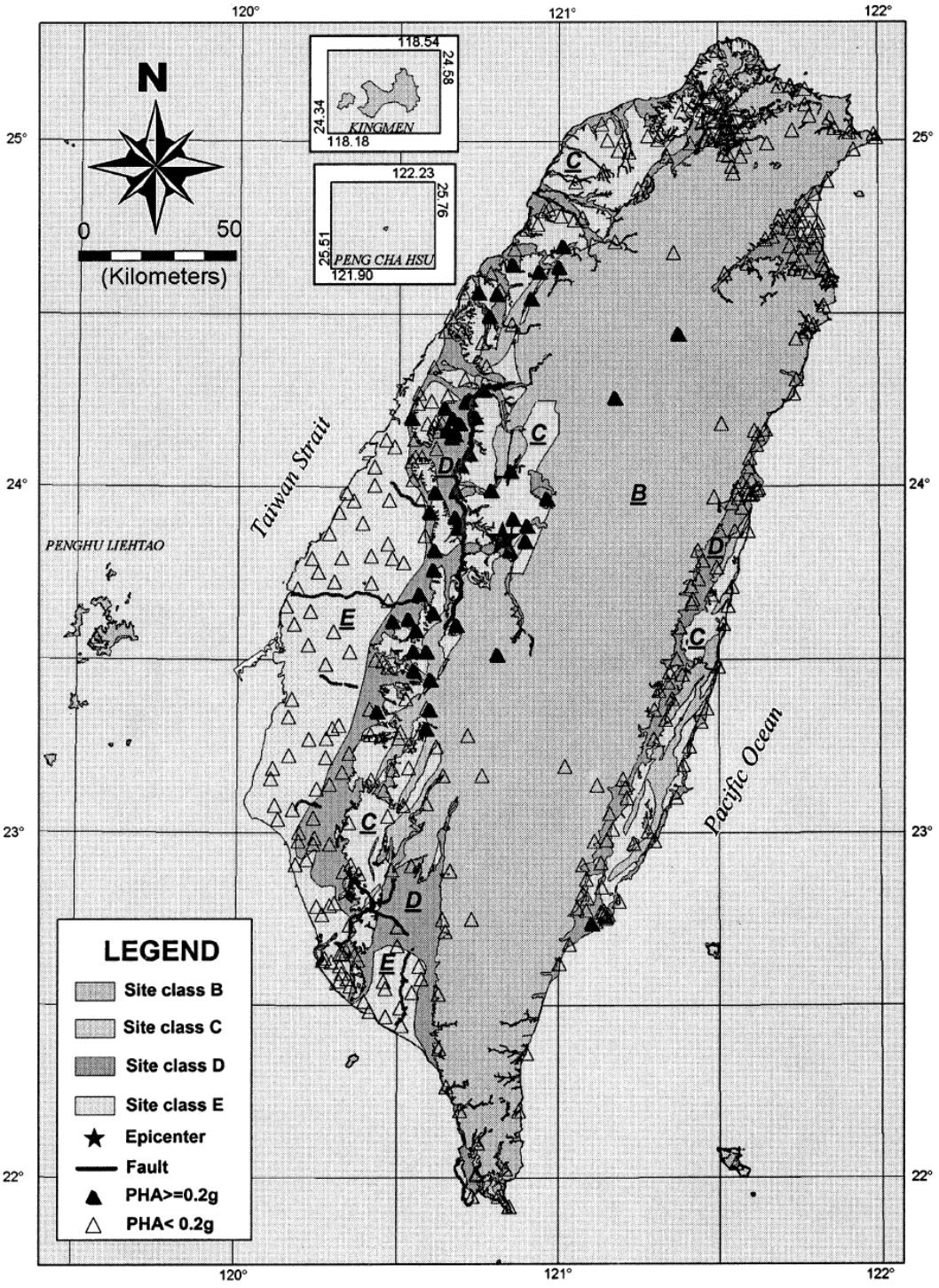

Figure 5.21 Map showing the 441 acceleration recording stations for Chi-Chi EQ

. Because some stations have more than one recorder accelerograph, essentially there are 412 stations. Among the 441 stations, 56 of them which are indicated by a solid black triangle show the stations to record maximum horizontal ground acceleration greater than 0.2 g.

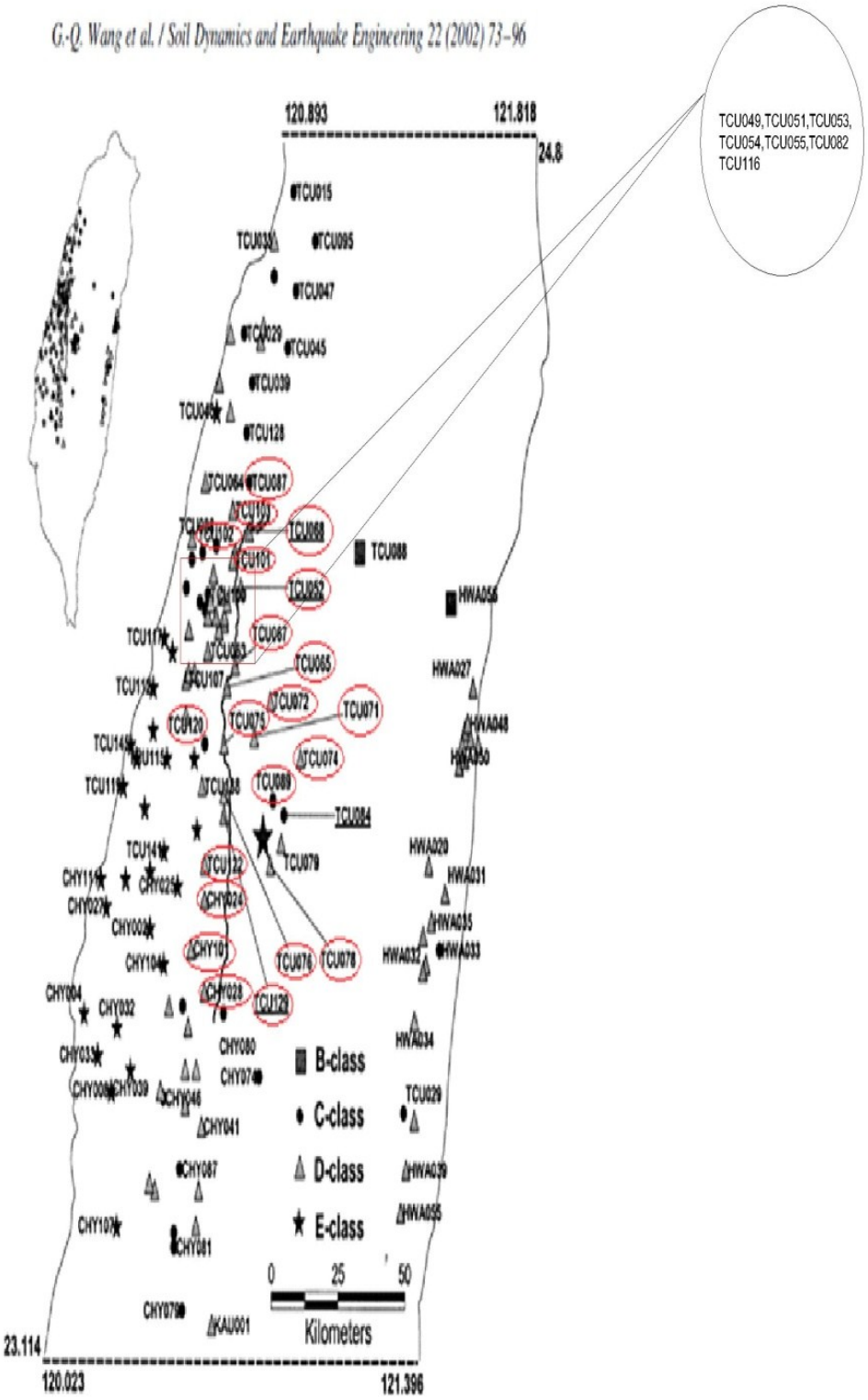

Figure 5.22 Map showing the location 130 stations nearby field.

The different symbols indicate the different geological characteristics of the soil. 2 stations are in soil category B, 30 in category C, 73 in D and 25 in E soil category respectively.

Figure 5.23 The surface ruptures zone and the locations of seismic. The star shows the focus of the main earthquake.

5.2.16 COYOTE LAKE, USA

Location	Mw	Dir/Ty	C/D	Displacement (m)	Limit State
GA1 230-1	5.6	F	9.0	0.1324	YIELD
GA1 360-1				0.04969	YIELD
GA2 050-1		F	7.2	0.04826	YIELD
GA2 140-1				0.1232	YIELD
GA3 050-1		F	5.1	0.08813	YIELD
GA3 140-1				0.1024	YIELD
GA4 270-1		F	3.5	0.06461	YIELD
GA4 360-1				0.0955	YIELD
GA6 230-1		F	1.2	0.5405	PARTIAL COLLAPSE
GA6 320-1				0.2521	YIELD
SMCC 160-1		B	0.2	0.3324	SLIGHT
SMCC 250-1				0.0496	YIELD

Table 18 Table of Displacements and damage levels for recording stations in Coyote Lake, USA.

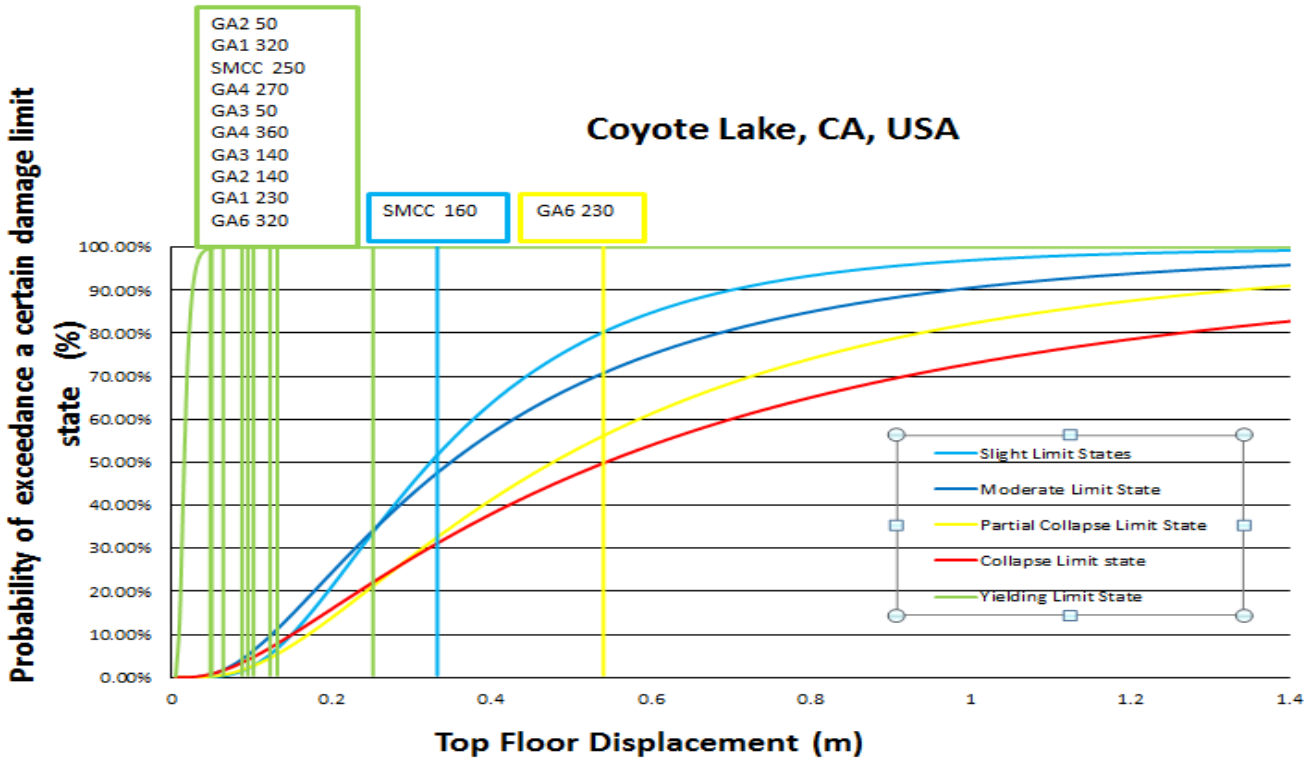

Figure 5.24 Fragility curves showing damage limit state for recording station in Coyote Lake, USA.

Coyote Lake earthquake had a magnitude of the 5.6. The stations recorded a forward directivity, exception being recorded by the SMCC station (backward directivity) which placed the building in the slight damage state show that the moderate placing of the building is mainly because of the small distance between the station and the rift. The other station of SMCC kept the building in the yielding area. While for GA6 recordings hold the forward directivity effect plus it's also near from the rift, around 1.2 Km which place the building in the partial collapse state.

5.2.17 DUZCE, TURKEY

Location	Mw	Dir/Ty	C/D	Displacement (m)	Limit State
DZC 180-1	7.1	N	8.3	0.2972	YIELD
DZC 270-1				0.3589	MODERATE
BOL 000-1		F	19.9	0.335	SLIGHT
BOL 090-1				0.2591	YIELD

Table 19 Table of Displacements and damage levels for recording stations in Duzce, TR.

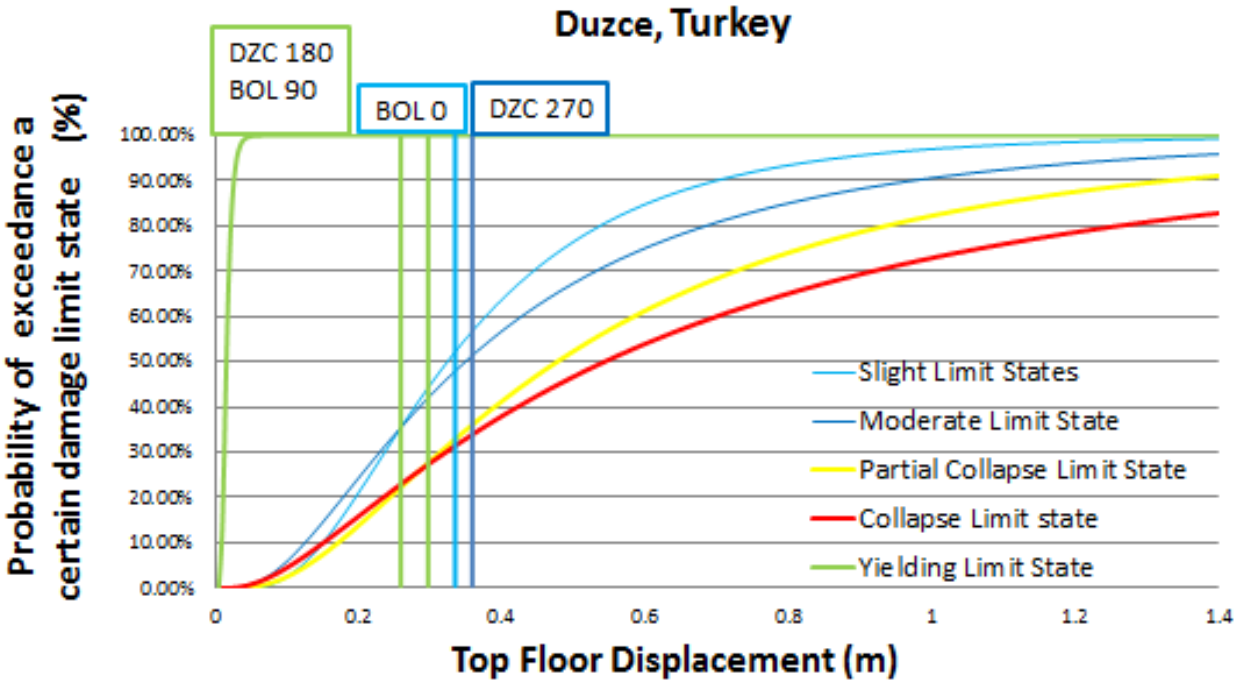

Figure 5.25 Fragility curves showing damage limit state for recording station in Duzce, Turkey.

Duzce earthquake had a seismic magnitude of 7.1 on Richter's scale. For this earthquake, two stations were used for recordings. The BOL, at a distance of 19.9 km from the rift, shows a forward directivity; the results showed that the building's displacements were smaller compared to the DZC station which was at a distance of 8.3 km, while holding a neutral directivity, placing the building in an area of moderate damage state. In this case it might, for the DZC station, the distance from the rift, may be affecting the building behavior more than the forward directivity effect since the EQ magnitude is the same.

5.2.18 GAZLI, URSS

Location	Mw	Dir/Ty	C/D	Displacement (m)	Limit State
KAR 000-1	6.7	N	3.0	0.2758	YIELD
KAR 090-1				0.3325	SLIGHT

Table 20 Table of Displacements and damage levels for recording stations in Gazli, URSS.

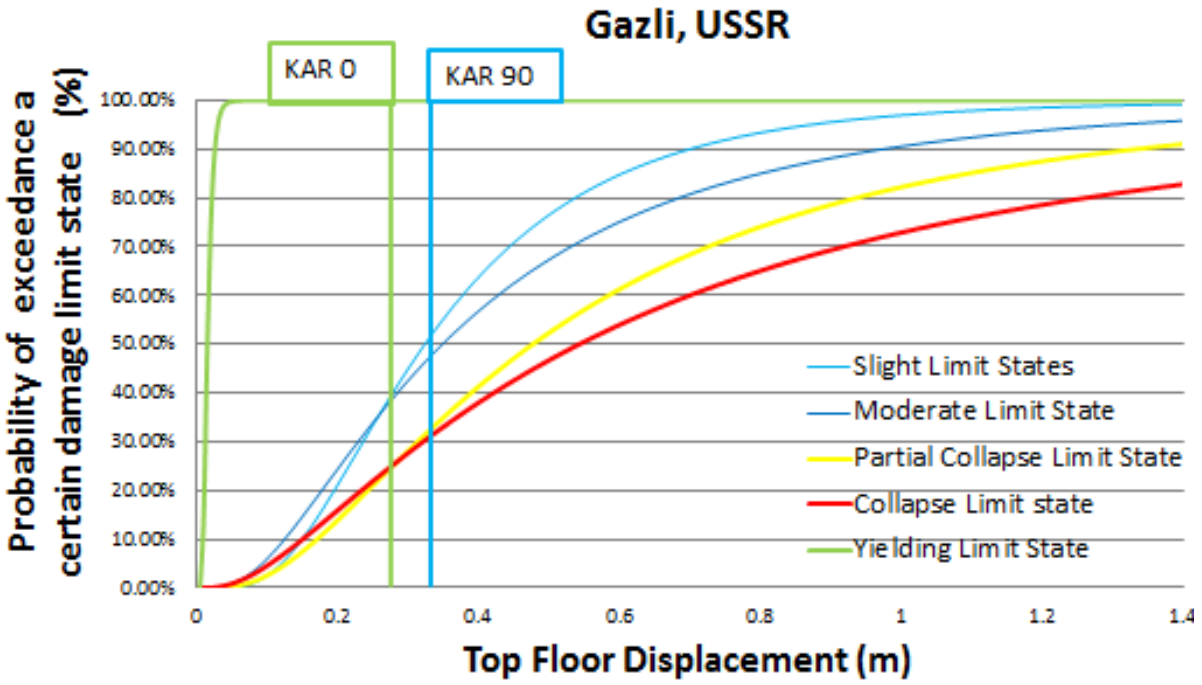

Figure 5.26 Fragility curves showing damage limit state for recording station in Gazli, URSS.

The earthquake in Gazli had a magnitude of 6.7 on Richter's scale. The displacements are somehow large close to each other and they place our building in the slight area may be due to the short distance of the station KAR (3km) and the neutral directivity recorded by it plus the large magnitude

5.2.19 HANSHIN (KOBE), JAPAN

Location	Mw	Dir/Ty	C/D	Displacement (m)	Limit State
KBU 000-1	6.8	F	3.2	0.3642	MODERATE
KBU 090-1				0.1694	YIELD
KPI 000-1		F	0.7	0.4943	P.COLLAPSE
KPI 090-1				0.2798	YIELD
TAZ 000-1		F	0.4	0.3718	MODERATE
TAZ 090-1				0.145	YIELD
TAK 000-1		F	1.1	0.5995	COLLAPSE
TAK 090-1				0.6641	COLLAPSE
NIS 000-1		N	10.5	0.2557	YIELD
NIS 090-1				0.2111	YIELD

Table 21 Table of Displacements and damage levels for recording stations in Kobe, Japan.

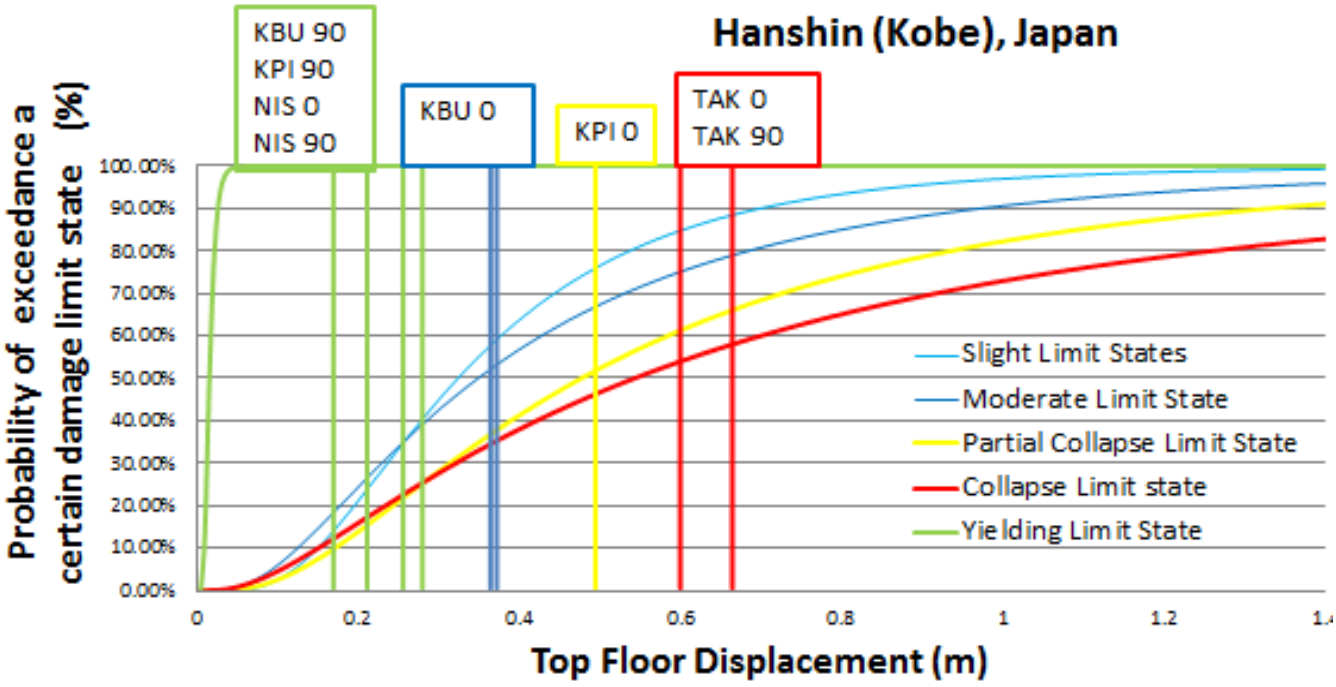

Figure 5.27 Fragility curves showing damage limit state for recording station in Kobe, Japan.

The intense earthquake in the area of Hanshin (Kobe) of Japan had a magnitude of 6.8 on the Richter's scale. An equal number of yielding and moderate results had revealed. An exception has the station KPI 000, where the distance of the station toward the rift is very small (0.7 km), so the results place the building into the partially collapse region. Also for TAK (0, 90) they are so close also to the rift at a distance about 1.1 Km, holding the forward directivity effect causing the building to collapse.

5.2.20 NORTHRIDGE, CA, USA

Location	Mw	Dir/Ty	C/D	Displacement (m)	Limit State
JFA 022-1	6.7	F	5.2	0.5878	COLLAPSE
JFA 292-1				0.5158	P.COLLAPSE
PKC 090-1		N	7.4	0.1858	YIELD
PKC 360-1				0.1575	YIELD
NHW 180-1		N	11.8	0.2954	YIELD
NHW 270-1				0.4254	YIELD
SFY 090-1		N	8.0	0.1476	YIELD
SFY 360-1				0.1596	YIELD
PCD 175-1		F	7.2	0.1085	YIELD
PCD 265-1				0.0985	YIELD
RRS 228-1		F	6.0	0.4891	COLLAPSE
RRS 318-1				0.5774	P.COLLAPSE
SCG 052-1		F	5.1	0.6409	COLLAPSE
SCG 142-1				0.6184	COLLAPSE

SCH 011-1	F	5.0	0.5327	P.COLLAPSE
SCH 281-1			0.5122	P.COLLAPSE
VSP 270-1	F	8.0	0.3269	SLIGHT
VSP 360-1			0.3401	SLIGHT
LDW 064-1	F	5.6	0.3801	YIELD
LDW 334-1			0.3021	MODERATE
SYH 090-1	F	5.5	0.3722	MODERATE
SYH 360-1			0.5834	COLLAPSE
CPC 106-1	N	13.7	0.371	YIELD
CPC 196-1			0.2157	MODERATE
CCY 000-1	F	12.9	0.2955	YIELD
CCY090-1			0.1502	YIELD
LF5 035-1	B	19.2	0.1411	YIELD
LF5 135-1			0.09639	YIELD
LF6 009-1	B	17.3	0.2835	YIELD
LF6 279-1			0.2712	YIELD
ULA 090-1	B	19.9	0.06151	YIELD
ULA 360-1			0.1895	YIELD
LWS 000-1	B	19.0	0.07637	YIELD
LWS 090-1			0.09689	YIELD
NWS 046-1	F	5.3	0.33	YIELD
NWS 316-1			0.4185	MODERATE
NWH 090-1	F	6.5	0.2225	YIELD
NWH 360-1			0.1937	MODERATE
NRG 090-1	F	11.5	0.1732	YIELD
NRG 180 -1			0.3863	MODERATE
SMI 000-1	N	12.4	0.1579	YIELD
SMI-090-1			0.1285	YIELD
SVG 000-1	N	9.3	0.1502	YIELD
SVG 090-1			0.1805	YIELD
TAR 090-1	B	14.8	0.1401	YIELD
TAR 360-1			0.3205	YIELD

Table 22 Table of Displacements and damage levels for recording stations in Northridge, USA.

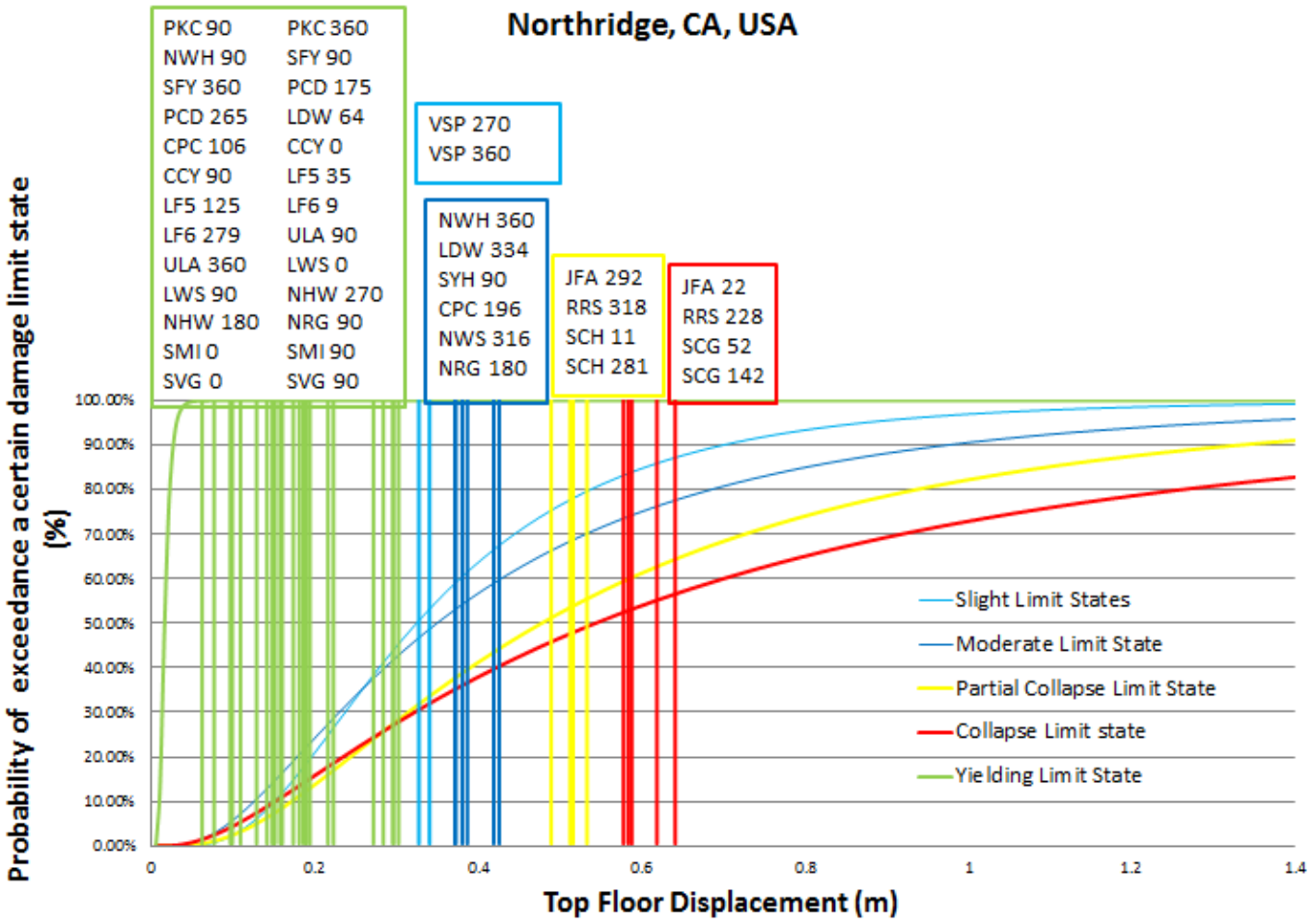

Figure 5.28 Fragility curves showing damage limit state for recording station in Northridge, USA.

The earthquake of Northridge California from 17-01-1994 had magnitude of 6.7 the stations which have maintained the building in the moderated area were mainly in position s which showed reverse and neutral directivity this is justified by the fact that all these stations were long distances from the surface of the rift, which is why we have experienced small movements. The recordings with the largest displacements were SCH, JFA, RRS, and SCG records holding forward directivity, although they have forward directivities like many other station records, they have the largest displacements as they are closer to the rift.

Again it begins to be clear that the effect of the seismological parameter "distance from the fault" has more impact on the building response than the other parameters.

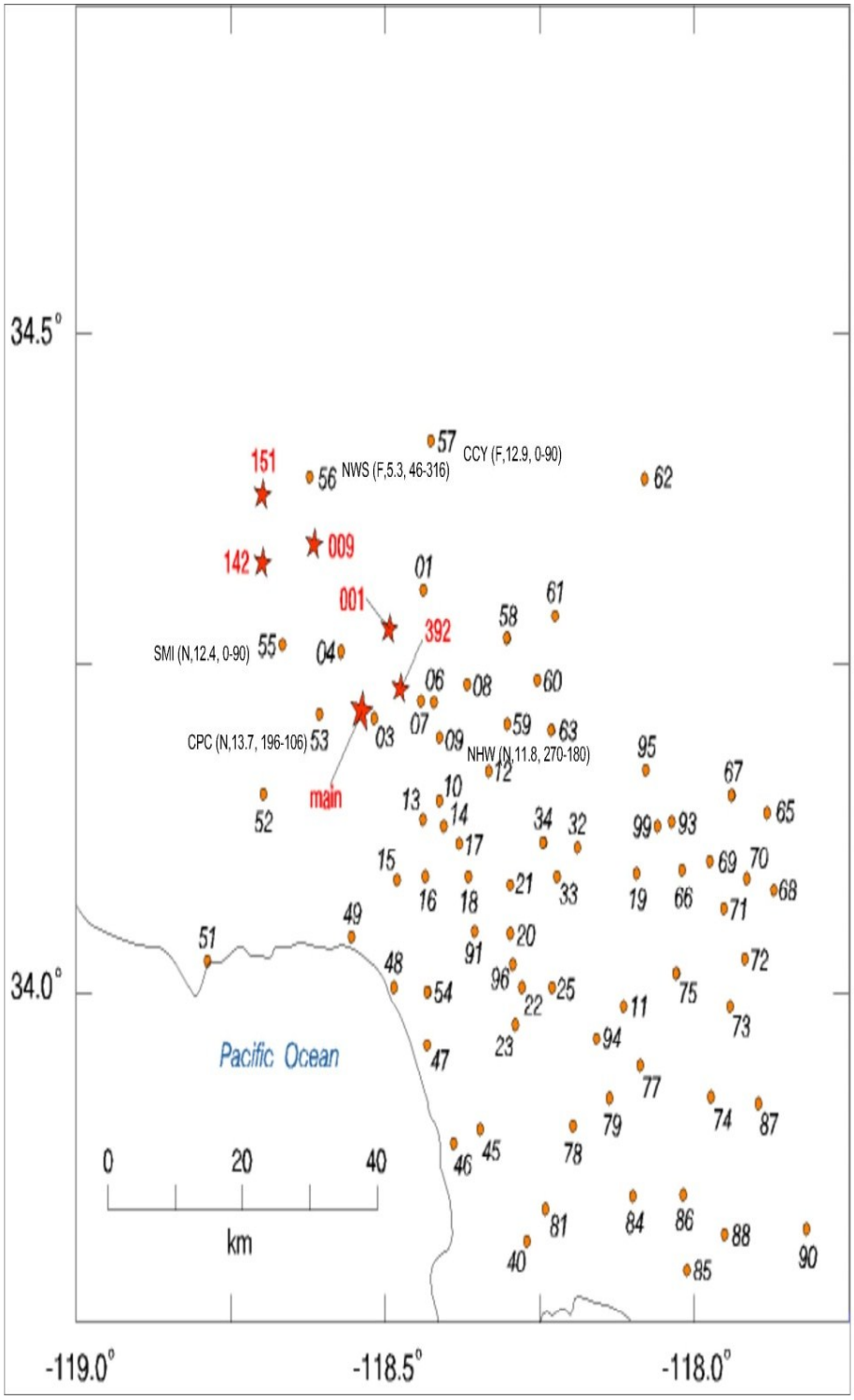

Figure 5.29 Stations DWP sensed the Northridge earthquake.

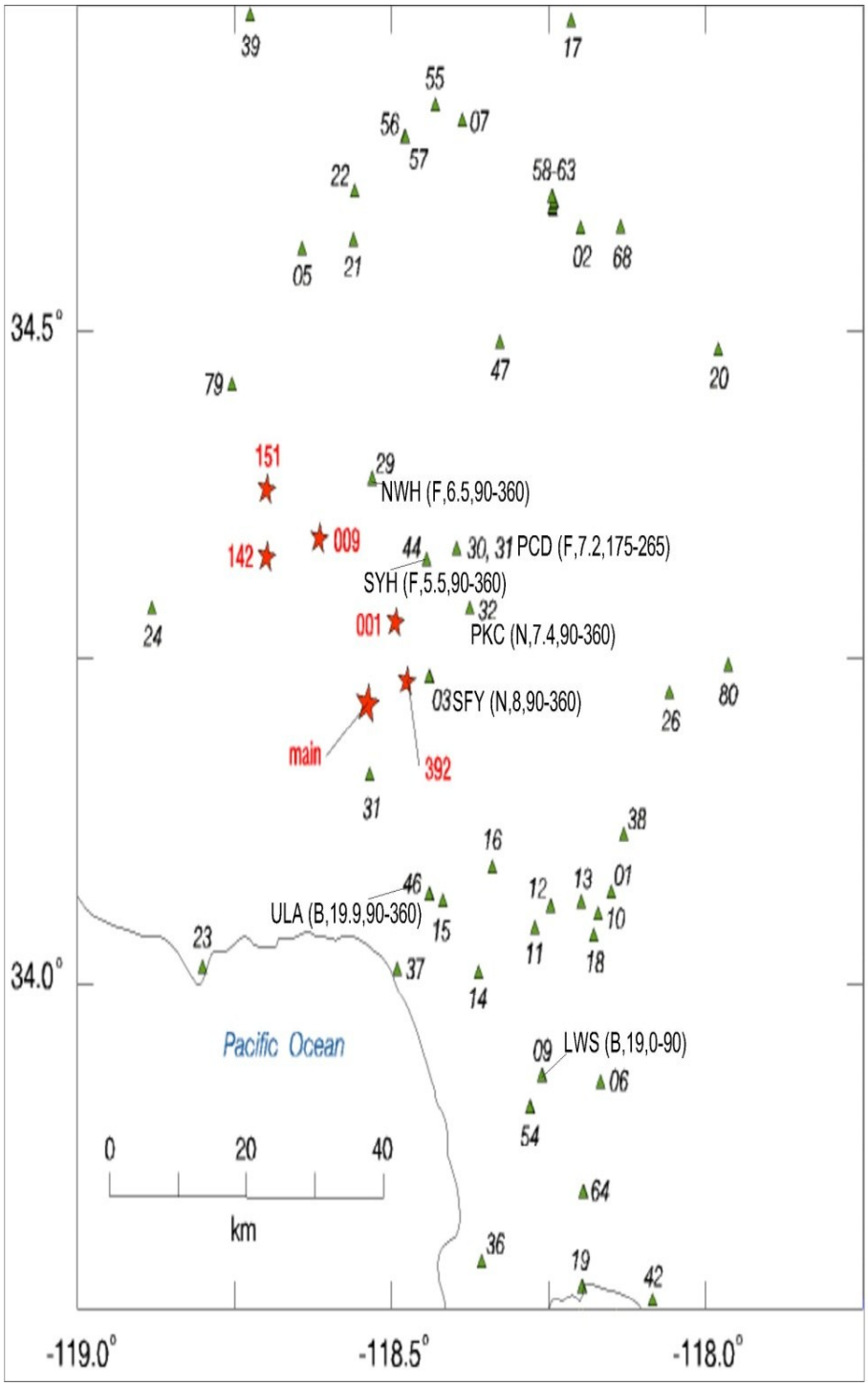

Figure 5.30 Stations DWP sensed the Northridge earthquake.

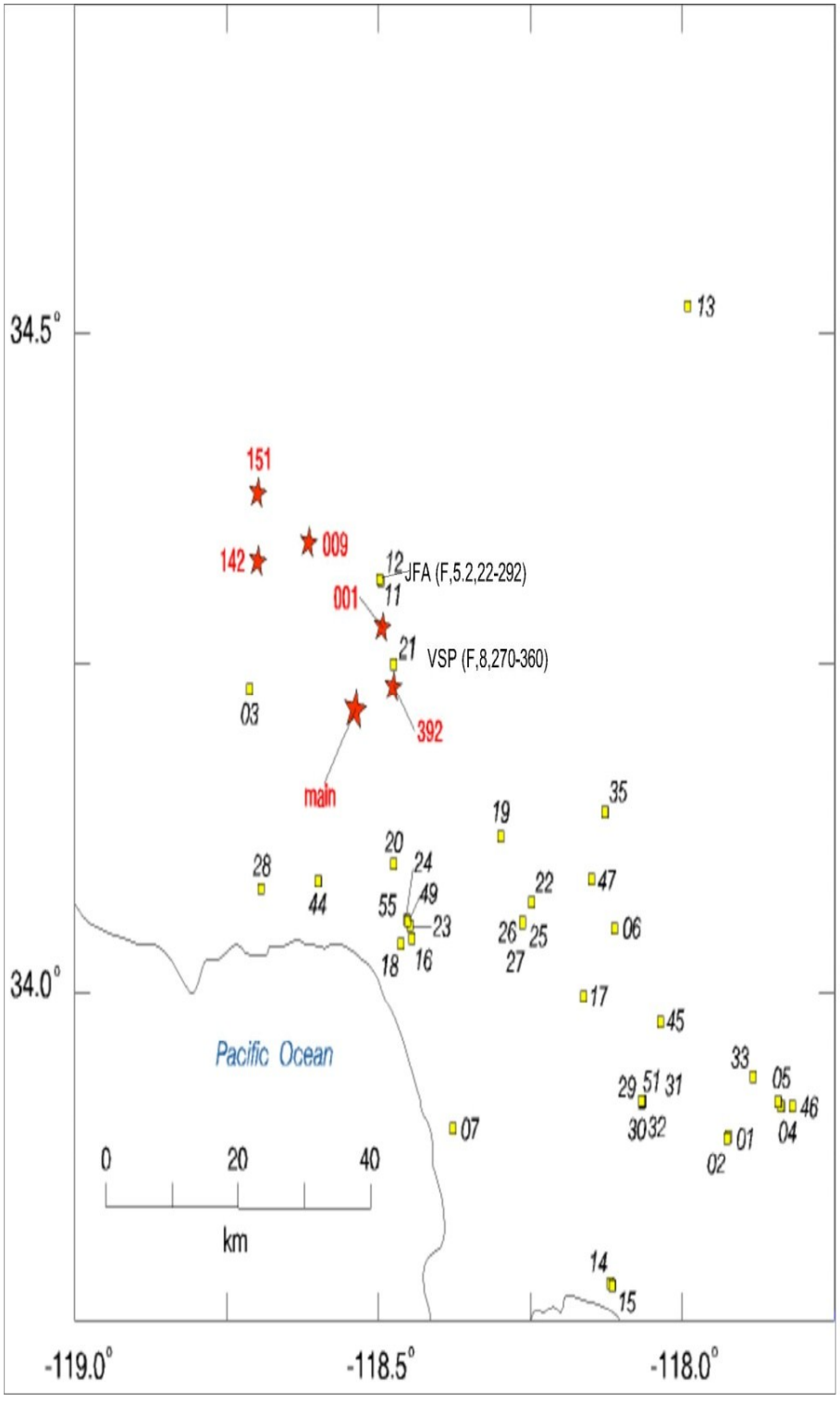

Figure 5.31 Stations USC sensed the earthquake Northridge.

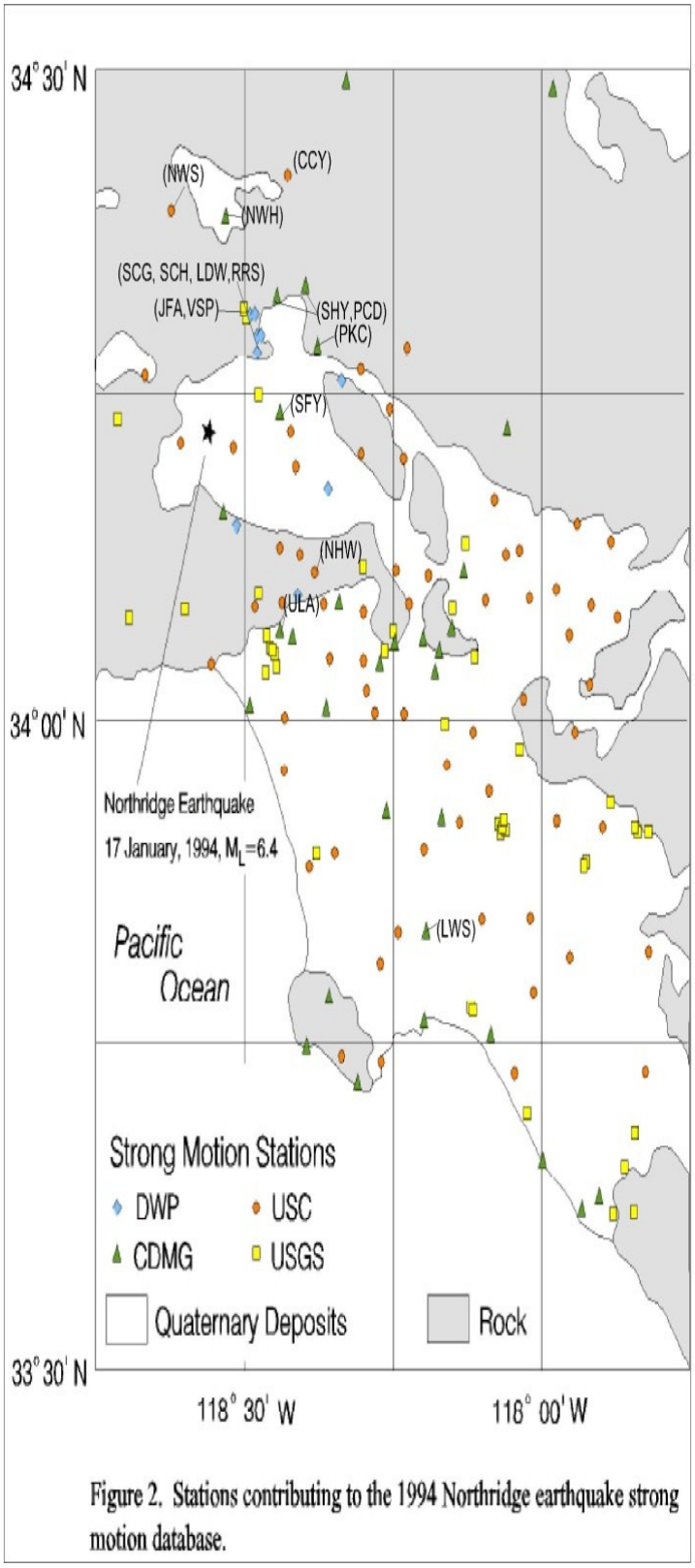

Figure 5.32 CDMG Stations sensed the Northridge earthquake.

5.2.21 WHITTER NARROWS, CA, USA

Location	Mw	Dir/Ty	C/D	Displacement (m)	Limit State
ALF 180-1	6.0	N	13.1	0.0539	YIELD
ALF 270-1				0.05177	YIELD
SNM 270-1		N	15.8	0.01526	NON-YIELD
SNM 360-1				0.06381	YIELD
OBP 270-1		F	12.7	0.04545	YIELD
OBP 360-1				0.05536	YIELD
ECP 000-1		N	19.1	0.03422	YIELD
ECP 090-1				0.0182	NON-YIELD
DOW 180-1		F	16.4	0.07834	YIELD
DOW 270-1				0.03	NON-YIELD
GVR 060-1		F	12.1	0.2905	YIELD
GVR 330-1				0.04603	YIELD
WND 062-1		F	12.3	0.03435	YIELD
WND 152-1				0.02454	NON-YIELD
ALH 000-1		N	14.3	0.09442	YIELD
ALH 090-1				0.04188	YIELD
WTR 090-1		F	11.1	0.0364	YIELD
WTR 180-1				0.08325	YIELD
LBM 010-1		F	12.7	0.03483	YIELD
LBM 280-1				0.08198	YIELD
VRN 007-1		F	13.6	0.05385	YIELD
VRN 277-1				0.04715	YIELD
NWK 090-1		N	15.7	0.02313	NON-YIELD
NWK 360-1				0.06591	YIELD
SGS 270-1		N	14.6	0.02327	NON-YIELD
SGS 180-1				0.09246	YIELD
EMC 270-1		N	15.2	0.0684	YIELD
EMC 000-1				0.01953	NON-YIELD
XWC 315-1		N	15.6	0.06503	YIELD
XWC 225-1				0.03906	YIELD
XHA 140-1		N	15.0	0.01791	NON-YIELD
XHA 230-1				0.01642	NON-YIELD
ARC 009-1		N	17.0	0.06093	YIELD
ARC 279-1				0.01068	NON-YIELD

Table 23 Table of Displacements and damage levels for recording stations in in Whittier Narrows, CA, USA.

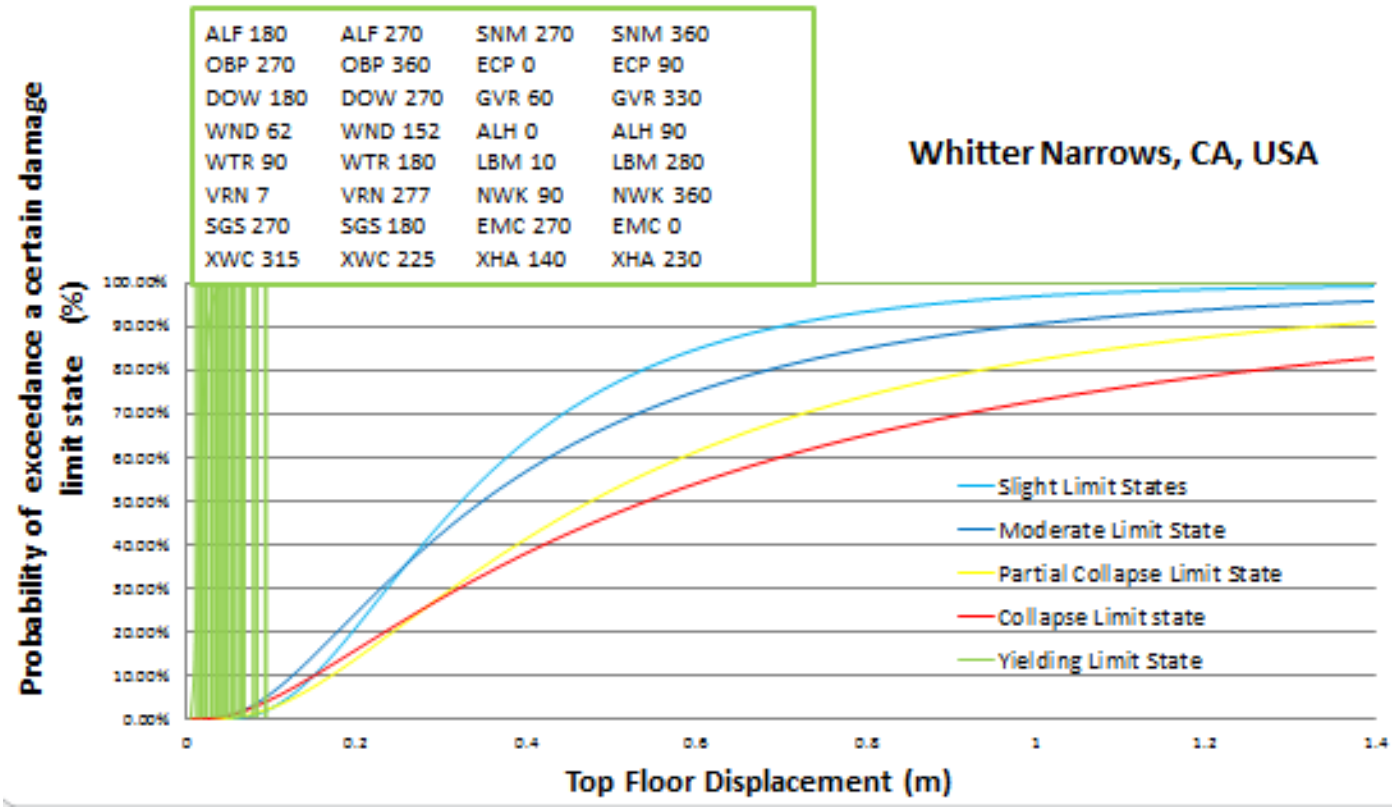

Figure 5.33 Fragility curves showing damage limit state for recording station in Whittier Narrows, CA, USA.

The Whittier Narrows Earthquake has a seismic magnitude of 6.0 on Richter's scale, The stations are showing a mix of forward and neutral directivity, the results attained after the analysis is so small, even some of the records doesn't place in any damage state even keeping it in the non-yield zone, this may be due to stations far position from the rift.

5.2.22 PETROLIA, CA, USA

Location	Mw	Dir/Ty	C/D	Displacement (m)	Limit State
CAP 000-1	7.6	F	7.8	0.2788	YIELD
CAP 090-1				0.2734	YIELD
PGS 000-1		F	8.9	0.2021	YIELD
PGS 090-1				0.4447	MODERATE
FOR 000-1		N	13.5	0.1755	YIELD
FOR 090-1				0.1192	YIELD
RIO 270-1		N	13.1	0.1528	YIELD
RIO 360-1				0.119	YIELD

Table 24 Table of Displacements and damage levels for recording stations in Petrolia, CA, USA.

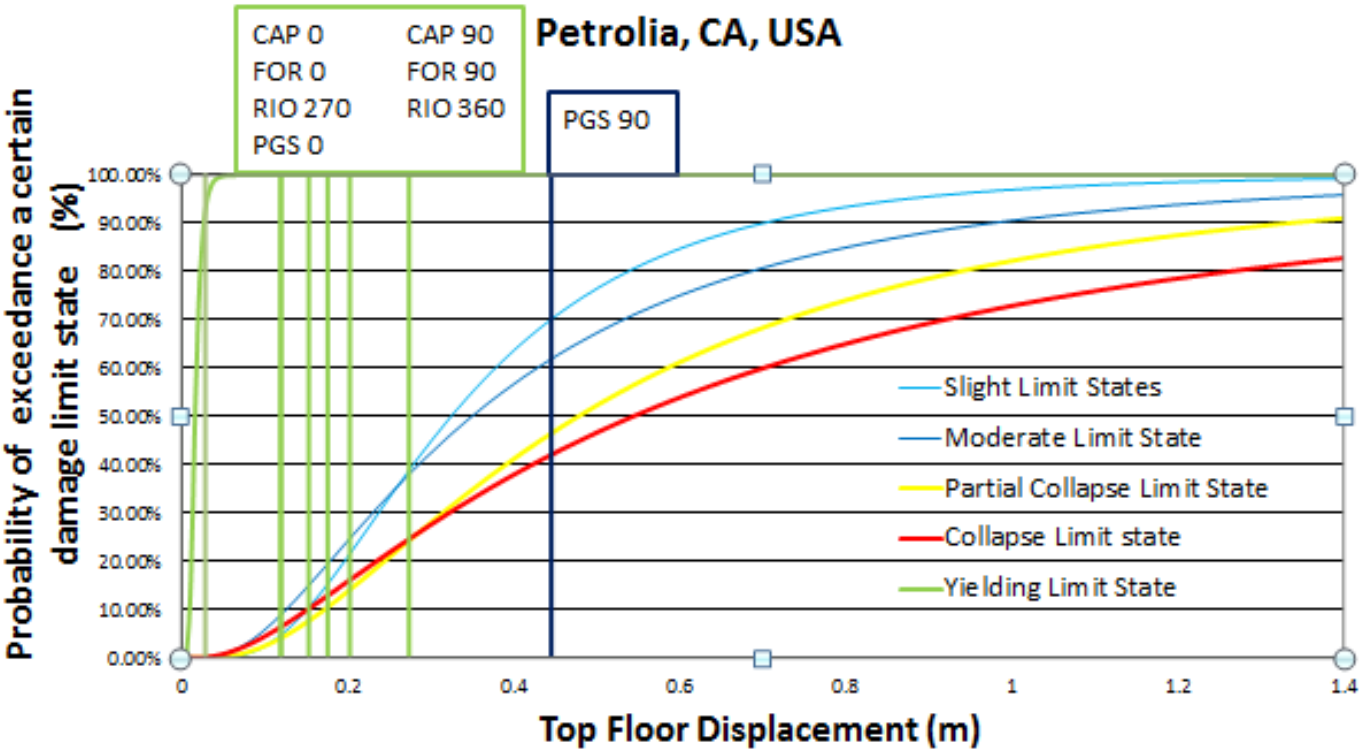

Figure 5.34 Fragility curves showing damage limit state for recording station in Petrolia, CA, USA.

Petrolia EQ has a magnitude of 6.9 on Richter's scale and having stations CAP, and PGS with forward directivity effects, and closer distance to the rift than the other 2 stations FOR, and Rio which has neutral directivity, thus the first two station records gives a higher effect on the response of the building due to the combination of Forward directivity and closer distance to the rift.

Chapter 6

6. Conclusion

As we saw for instance the intense earthquake in the area of Hanshin (Kobe) of Japan had a magnitude of 6.8 on the Richter's scale. An equal number of yielding and moderate results had revealed. An exception has the station KPI 000, where the distance of the station toward the rift is very small (0.7 km), so the results place the building into the partially collapse region. Also for TAK (0, 90) they are so close also to the rift at a distance about 1.1 Km, Plus holding the forward directivity effect causing the building to collapse.

Also in Duzce earthquake that had a seismic magnitude of 7.1 on Richter's scale. For this earthquake, two stations were used for recordings. The BOL, at a distance of 19.9 km from the rift, shows a forward directivity; the results showed that the building's displacements were smaller compared to the DZC station which was at a distance of 8.3 km, while holding a neutral directivity, placing the building in an area of moderate damage state, it would be clear that the distance from the rift, may be affecting the building behavior more than the forward directivity effect since the EQ magnitude is the same.

And after reviewing all the previous results presented in chapter 5 we can conclude that:

Analytical analysis revealed that the forward directivity pattern and a near distance of a station from the fault will result in large displacements of the building. And also the seismic magnitude play a major role in amplification the response of the building toward this direction.

The seismic records which present the fault normal component showed more displacement than those presented by the fault parallel component.

One can say that the magnitude effect has already been appreciated as a crucial factor affecting structural response. This investigation indicates that the directivity and distance to the fault effects are of equal significance.

Characteristically, the range of structural response values for different directivity or attenuation effects may present a difference of an order of magnitude. The sensitivity of the estimation of seismic risk to the referred parameters indicates that their incorporation in procedures such as HAZUS must be as detailed and accurate as possible.

References

1) "A review of the seismic hazard zonation in national building codes in the context of Euro code 8- G. Solomon, A. Pinto, S. Dimova.
2) An Introduction to Probabilistic Seismic Hazard Analysis (PSHA), Jack W. Baker, 2008
3) Deterministic vs. Probabilistic earthquake hazards and risks, Robin K. Maguire
4) http://peer.berkeley.edu/course_modules/eqrd/index.htm?c227top.htm&227cont.htm&EQDef/eqdef7.htm
5) Seismic Hazards: Issues and Alternatives, Zhenming Wang, 2010
6) A Methodology for Assessing the seismic risk of Buidings, Katherine Marie Thibert, 2003
7) Earthquake loss estimation and risk assessment methodology from concept to real applications, Yasin M. Fahjan, 2010
8) Wikipedia.com
9) Earthquake Engineering and Engineering Seismology, Rajesh Rupakhety, 2008
10) Effects of Fling step and Forward Directivity on Seismic Response of Buildings, Sashi K. Kunnath, 2005
11) Identification of near-fault earthquake record characteristics, Ch.A. Maniatakis, I.M. Taflampas and C.C. Spyrakos, 2008
12) Hazus MH